Meereswissenschaftliche Berichte

Marine Science Reports


No 127 2024

# Hydrographic-hydrochemical assessment of the Baltic Sea 2022

Michael Naumann, Ulf Gräwe, Lars Umlauf, Hans Burchard, Volker Mohrholz, Joachim Kuss, Marion Kanwischer, Helena Osterholz, Susanne Feistel. Ines Hand. Joanna J. Waniek. Detlef E. Schulz-Bull

"Meereswissenschaftliche Berichte" veröffentlichen Monographien und Ergebnisberichte von Mitarbeitern des Leibniz-Instituts für Ostseeforschung Warnemünde und ihren Kooperationspartnern. Die Hefte erscheinen in unregelmäßiger Folge und in fortlaufender Nummerierung. Für den Inhalt sind allein die Autoren verantwortlich.

"Marine Science Reports" publishes monographs and data reports written by scientists of the Leibniz-Institute for Baltic Sea Research Warnemünde and their co-workers. Volumes are published at irregular intervals and numbered consecutively. The content is entirely in the responsibility of the authors.

Schriftleitung / Editorship: Dr. Sandra Kube (sandra.kube@io-warnemuende.de)

Die elektronische Version ist verfügbar unter / The electronic version is available on: http://www.io-warnemuende.de/meereswissenschaftliche-berichte.html



ISSN 2195-657X

---

Dieser Artikel wird zitiert als /This paper should be cited as:

Michael Naumann[1], Ulf Gräwe[1], Lars Umlauf[1], Hans Burchard[1], Volker Mohrholz[1], Joachim Kuss[1], Marion Kanwischer[1], Helena Osterholz[1], Susanne Feistel[1], Ines Hand[1], Joanna J. Waniek[1], Detlef E. Schulz-Bull[1]: Hydrographic-hydrochemical assessment of the Baltic Sea 2022. Meereswiss. Ber., Warnemünde, 127 (2024), doi:10.12754/msr-2024-0127.

Adressen der Autoren:
[1] Leibniz Institute for Baltic Sea Research (IOW), Seestraße 15, D-18119 Rostock-Warnemünde, Germany

Corresponding author: michael.naumann@io-warnemuende.de

## Table of content

## Kurz- /Zusammenfassung

Die Arbeit beschreibt die hydrographisch-hydrochemischen Bedingungen in der westlichen und zentralen Ostsee im Jahr 2022. Basierend auf den meteorologischen Verhältnissen werden die horizontalen und vertikalen Verteilungsmuster von Temperatur, Salzgehalt, Sauerstoff, Schwefelwasserstoff und Nährstoffen mit saisonaler Auflösung dargestellt.

Der Winter 2021/2022 belegt mit einer Kältesumme von 15,9 Kd in Warnemünde den sechsten Platz der wärmsten Winter der Datenreihe seit dem Jahr 1948. Die Wärmesumme des Sommers 2022 ist mit 281,4 Kd nur knapp unter dem Vorjahr (284,7 Kd), jedoch deutlich über dem Mittelwert von 161,4 Kd. Im gesamten Jahresverlauf 2022 blieben intensive Einstromereignisse erneut aus. Zwei kleinere Ereignisse mit Gesamtvolumina von 140 $km^3$ und 158 $km^3$ sorgten für die Belüftung des Tiefenwassers im Gebiet des Arkona Beckens. Im Dezember sorgten zusätzlich drei aufeinanderfolgende kleine Einschübe für ein Einstromvolumen von etwa 141 $km^3$ mit einem Salzimport von 1,15 Gt.

Der insgesamt abnehmende Trend von Sauerstoff, also tatsächlich die Zunahme von Schwefelwasserstoff, im Tiefenwasser der tiefen Ostseebecken ging im Jahr 2022 grundsätzlich weiter. Seit einiger Zeit wird immer deutlicher, dass auch flache Bereiche der Ostsee immer öfter von saisonalem Sauerstoffmangel betroffen sind. Der Abbau der großen Mengen an organischem Material, die aufgrund der anhaltenden Eutrophierung produziert werden, verbraucht im beträchtlichen Umfang Sauerstoff, was sich besonders im Bereich des Meeresbodens auswirkt. Zwar hatte sich im Februar 2022 im westlichen und zentralen Arkonabecken sauerstoffreiches Bodenwasser mit einer Konzentration von 310-335 µmol $l^{-1}$ Sauerstoff gebildet, das aber letztendlich nur in einigen Bereichen eine vorübergehende Verbesserung brachte. Es passierte das Bornholmsgatt und mischte sich dann in das Bornholmbecken Tiefenwasser ein. Über das Frühjahr und den Sommer wurde es mit 130-270 µmol $l^{-1}$ Sauerstoff weiter ostwärts bis in die südliche Gotlandsee transportiert, wo es in einer Tiefe von etwa 100 m noch eine Konzentration von bis zu etwa 45 µmol $l^{-1}$ Sauerstoff aufwies.

Die ausgewählten Stationen westlich der Darsser Schwelle (Fehmarn Belt, Lübecker und Mecklenburger Bucht) wiesen im Februar 2022 relativ hohe winterliche Nitratkonzentrationen im Oberflächenwasser im Vergleich zu den letzten Jahren auf, was eventuell einen Einfluss von Nordseewasser anzeigte. Dagegen waren die Stationen in der zentralen Ostsee eher durch niedrigere Nitratkonzentrationen im Februar gekennzeichnet, was eventuell auf dem zunehmenden Sauerstoffmangel und verstärktem Nitratabbau im Tiefenwasserkörper beruhte. Die relativ niedrigen Werte von 3,4 µmol $l^{-1}$ Nitrat im Oberflächenwasser der Station Gotlandtief und 2,9 µmol $l^{-1}$ am Bornholmtief im Winter verursachten eine frühe Aufzehrung von Nitrat, bereits bei noch niedrigen Temperaturen. Dies ermöglichte wahrscheinlich, dass Phosphat über das Sommerhalbjahr 2022 praktisch permanent vorhanden war. Nur Anfang August lag die Konzentration im Gotlandtief unter der Nachweisgrenze. Die Jahresmittelwerte der Phosphatkonzentration im Tiefenwasser des Bornholmbeckens spiegelten eine beträchtliche Variabilität seit 2018 auf hohem Niveau von 4,2 ± 0,9 µmol $l^{-1}$ in der Referenztiefe wider. Wogegen die Phosphatkonzentrationen im Landsorttief und dem Karlsötief mit 3,7 ±0,4 µmol $l^{-1}$ und 3,8 ±0,3 µmol $l^{-1}$ Phosphat in den entsprechenden Referenztiefen stabiler waren. Das Gotlandtief zeigte die deutlichste Akkumulation von Phosphat, bis auf 6,1 µmol $l^{-1}$, und von Ammonium,

sogar bis auf 27,9 µmol $l^{-1}$ in 2022. Wobei im Fårötief die Phosphat- und Ammoniumkonzentration auf 4,7 µmol $l^{-1}$ bzw. 15,9 µmol $l^{-1}$ n der Referenztiefe anstieg, und nur im Jahr 2020 durch etwas niedrigere Jahresmittelwerte unterbrochen wurde. Im Bornholmtief bewegte sich die Ammoniumkonzentration bei hoher interannueller Variabilität auf niedrigerem Niveau von 2,2 ±1,4 µmol $l^{-1}$.

POC und PON Konzentrationen waren im Jahr 2022 im Oberflächenwasser hauptsächlich in den Monaten März, Juli, und teilweise im Mai aufgrund von Primärproduktion während der Frühjahrs- und Sommerblüten erhöht. Oberflächen- und Tiefenwasser POC, PON, sowie C/N Verhältnis unterschieden sich nicht signifikant vom Langzeitmittel.

In diesem Bericht sind die während des Ostsee-Umweltmonitorings im Februar 2022 ermittelten Oberflächenwasserkonzentrationen für chlorierte Kohlenwasserstoffe (CHC) und Oberflächensedimentgehalte für CHC, polyzyklische aromatische Kohlenwasserstoffe (PAH, U.S. EPA PAH) sowie für Organozinnsubstanzen (OT) zusammengefasst. Die Bestimmung der PAH in den Seewasserproben war aus technischen Gründen nicht möglich. Erstmals erfolgte die Bestimmung des Pestizids Heptachlor und des Metaboliten Heptachlorepoxid (HEPEP) in den Seewasserproben.

In den Oberflächenwasserproben wurden für DDT und Metabolite ($\Sigma DDT_{sum}$) Konzentrationen von 2,7 pg $l^{-1}$ - 9,1 pg $l^{-1}$ ermittelt; die höchste Konzentration von 9,1 pg $l^{-1}$ für den Bereich Pommersche Bucht. Die Konzentrationen des langlebigen Abbauproduktes p,p‘-DDE waren höher im Vergleich zu p,p‘-DDT, was darauf deutet, dass aktuell keine wesentlichen neuen DDT-Einträge erfolgten. Für $PCB_{ICES}$ und HCB wurden Konzentrationen von 1,6 pg $l^{-1}$ – 13,1 pg $l^{-1}$ für $\Sigma PCB_{ICES,SUM}$ bzw. 4,8 pg $l^{-1}$ – 9,9 pg $l^{-1}$ für $HCB_{SUM}$ ermittelt. Die höchsten PCB-Konzentrationen wurden im Bereich Kieler Bucht/Fehmarn Belt und für HCB in der Pommersche Bucht ermittelt, d.h. 13,1 pg $l^{-1}$ $\Sigma PCB_{ICES,SUM}$ und 9,9 pg $l^{-1}$ $HCB_{SUM}$. HEPEP wurde in allen Oberflächenwasserproben mit Konzentrationen von 0,28 pg $l^{-1}$ –0,83 pg $l^{-1}$ $HEPEP_{SUM}$ nachgewiesen. Heptachlor wurde dagegen in keiner der Transektproben gefunden.

In den Oberflächensedimentproben wurden für DDT und Metabolite (ΣDDT) Gehalte von 29,3 ng $g^{-1}$ - 168,7 ng $g^{-1}$ TOC ermittelt; der höchste Gehalt von 168,7 ng $g^{-1}$ TOC für die Pommersche Bucht. Für $PCB_{ICES}$ und HCB wurden Konzentrationen von 63,7 ng $g^{-1}$ –166,0 ng $g^{-1}$ TOC für $\Sigma PCB_{ICES}$ bzw. 0,34 ng $g^{-1}$ – 44,0 ng $g^{-1}$ TOC für HCB ermittelt. Die jeweils höchsten Gehalte wurden für die Station in der Pommerschen Bucht ermittelt, d.h. 166,0 ng $g^{-1}$ TOC $\Sigma PCB_{ICES}$ und 44,0 ng $g^{-1}$ TOC HCB. Für PAH wurden Gehalte von 16951,8 ng $g^{-1}$ - 40000,0 ng $g^{-1}$ TOC ΣPAH ermittelt; der höchste Gehalt von 40000,0 ng $g^{-1}$ TOC an der Station in der Pommerschen Bucht. Es wurden Organozinngehalte von bis zu 278,7 ng $g^{-1}$ TOC ΣOT (MBT, DBT, TBT, TPhT) detektiert. Dabei wurde an keiner der untersuchten Stationen TPhT nachgewiesen. An der Station in der Pommerschen Bucht wurde keine der Organozinnverbindungen detektiert.

Die Bewertung der ermittelten Daten erfolgte auf Grundlage der Umweltqualitätsnormen (UQN) der Wasserrahmenrichtlinie und HELCOM-Indikatoren. Alle in den Oberflächenwasserproben ermittelten Konzentrationen für HEPEP überschreiten die Jahresdurchschnitts-UQN von 0,01 pg $l^{-1}$. Die nachgewiesenen Gehalte für TBT in den Oberflächensedimentproben überschreiten den *threshold value* des HELCOM Indikators *TBT and imposex* von 1,6 µg $kg^{-1}$ TS,

5 % TOC. Der für die Pommersche Bucht ermittelte Anthracen-Gehalt (0,3 ng $g^{-1}$ TS ≙ 50 µg $kg^{-1}$, 5 %TOC) überschreitet den *threshold value* des HELCOM Indikators *Polycyclic aromatic Hydrocarbons and their Metabolites* von 24 µg $kg^{-1}$ TS, 5 %TOC.

## Abstract /Summary

The article summarizes the hydrographic-hydrochemical conditions in the western and central Baltic Sea in 2022. Based on the meteorological conditions, the horizontal and vertical distribution of temperature, salinity, oxygen/hydrogen sulphide and nutrients are described on a seasonal scale.

The winter season 2021/22 shows a "cold sum" of 15.9 Kd recorded at station Warnemünde, which is ranked on 6$^{th}$ place of warm winters in comparative data from 1948 to date. The summer "heat sum" of 281.4 Kd is far above the long-term average of 161.4 Kd and only slightly below the previous year 2021 (284.7 Kd). In the course of 2022, the Baltic Sea experienced again no strong inflow activity. Only two smaller inflow pulses occurred with total volumes of 140 km$^3$ and 158 km$^3$ all over the year which ventilated the Arkona Basin. During December occured a stepwise sealevel rise of three small pulses which led to an total inflow volume of 141 km$^3$ and salt mass import of 1.15 Gt.

The overall decreasing trend of the oxygen concentration, in fact, the increase of hydrogen sulphide in deep waters of Baltic Sea deeps was basically ongoing in 2022. Recently, it became obvious that also shallow areas of the Baltic Sea are more often subjected to saisonal low oxygen values. The degradation of large amounts of organic matter that is produced because of ongoing eutrophication, causes a high oxygen demand impacting especially the seafloor. However, in February an oxygenated bottom layer in the western and central part of the Arkona Basin with a concentration of 310-335 µmol l$^{-1}$ oxygen was formed that only temporarily and locally improved the conditions. The oxygenated water passed the Bornholmsgatt and was mixed with Bornholm Sea deep water. The newly formed water mass contained 130-270 µmol l$^{-1}$ oxygen. It was further transported eastward and reached the southern part of the Eastern Gotland Basin in spring and summer 2022 with oxygen concentration of about 45 µmol l$^{-1}$ at a depth of 100 m.

The selected stations in the regions west of Darss Sill (Fehmarn Belt, Lübeck and Mecklenburg Bights) showed relatively high winter nitrate concentrations in surface water in comparison to recent years, which might hint to an influence of North Sea water. Whereas the stations in the Baltic Proper were characterized by low nitrate values in February, perhaps originating from an increasing oxygen debt and nitrate consumption in the deep water body. The relatively low winter nitrate concentration of 3.4 µmol l$^{-1}$ in Gotland Deep surface water and 2.9 µmol l$^{-1}$ at Bornholm Deep station, caused an early exhaustion of nitrate already at low temperatures. This likely enabled availability of phosphate almost throughout the summer half-year in 2022. Only in early August, the value was below the detection limit. The annual mean phosphate concentration in the Bornholm Sea deep water depicted a considerable interannual variability since 2018 on a high level of 4.2 ±0.9 µmol l$^{-1}$ at the reference depth. Whereas, the Landsort and Karlsö Deeps with 3.7 ±0.4 µmol l$^{-1}$ and 3.8 ±0.3 µmol l$^{-1}$, repectively, in the selected reference depths were more stable. The Gotland Deep showed the strongest accumulation of phosphate to 6.1 µmol l$^{-1}$ and ammonium of even 27.9 µmol l$^{-1}$ in 2022. Thereby, the phosphate and ammonium concentrations increased in the Fårö Deep to 4.7 µmol l$^{-1}$ and 15.9 µmol l$^{-1}$, respectively, in the reference depth. This increase was interrupted only in 2020 by slightly lower annual averages. In the Bornholm Deep, the ammonium concentration scattered around relativ low values of 2.2 ±1.4 µmol l$^{-1}$ in 2022 at high interannual variability.

In 2022, POC and PON concentrations were elevated in the surface water of the Baltic Sea in March, July, and partially May, induced by primary production during spring and summer blooms. Surface and deep POC and PON or particulate C/N ratios were not significantly different from long term means.

This report summarizes surface water concentrations for chlorinated hydrocarbons (CHC) and surface sediment contents for CHC, polycyclic aromatic hydrocarbons (PAH, U.S. EPA PAH) as well as organotin substances (OT) which were determined during the Baltic Sea monitoring in February 2022. Due to the occurrence of technical problems PAH data for surface water samples cannot be reported. Since 2022 the determination of the pesticide heptachlor and its metabolite heptachlorepoxide (HEPEP) is included in the assessment.

Concentrations of 2.7-9.1 pg $l^{-1}$ were determined for DDT and metabolites (ΣDDTsum); highest concentration of 9.1 pg $l^{-1}$ for the area Pomeranian Bight. Concentrations of the long-lived degradation product p,p'-DDE were higher compared to p,p'-DDT, indicating no significant new DDT inputs. For $\Sigma PCB_{ICES,SUM}$ and $HCB_{SUM}$, concentrations of 1.6-13.1 pg $l^{-1}$ and 4.8-9.9 pg $l^{-1}$ were determined. Highest PCB concentrations were detected in the Kiel Bight/Fehmarn Belt area and for HCB in the Pomeranian Bight, i.e., 13.1 pg $l^{-1}$ $\Sigma PCB_{ICES,SUM}$ and 9.9 pg $l^{-1}$ $HCB_{SUM}$. HEPEP was detected in all seawater samples with concentrations ranging from 0.28-0.83 pg $l^{-1}$ $HEPEP_{SUM}$. Heptachlor was not detected in any of the transect samples.

In the surface sediment samples 29.3 ng $g^{-1}$ - 168.7 ng $g^{-1}$ TOC were determined for DDT and metabolites (ΣDDT); the highest content of 168.7 ng $g^{-1}$ TOC for the Pomeranian Bight. For $\Sigma PCB_{ICES}$ and HCB, contents ranging from 63.7 ng $g^{-1}$ - 166.0 ng $g^{-1}$ TOC and 0.34 ng $g^{-1}$ - 44.0 ng $g^{-1}$ TOC were determined, highest contents for the site in the Pomeranian Bight, i.e. 166.0 ng $g^{-1}$ TOC $\Sigma PCB_{ICES}$ and 44.0 ng $g^{-1}$ TOC HCB. PAH contents ranged from 16951.8 ng $g^{-1}$ - 40000.0 ng $g^{-1}$ TOC ΣPAH; the highest content was obtained for the station in Pomeranian Bight with 40000.0 ng/g TOC. Organotin contents of up to 278.7 ng $g^{-1}$ TOC ΣOT (MBT, DBT, TBT, TPhT) were detected. TPhT was not detected at any of the sites and none of the organotin compounds was detected at the station in the Pomeranian Bight.

The assessment of the obtained data was based on the environmental quality standards (EQS) of the Water Framework Directive and HELCOM indicators. All surface seawater concentrations for HEPEP exceed the annual average EQS of 0.01 pg $l^{-1}$. The detected surface sediment TBT contents exceed the threshold value of 1.6 µg $kg^{-1}$ DW, 5 % TOC of the HELCOM indicator "TBT and imposex". The anthracene content of 0.3 ng $g^{-1}$ DW (≙ 50 µg $kg^{-1}$ DW, 5 % TOC) determined for the Pomeranian Bight exceeds the threshold value of the HELCOM indicator "Polycyclic aromatic Hydrocarbons and their Metabolites" of 24 µg $kg^{-1}$ DW, 5 % TOC.

# 1 Introduction

This assessment of hydrographic and hydrochemical conditions in the Baltic Sea in 2022 has partially been produced on the basis of the Baltic Sea Monitoring Programme that the Leibniz Institute for Baltic Sea Research Warnemünde (IOW) undertakes on behalf of the Federal Maritime and Hydrographic Agency, Hamburg and Rostock (BSH). Within the scope of an administrative agreement, the German contribution to the Helsinki Commission's (HELCOM) monitoring programme (COMBINE) for the protection of the marine environment of the Baltic Sea has been devolved to IOW. It basically covers Germany's Exclusive Economic Zone. Beyond these borders, the IOW is running an observation programme on its own account in order to obtain and maintain long-term data series and to enable analyses of the conditions in the Baltic Sea's central basins, which play a decisive role in the overall health of the sea.

The combination of both programmes leads to a yearly description of the water exchange between the North Sea and the Baltic Sea, the hydrographic and hydrochemical conditions in the study area, their temporal and spatial variations, as well as the investigation and identification of long-term trends.

Five routine monitoring cruises are undertaken each year covering all four seasons. The data obtained during these cruises, as well as results from other research activities by IOW, form the basis of this assessment. Selected data from other research institutions, especially the Swedish Meteorological and Hydrological Institute (SMHI) and the Maritime Office of the Polish Institute of Meteorology and Water Management (IMGW), are also included in the assessment.

HELCOM guidelines for monitoring in the Baltic Sea form the basis of the routine hydrographical and hydrochemical monitoring programme within its COMBINE Programme (HELCOM 2017). The five monitoring cruises in February, March, May, August and November were performed by RV Elisabeth Mann Borgese. Details about water sampling, investigated parameters, sampling techniques and their accuracy are given in NEHRING et al. (1993, 1995).

Ship-based investigations were supplemented by measurements at three autonomous stations within the German MARNET environmental monitoring network, the ARKONA BASIN (AB), the DARSS SILL (DS) station and the ODER BANK (OB) station. At the Darss Sill the autonoumous measuring pile was removed for a usual 10-years general overhaul. A mooring was deployed as replacement. At December 12$^{th}$ the measuring pile was deployed again after its maintenance period, but fully technical equipped during February 2023. The Oder Bank buoy was in operation from mid-April to the end of December 2022. The buoy was not taken out of service like usual in wintertime. In 2022 again a second system of a new buoy construction more resistant against damages caused by ice was operated in parallel at the Oder Bank position, to have a longer test period for data evaluation and technical approval.

Besides meteorological parameters at these stations, water temperature and salinity as well as oxygen concentrations were measured at different depths:

| | | | |
|---|---|---|---|
| AB: | 8 horizons T + S | + | 2 horizons $O_2$ |
| DS: | 6 horizons T + S | + | 2 horizons $O_2$ |
| OB: | 2 horizons T + S | + | 2 horizons $O_2$ |

All data measured at the MARNET stations are transmitted via METEOSAT to the BSH database as hourly means of six measurements (KRÜGER et al. 1998, KRÜGER 2000). An acoustic doppler current profiler (ADCP) records current speeds and directions at AB and DS. The ADCP are moored on the seabed in some two hundred metres distance from the main stations and protected by a trawl-resistant bottom mount mooring. ADCP data are transmitted to the main station in real time via an hourly acoustic data link, for storage and satellite transmission. In perallel the data are stored in the ADCPs for quality assurance and service purposes. These data are retreaved during maintenance measures at the station once or twice a year.

Oxygen deficiency is one of the major factors influencing the Baltic Sea ecosystem. As a general overview of the state of the Baltic Sea Fig. 1 shows the recent hypoxic to euxinic conditions. The conditions in winter-spring and summer that are shown, visualising the development during the year 2022. A large extend of bottom water in the deep basins is influenced by hypoxia (black dotted areas). The situation is more or less stagnant comparing the winter to spring situation (March) with summer measurements in August at the Eastern, Northern and Western Gotland Basin, but the situation worsened at the Bornholm basin with a spreading of hydrogen sulphide in summertime (Fig. 1b).

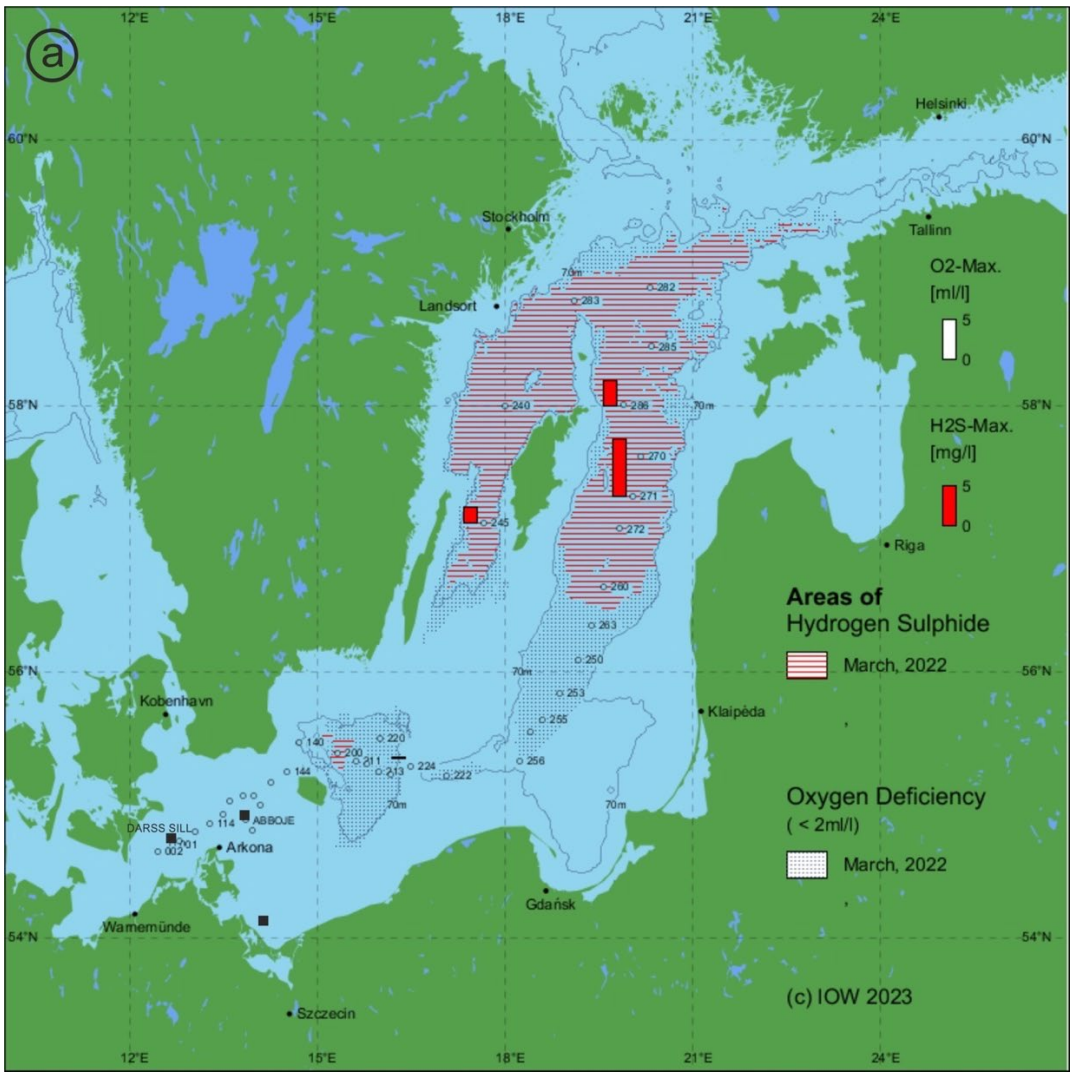

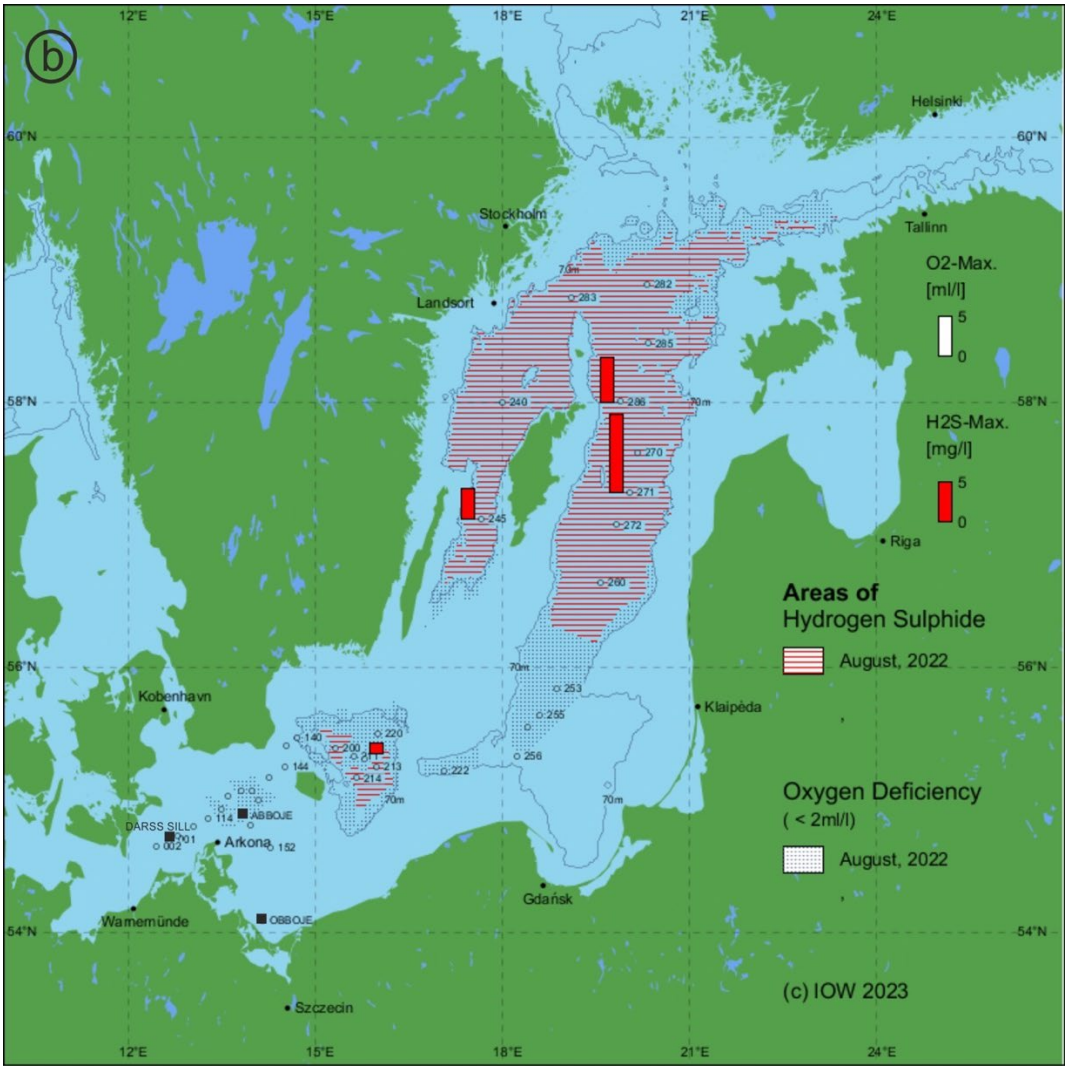


*Fig. 1: Areas of oxygen deficiency and hydrogen sulphide in the near bottom layer of the Baltic Sea. Bars show the maximum oxygen and hydrogen sulphide concentration. The location of measurements is indicated by circles (CTD casts) and bold squares (MARNET- stations). The figure additionally contains the 70 m -depth line. a) The situation in March 2022. b) The situation in August 2022.*

# 2 General meteorological conditions

The following description of weather conditions in the southern Baltic Sea area is based on an evaluation of data from the Germany's National Meteorological Service (DWD), the Federal Maritime and Hydrographic Agency (BSH), the Swedish Meteorological and Hydrological Institute (SMHI), the Institute of Meteorology and Water Management (IMGW), Freie Universität Berlin (FU) as well as IOW itself. Table 1 gives a general outline of the year's weather with monthly mean temperature, sunshine duration, precipitation as well as the number of days of frost and ice at Arkona weather station. Solar irradiance at Gdynia weather station is given in addition. The warm and cold sums at Warnemünde and Arkona weather stations are listed in Table 2 and Table 3.

According to the analysis of DWD (DWD 2023), 2022 was recorded as warm like the year 2018, in the mid range of precipitation and set a new record of sunshine duration. With 10.5 °C, Germany's annual mean temperature was on the same record high level like in 2018 and both years are the warmest ones since 1881. It was 2.3 K warmer than those of the international reference period 1961-1990 and 1.2 K warmer compared to the actual national reference period 1991-2020. It was the twelfth year in a row of a too warm mean temperature. In Germany a warming trend of 0.012 K $a^{-1}$1 occurred since the year 1881, a total warming of 1.7 K. All months showed warmer temperatures compared to the mean of the reference period 1961-1990. Several heat waves during June and July led to new temperature records across Europe. Germany's annual temperature maximum of 40.1 °C was recorded on July 20th at Station Hamburg-Neuwiedenthal (DWD 2023).

Focussing at the Baltic Sea, the meteorological data reflect the same situation (station Arkona, cf. Table 1). Most monthly mean temperature values were above average, but April, September and December were 0.4 to 0.7 K below average 1991-2020. At the southern Baltic Sea coast the warm sum of 281.4 Kd (station Warnemünde, cf. Table 2) was only slightly below the previous year (284.7 Kd), which is far above the long-term mean of 161.4 Kd. The warm sum of 2022 is on 8th place of warmest summers (1948-2021) and the considered months showed temperature anomalies as follows: April -1.1 K, May +0.9 K, June +1.2 K, July +0.2 K, August +1.7 K, September -0.5 K, October +2.8 K (warm sums cf. Table 2). The warm sum of August (127.4 Kd) is more than twice as high as the long-term monthly mean of 56.1 Kd and is fourth placed in this time series. August 1997 is the actual "number one" with 173 Kd. The warm sum of June 2022 is as well in "top 10" on 5th place in the long-term data.

The mean amount of precipitation in Germany in 2022 was 670 l $m^{-2}$, 15 % less than the long-term mean value (791 l $m^{-2}$ - reference period 1991-2020 and former reference period 1961-1990 of 789 l $m^{-2}$). During summer precipitation was 40 % less compared to the reference period 1961-1990 and led the lowest subsoil moisture since 1961. In contrast, February and September were much too wet. The highest daily rainfall of 112.1 l $m^{-2}$ was registered on August 19th in Babenhausen (Bavaria, southern Germany). In the Alps an amount of 1,500-2,000 l $m^{-2}$ were fallen during 2022 and in the Northeast in some regions precipitation was below 500 l $m^{-2}$. In the coastal states along Germany's Baltic Sea coast precipitation ranged from 732 l $m^{-2}$ (avg. 788 l $m^{2}$) in Schleswig-Holstein to 481 l $m^{-2}$ (avg. 595 l $m^{-2}$) in Mecklenburg-Vorpommern.

In Germany, the average annual sum of 2025 sunshine hours set a new record. The value was 30 % above the average of 1544 hours (international reference period 1961-1990) and 20 %

above the national reference period 1991-2020. The former record-breaking value was observed in the year 2018 with 2020 hours of sunshine. At the coast the sunshine duration was as well far above the average. Schleswig-Holstein registered 1910 hours in 2022 (long-term mean: 1567 hours) and Mecklenburg-Vorpommern recorded 2015 hours (long-term mean: 1648 hours).

At Gdynia station (Gdansk Bight), an annual sum of 403 155 J $cm^{-2}$ of solar irradiance was recorded. Within a data series covering 67 years back in time (first compiled by FEISTEL et al. 2008, continued to date), this value takes the 7th rank of these long-term data series 1956-2022. It is much lower than the long-term maximum in 1959 with 457 751 J $cm^{-2}$, but well above the mean value of 375 742 J $cm^{-2}$. The sunniest month in 2022 was like in 2021 June (Table 1). With 62 771 J $cm^{-2}$, it takes the 29th place in the midrange of long-term comparison of monthly mean values and is far below the peak value of 80 389 J $cm^{-2}$ in July 1994, which represents the absolute maximum of the entire series since 1956. March set a new record with 36 370 J $cm^{-2}$ and February (10th), April (6th) and August (9th) had values in the "Top 10" of the data series. All other months showed solar irradiance monthly mean values compared to those of the last 67 years as follows: January rank 39; Mai rank 38; July rank 31; September rank 24; October rank 12; November rank 49 and December rank 44.

*Table 1: Monthly averaged weather data at Arkona station (Rügen Island, 42 m MSL) from DWD (2023). t: air temperature, Δt: air temperature anomaly 1991-2020, s: sunshine duration, r: precipitation, Frost: days with minimum temperature below 0 °C, Ice: days with maximum temperature below 0 °C. Solar: solar irradiance in J $cm^{-2}$ at Gdynia station, 54°31' N, 18°33' O, 22 m MSL from IMGW (2023). Percentages are given with respect to the long-term mean (period 1991-2020). Maxima and minima of the year 2022 are shown in bold. Due to a lack of data from October 10th to 18th no monthly values are available for this station.*

| Month | *t*/°C | Δ*t*/K | *s*/% | *r*/% | Frost/d | Ice/d | Solar/J $cm^{-2}$ |
|---|---|---|---|---|---|---|---|
| November 2021 | 7.2 | 1.3 | 49 | 117 | - | - | 6052 |
| December 2021 | 2.2 | -0.6 | 89 | 124 | 14 | 1 | 4389 |
| January | 3.3 | 1.8 | 127 | 105 | 6 | **-** | 5440 |
| February | 4.1 | **2.5** | **135** | **272** | 1 | - | 13519 |
| March | 4.1 | 0.8 | 171 | 3 | 1 | - | 36370 |
| April | 6.2 | -0.4 | 126 | 125 | 2 | - | 49127 |
| May | 11.9 | 1.1 | 109 | 145 | - | - | 57289 |
| June | 15.8 | 1.2 | 107 | 39 | - | - | **62771** |
| July | 17.4 | 0.0 | 106 | 84 | - | - | 59594 |
| August | **19.8** | 2.0 | 115 | 44 | - | - | 55312 |
| September | 14.3 | -0.4 | 108 | 96 | - | - | 33207 |
| October | - | - | - | - | - | - | 20339 |
| November | 7.4 | 1.4 | 83 | 35 | 3 | - | 6132 |
| December | 2.1 | -0.7 | 122 | 124 | **11** | **4** | 4055 |

*Table 2: Sums of daily mean air temperatures at the weather station Warnemünde (data: DWD 2023b. The 'cold sum' (CS) is the time integral of air temperatures below the line t = 0 °C, in Kd, the 'heat sum' (HS) is the corresponding integral above the line t = 16 °C. For comparison, the corresponding mean values 1948–2021 are given.*

| Month | CS 2021/22 | Mean | Month | HS 2022 | Mean |
|---|---|---|---|---|---|
| November | 0 | 2.3 ± 5.9 | April | 0 | 0.9 ± 2.3 |
| December | 15.9 | 19.9 ± 27.3 | May | 10.9 | 6.0 ± 7.4 |
| January | 0 | 37.0 ± 38.9 | June | 53.1 | 25.9 ± 18.5 |
| February | 0 | 29.7 ± 36.9 | July | 79.8 | 59.4 ± 36.9 |
| March | 0 | 8.1 ± 12.0 | August | 127.4 | 56.1 ± 33.8 |
| April | 0 | 0 ± 0.2 | September | 10.2 | 12.6 ± 13.2 |
| | | | October | 0 | 0.5 ± 1.5 |
| **Σ 2021/2022** | **15.9** | 97.0 ± 84.3 | **Σ 2022** | **281.4** | 161.4 ± 75.9 |

*Table 3: Sums of daily mean air temperatures at the weather station Arkona (data: DWD 2023b). The 'cold sum' (CS) is the time integral of air temperatures below the line t = 0 °C, in Kd, the 'heat sum' (HS) is the corresponding integral above the line t = 16 °C.*

| Month | CS 2021/22 | Month | HS 2022 |
|---|---|---|---|
| November | 0 | April | 0 |
| December | 9.1 | May | 3.7 |
| January | 2.1 | June | 28.4 |
| February | 0 | July | 50 |
| March | 0 | August | 116.6 |
| April | 0 | September | 4 |
| | | October | 0 |
| **Σ 2021/2022** | **11.2** | **Σ 2022** | **202.7** |

## 2.1 Ice winter 2021/22

For the southern Baltic Sea area, the Warnemünde station shows a cold sum of 15.9 Kd (Table 2) referring to the air temperature of the winter 2021/2022. After the record winter 2019/2020 (cold sum of 0 Kd) the recent winter season is ranked on 6$^{th}$ place of warm winters in comparative data from 1948 to date. It continues the series of warm winters during the latest years showing low cold sums: 2020/2021 (32.7 Kd), 2019-2020 (0 Kd), 2018/2019 (18.3 Kd), 2017/18 (67.7 Kd) and 2016/17 (31.7 Kd). Since the year 2012 all values plot below the long-term average of 97 Kd. In comparison, the cold sum at Arkona station is in the same magnitude of 11.2 Kd (Table 3) and represents as well a warm winter. Recent winter seasons show at Arkona slightly lower values than in Warnemünde (station Arkona: 2020/21 with 30.2 Kd, 2019/20 with 0 Kd, 2018/2019 with 14.6 Kd, 2017/18 with 53.8 Kd and 2016/17 with 27.2 Kd). Given the exposed location of the Arkona station at a headland surrounded by water masses at the northernmost coast of Rügen Island, the local air temperature development is under an even stronger influence by the water temperature of the Baltic Sea than at Warnemünde. Thus, winter values at Arkona are frequently higher, while summer values are lower.

The winter season recorded 24 days of frost and 1 ice days (daily max below 0 °C) in the time span December 2021 to April 2022 (Table 1). A longer cold spell occurred around Christmas 2021 from December 21st to 28th with 8 days of frost and 1 ice day. At station Arkona a cold sum of 11.2 Kd was registered. December and January reached cold sums of 9.1 Kd and 2.1 Kd in the north of Rügen Island (Table 3). All other winter months showed cold sums of 0 Kd.

The local ice conditions at the German Baltic Sea coast were generally classified as weak (ALDENHOFF 2022). Icing occurred only in small areas in sheltered lagoons for a short period in the end of December. All offshore areas stayed free of ice during this winter season (Fig. 3). Another measure for the strength of an ice winter is the accumulated areal ice volume (KOSLOWSKI 1989, BSH 2009). The season 2021/22 showed a low accumulated areal ice volume of 0.026 m (ALDENHOFF 2022), like typical for the last two decades. Winter season 2009/2010 was the only exception with a high value of 4.22 m. In contrast, the highest values recorded in this data series are as follows: 26.83 m in 1942; 26.71 m in 1940; 25.26 m in 1947; and 23.07 m in 1963. In all other winters, values were well below 20 m (KOSLOWSKI 1989).

For the whole Baltic Sea a maximum ice coverage of 93,000 km² was observed at February 3rd (Fig. 3). This maximum extent of ice corresponds to some 22 % of the Baltic Sea's total area (415 266 km²), and was largely centred in the Bothnian Bay, eastern Gulf of Finland and northern Gulf of Riga. The observed maximum ice extent is classified as mild in the time series of 303 years (Fig. 2). First icing occurred at the end of October in the Bothnian Bay and last ice melted at the beginning of June, which was a longer period than average. Other regions showed much shorter icing periods than average (ALDENHOFF 2022).

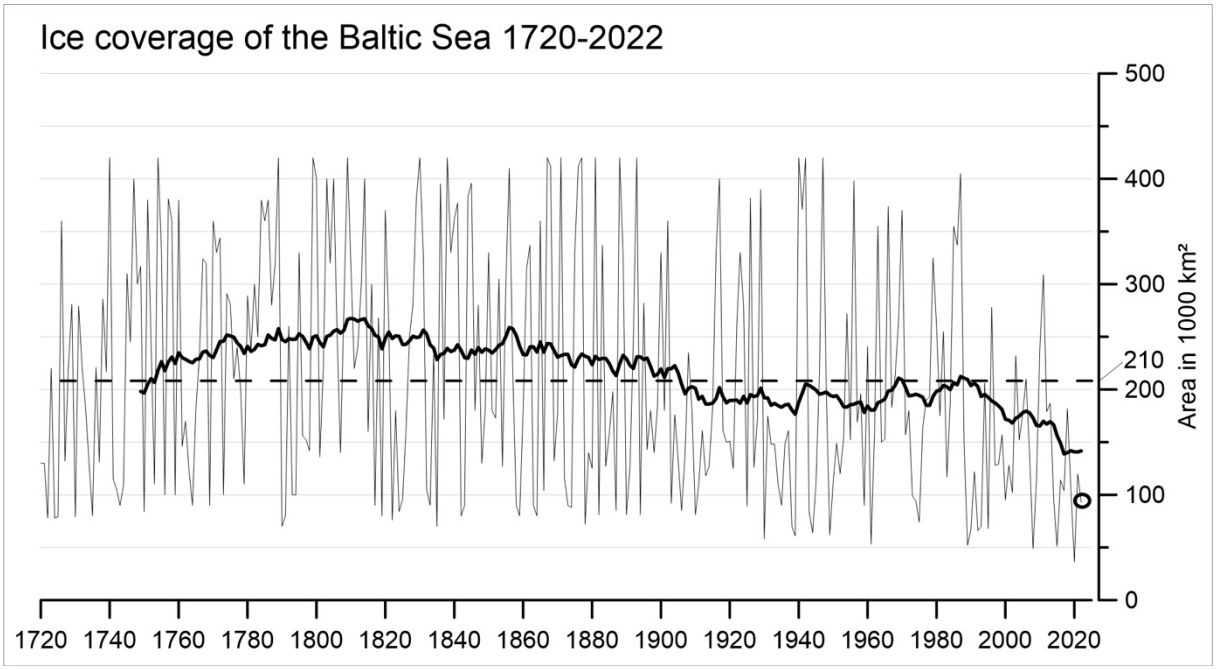


*Fig. 2: Maximum ice covered area in 1 000 km² of the Baltic Sea in the years 1720 to 2022 (from data of SCHMELZER et al. 2008, ALDENHOFF 2022). The long-term average of 210 000 km² is shown as dashed line. The bold line is a running mean value over the past 30 years. The ice coverage in the winter 2021/2022 with 93 000 km² is encircled.*

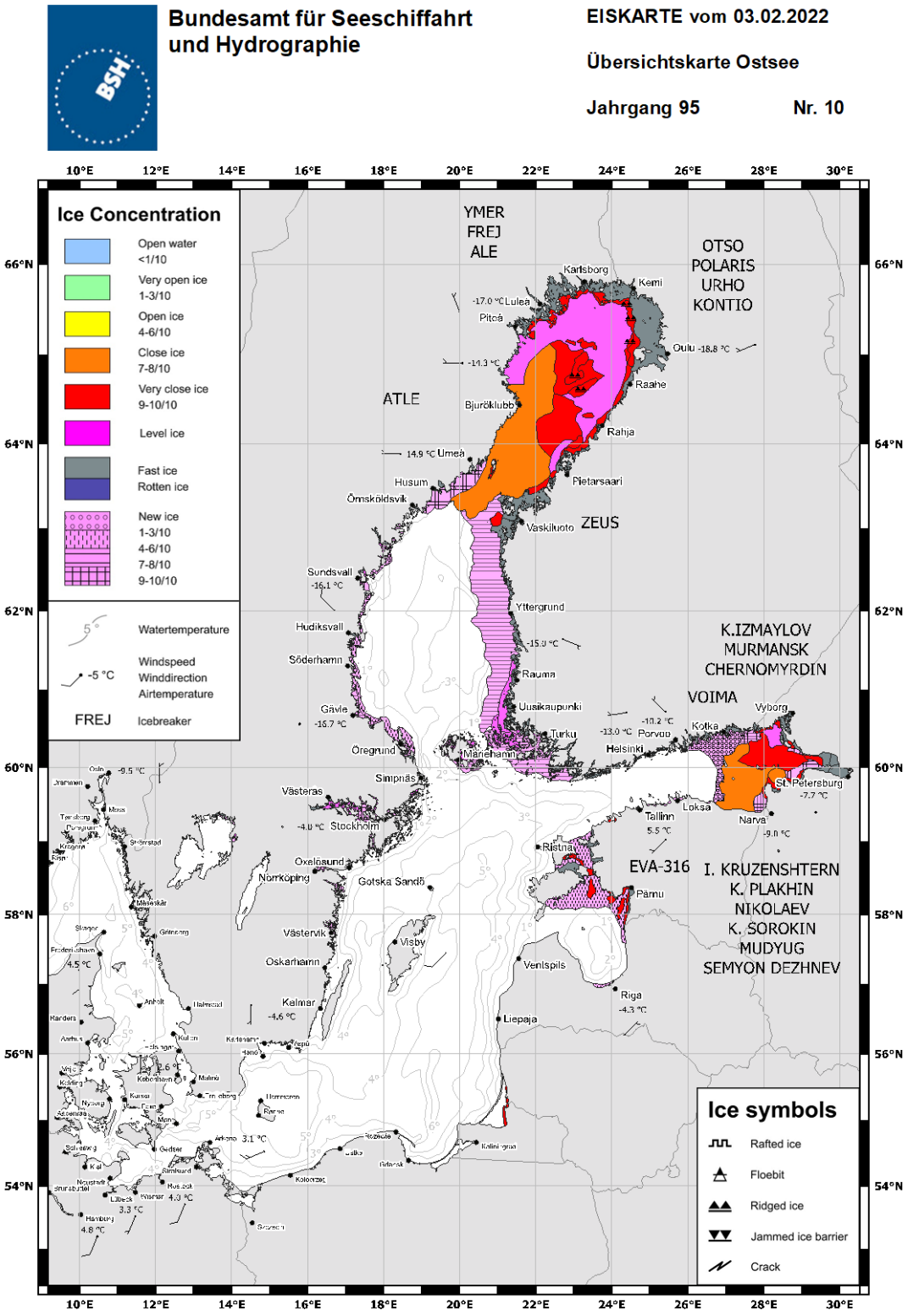


*Fig. 3: Maximum ice coverage in the winter 2021/2022 on February 3rd – ice concentration in colour code and ice type in symbols (ALDENHOFF 2022).*

## 2.2 Wind conditions

The year 2022 was again a light windy one and westerly to south-westerly wind directions dominated the situation, comparable to the climatic mean for this region.

Fig. 4 to Fig. 5 and Fig. 6b illustrate the wind conditions at Arkona throughout 2022. The year 2022 of intensified westerly to southwesterly winds (Fig. 5) match with the trend towards prevailing south-west winds that began in 1981 (HAGEN & FEISTEL 2008) and continues today. Comparing the east component of the wind (positive for westerly winds, i.e. wind directed eastward) with an average of 2.8 m/s (Fig. 4b) with the climatic mean of 1.9 m/s (reference period 1991-2020), westerly winds were in 2022 much more dominant than the mean.

According to the wind-rose diagram (Fig. 5), north-western to south-western directed winds account for about 60 % of the annual sum, which is a bit lower compared to 2021 (67 %) and comparable to 2020 (61 %). These directions can potentially lead to inflow conditions of saltwater from the North Sea. Easterly to north-easterly winds account for another 20 % in 2022 (18 % in 2021, 24 % in 2020) and can induce outflow conditions. The annual mean wind speed of 6.74 m/s (Fig. 4a) is below the average and root mean square of 7.37 +/- 0.44 m/s of the 49 years long time-series at staion Arkona (1973-2020) and the reference period 1991-2020 with a mean of 7.34 m/s . The maximum wind speed in that period was reached with 8.41 m/s in 1990 and the minimum value occurred in 2018 – the warmest year on record – with 6.5 m/s (based on DWD data, 2023b). Since the year 2009 all following years showed an annual mean value below the long-term mean 7.37 m/s. Seven high-wind days of over 15 m/s daily mean are registered during 2022 all from western directions: February 19th (17.6 m/s, W), February 21st (17.4 m/s, SW-W), January 27th (16.4 m/s, WSW), February 17th (16.1 m/s, WSW-W), January 29th (16 m/s, SW), April 4th and 8th (15.7m/s, SW-W / 15.1 m/s, W). In addition to the daily means, a view at high values of hourly means and maximum gusts enables to detect short, but intensive wind events of violent character. Some storms are regionally restricted to some hours only with no significant impact on the daily mean value. However, they can lead to major damages. Like in the previous year 2021 as well in 2022 the maximum daily mean, hourly mean and gust were registered all at the same day. At February 19th the maximum daily mean (17.6 m/s), maximum hourly mean (26.3 m/s) and the maximum gust of the year (37.2 m/s, 12 Bft) was registered at station Arkona. The daily mean value is relativly low compared to hourly mean and maximum gust, which means it was only a short storm phase of several hours. This 2022 hourly maximum value of 26.3 m/s is comparable to previous peak values, for example an hourly mean of 30 m/s in 2000, 26.6 m/s in 2005; and 25.9 m/s in December 2013.

At the western Baltic Sea three storm surges of slight category (January 17th, January 20th-21st) and average category (January 28th-31st) occurred during 2022. For these events the highest water levels are registered as follows:

- January 17th with maximum levels of +90 cm MSL Warnemünde and Travemünde to +105 cm MSL at Flensburg (HOLFORT 2022a)
- January 20th-21st with maximum levels of +123 cm MSL Koserow /Usedom island, +124 cm MSL Warnemünde, +122 cm MSL Travemünde, +115 cm MSL Flensburg (HOLFORT 2022b)

– January 28th-31st with maximum levels of +103 cm MSL Greifswald, +119 cm MSL Warnemünde, +124 cm MSL Travemünde, +149 cm MSL Flensburg (WEIDIG 2022)

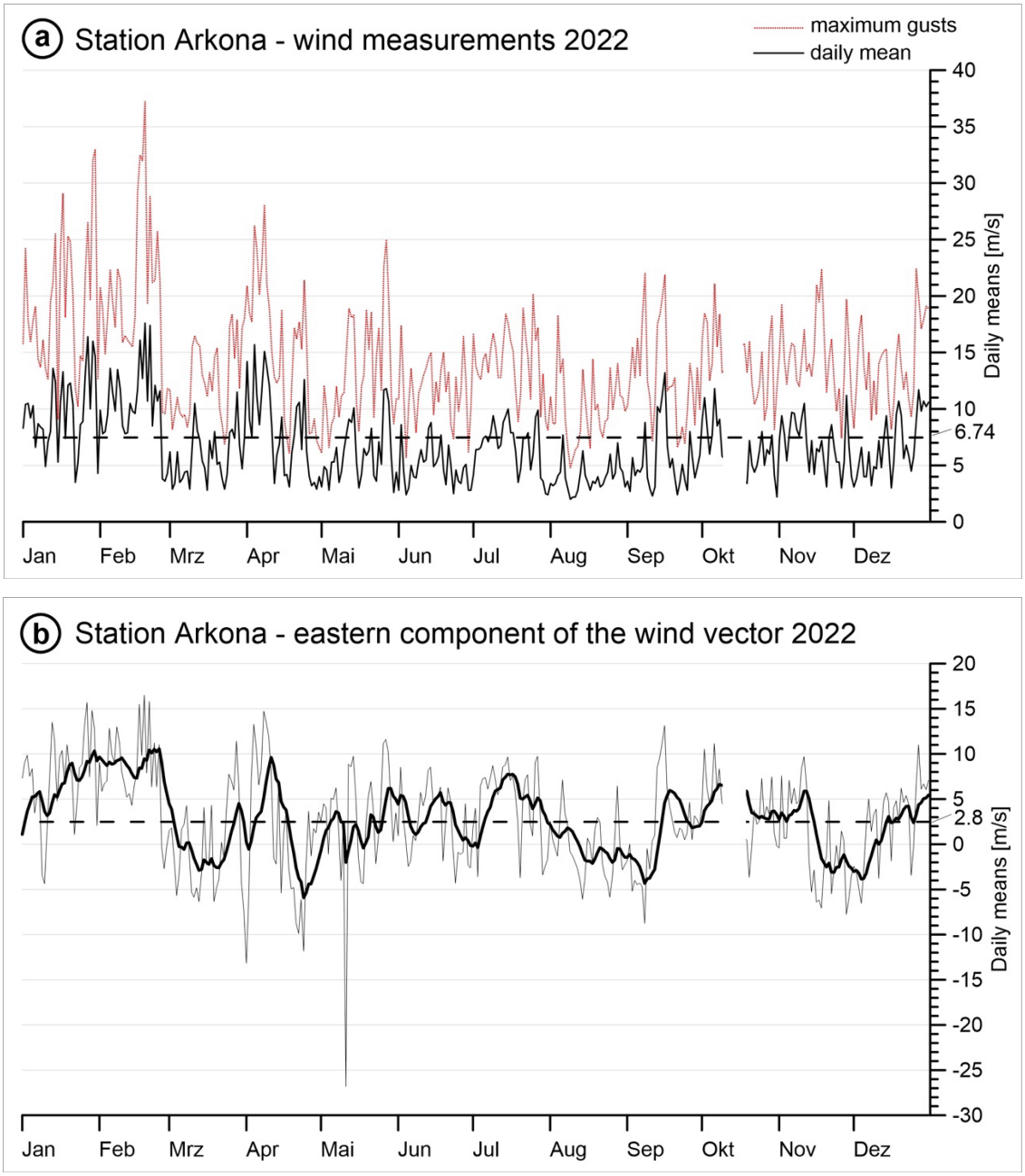


*Fig. 4: Wind measurements at the weather station Arkona (from data of DWD, 2023a). a) Daily means and maximum gusts of wind speed, in m/s, the dashed black line depicts the annual average of 6.74 m/s. b) Daily means of the eastern component (for westerly wind positive), the dashed line depicts the annual average of 2.8 m/s. The line in bold is filtered with a 10-days exponential memory. Due to a lack of data from October 10th to 18th no values are available in that time for this station.*

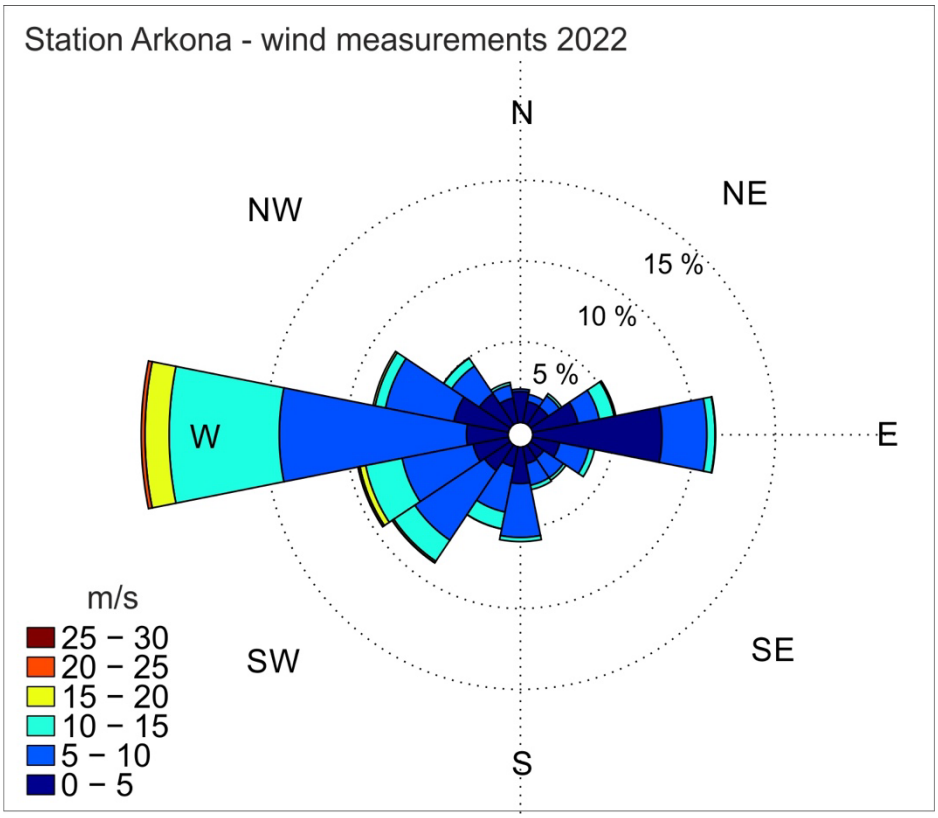


*Fig. 5: Wind measurements at the weather station Arkona (from data of DWD 2023a) as windrose plot. Distribution of wind direction and strength based on hourly means of the year 2022.*

# 3 Water exchange through the straits

## 3.1 Water level at Landsort

The Swedish tide gauge station at Landsort Norra, south of Stockholm, provides a good description of the mean water level in the Baltic Sea (Fig. 6a), as it is more or less unaffected by windshift and located in the centre of the large scale seiche of the Baltic Basin (LISITZIN 1974, JACOBSEN 1980, FEISTEL et al. 2008). In the course of 2022, the Baltic Sea experienced again no strong inflow activity. Only two smaller inflow pulses occurred with total volumes of 140 $km^3$ and 158 $km^3$ (April 2nd - 11th / September 11th – 20th) all over the year which ventilated the Arkona Basin. During December occured a stepwise sealevel rise of three small pulses (December 5th – 29th) which led to an total inflow volume of 141 $km^3$ and salt mass import of 1,15 Gt. Compared to the events in April and September (0.44 Gt, 0.56 Gt) a quit effective period.

These total volumes of inflow water are calculated after NAUSCH et al. 2002, FEISTEL et al. 2008. No “classic” situations of continuous and rapid sea level changes of more than 50 cm could be observed, which indicate major events. Rapid rises of the sea level are usually only caused by an inflow of North Sea water through the Sound and Belts. They are of special interest for the ecological conditions of the deep-water in the Baltic Sea. Such events are produced by storms from westerly to north-westerly directions, as the correlation between the sea level at Landsort Norra and the filtered wind curves illustrates (Fig. 6b). Only in mid January to mid March a longer intensified phase (weeks) of a positive southeastern wind component (northwesterly wind) occurred during 2022, which caused a stepwise sea level rise. The wind events were interupted (Fig. 4a) and hampered a steady inflow. For example, the accumulated inflow curve of the Öresund (Fig. 7) runs rather flat and unsteady.

Sea level fluctuations in the course of the year 2022 registered a high stand of +77.44 cm MSL at February 19th right after this longer period of westerly winds with stormy days above 15 m $s^{-1}$ (7 Bft). The lowest water level was reached at September 9th with -32.8 m MSL after a longer period of easterly winds in August to September (Fig. 6a, b).

For example, the large Major Baltic Inflow of December 2014 showed a rapid continnous sea level rise from -47 cm MSL to +48 cm MSL within 22 days (MOHRHOLZ et al. 2015).

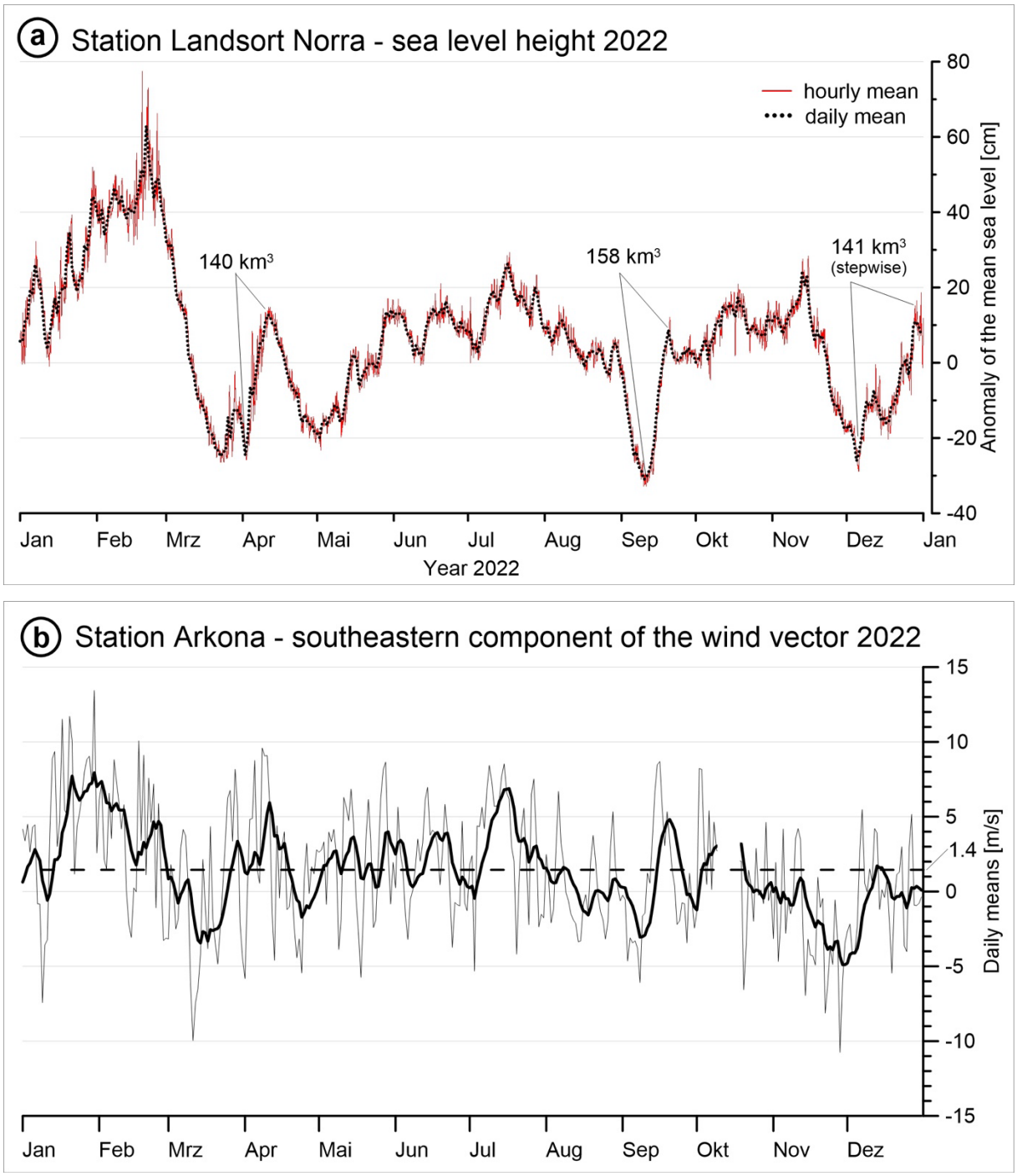


*Fig. 6: (a): Sea level at Landsort as a measure of the Baltic Sea fill factor (from data of SMHI 2023a). (b): Strength of the southeastern component of the wind vector (for northwesterly wind positive) at the weather station Arkona (from data of DWD 2023a). The bold curve appeared by filtering with an exponential 10-days memory and the dashed line depicts the annual average of 1.4 m s-1.*

An overview of the inflow situation at the entrance of Baltic Sea is shown in Fig. 7. The curve of the accumulated inflow volume through the Öresund runs mainly in the root mean square of the long-term mean 1977-2020 (SMHI 2023b). Only a short period from January to February runs above caused by several high wind phases /storms from western direction (c.f. chapter 2.2). As in 2021, the short inflow pulses do not exceed 20-25 km³. For comparison, the previous year 2021, the year 2017 of very low inflow activity and the curve of 2014, the year in which in

December the latest very strong Major Baltic Inflow occurred (MOHRHOLZ et al. 2015) are shown. Another method to classify inflow events is the salt mass import (Fig. 8), where the overflow volumes of saline water above 17 PSU are taken into account in more detail. MOHRHOLZ (2018) reviewed all sources of hydrographic long-term data for the historic events and set up a new calculation method in comparison to the criteria of MATTHÄUS & FRANCK (1992). The classic criterium for a Major Baltic Inflow is an import volume of at least 1 Gt.

Fig. 8 shows the import of salt into the western Baltic Sea for the time span 2018 to 2022 (calculated after MOHRHOLZ 2018). This two smaller inflow pulses during April and September 2022 imported 0.44 Gt and 0.56 Gt of salt. The phases of stepwise sea level rise during February to March and in December exceeded the threshold of 1 Gt. However, the water passed the sills in the western Baltic with interuptions of the overflow in very long time spans of 17 days and 29 days in total.

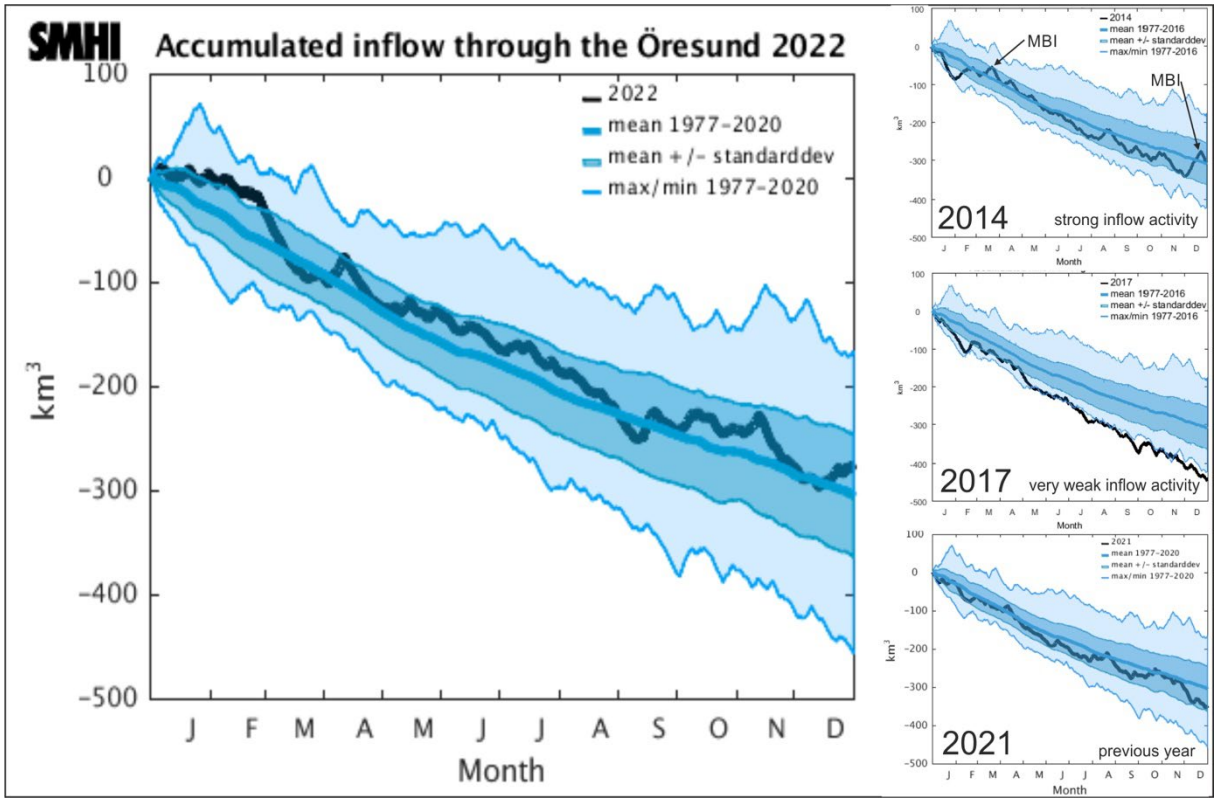


*Fig. 7: Accumulated inflow (volume transport) through the Öresund during 2022 in comparison to the previous year and year 2017 of very weak inflow activity and 2014, characterized by the very strong Major Baltic Inflow in December (SMHI 2023b).*

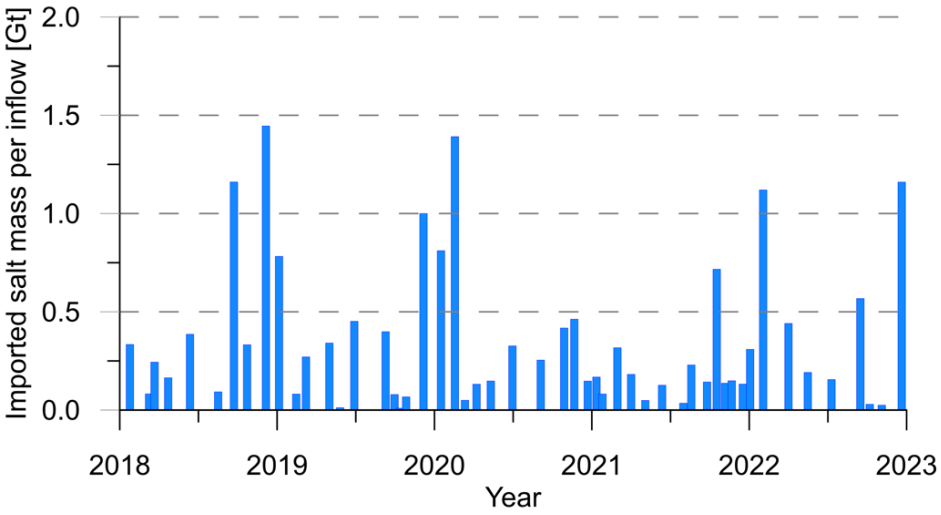


*Fig. 8: Inflow activity into the Baltic Sea during 2018-2023 - salt mass import in Gt per barotrope inflow event (calculated after MOHRHOLZ 2018).*

## 3.2 Observations at the MARNET monitoring platform "Darss Sill"

In 2022, the monitoring station at the Darss Sill provided full records for all mounted devices, except for very few small data gaps that, however, had no relevant effect on any of the analyses presented in the following.

As usual, in addition to the automated oxygen readings taken at the observation mast, discrete comparative measurements of oxygen concentrations were taken at the depths of the station's sensors using the Winkler method (cf. GRASSHOFF et al. 1983) during the regular maintenance cruises. Oxygen readings were corrected accordingly.

### 3.2.1 Statistical Evaluation

The bulk parameters determining the water mass properties at Darss Sill were gathered from a statistical analysis based on the temperature and salinity time series at different depths.

Table 4 summarizes the annual mean temperatures and standard deviations at different depth levels, ranging from the surface to the near-bottom region. These data show that water temperatures in 2022 were significantly warmer than in the previous year, and ranked, at all depth levels, among the top 20% of all years since the beginning of the record in 1992.

This is consistent with Fig. 10, showing the anomaly of the near-surface temperature compared to the long-term climatology at this location. The climatology was based on the data set of REYNOLDS et al. 2007, and covers the period 1982-2011, close to the national reference period 1981-2010. Near-surface temperatures in Fig. 10 are seen to significantly exceeded the reference values during most time of the year, except for a 7-week period from end of July to the second week of September, and a short period in December that, however, only had a marginal impact on the annual statistics. A more detailed analysis showed that especially the unusually mild weather conditions of the winter 2021/2022 and the fall season contributed to these overall high water temperatures at Darss Sill. It is surprising that the extremely warm weather conditions in August (see Chapter 2) were not reflected in the surface temperatures at the MARNET station (Fig. 10). As discussed in more detail below, this effect is related to the occurrence of frequent

upwelling events at the German coast in August and early September, leaving a clear and statistically significant imprint in the temperature records at the Darss Sill (Fig. 9, Fig. 10). Without these unusual events, the annual mean temperatures would have been significantly higher, and 2022 would have developed into one of the warmest years in the record.

*Table 4: Annual mean values and standard deviations of temperature (T) and salinity (S) at the Darss Sill. Maxima in boldface.*

| Year | 7 m depth | | 17 m depth | | 19 m depth | |
|---|---|---|---|---|---|---|
| | T °C | S g kg$^{-1}$ | T °C | S g kg$^{-1}$ | T °C | S g kg$^{-1}$ |
| **1992** | 9.41 ± 5.46 | 9.58 ± 1.52 | 9.01 ± 5.04 | 11.01 ± 2.27 | 8.90 ± 4.91 | 11.77 ± 2.63 |
| **1993** | 8.05 ± 4.66 | 9.58 ± **2.32** | 7.70 ± 4.32 | 11.88 ± 3.14 | 7.71 ± 4.27 | 13.36 ± 3.08 |
| **1994** | 8.95 ± 5.76 | 9.55 ± 2.01 | 7.94 ± 4.79 | 13.05 ± 3.48 | 7.87 ± 4.64 | 14.16 ± 3.36 |
| **1995** | 9.01 ± 5.57 | 9.21 ± 1.15 | 8.50 ± 4.78 | 10.71 ± 2.27 | – | – |
| **1996** | 7.44 ± 5.44 | 8.93 ± 1.85 | 6.86 ± 5.06 | 13.00 ± 3.28 | 6.90 ± 5.01 | 14.50 ± 3.14 |
| **1997** | 9.39 ± 6.23 | 9.05 ± 1.78 | – | 12.90 ± 2.96 | 8.20 ± 4.73 | 13.87 ± 3.26 |
| **1998** | 8.61 ± 4.63 | 9.14 ± 1.93 | 7.99 ± 4.07 | 11.90 ± 3.01 | 8.10 ± 3.83 | 12.80 ± 3.22 |
| **1999** | 8.83 ± 5.28 | 8.50 ± 1.52 | 7.96 ± 4.39 | 12.08 ± **3.97** | 7.72 ± 4.22 | 13.64 ± **4.39** |
| **2000** | 9.21 ± 4.27 | 9.40 ± 1.33 | 8.49 ± 3.82 | 11.87 ± 2.56 | 8.44 ± 3.81 | 13.16 ± 2.58 |
| **2001** | 9.06 ± 5.16 | 8.62 ± 1.29 | 8.27 ± 4.06 | 12.14 ± 3.10 | 8.22 ± 3.86 | 13.46 ± 3.06 |
| **2002** | 9.72 ± 5.69 | 8.93 ± 1.44 | 9.06 ± 5.08 | 11.76 ± 3.12 | 8.89 ± 5.04 | 13.11 ± 3.05 |
| **2003** | 9.27 ± 5.84 | 9.21 ± 2.00 | 7.46 ± 4.96 | **14.71** ± 3.80 | 8.72 ± 5.20 | 15.74 ± 3.27 |
| **2004** | 8.95 ± 5.05 | 9.17 ± 1.50 | 8.36 ± 4.52 | 12.13 ± 2.92 | 8.37 ± 4.44 | 12.90 ± 2.97 |
| **2005** | 9.13 ± 5.01 | 9.20 ± 1.59 | 8.60 ± 4.49 | 12.06 ± 3.06 | 8.65 ± 4.50 | 13.21± 3.31 |
| **2006** | 9.47 ± 6.34 | 8.99 ± 1.54 | 8.40 ± 5.06 | 14.26 ± 3.92 | 9.42 ± 4.71 | **16.05** ± 3.75 |
| **2007** | 9.99 ± 4.39 | 9.30 ± 1.28 | 9.66 ± 4.10 | 10.94 ± 1.97 | 9.63 ± 4.08 | 11.39 ± 2.00 |
| **2008** | 9.85 ± 5.00 | 9.53 ± 1.74 | 9.30 ± 4.60 | - | 9.19 ± 4.48 | - |
| **2009** | 9.65 ±5.43 | 9.39 ±1.67 | 9.38 ±5.09 | 11.82 ±2.47 | 9.35 ±5.04 | 12.77 ±2.52 |
| **2010** | 8.16 ± 5.98 | 8.61 ± 1.58 | 7.14 ± 4.82 | 11.48 ± 3.21 | 6.92 ± 4.56 | 13.20 ± 3.31 |
| **2011** | 8.46 ± 5.62 | - | 7.76 ± 5.18 | - | 7.69 ± 5.17 | - |
| **2012** | - | - | - | - | - | - |
| **2013** | - | - | - | - | - | - |
| **2014** | 10.58 ± 5.58 | **9.71** ± 2.27 | 10.01 ± 4.96 | 13.75 ± 3.53 | 9.99 ± 4.90 | 14.91 ± 3.40 |
| **2015** | - | - | - | - | - | - |
| **2016** | 10.23 ± 5.63 | 9.69 ± 1.98 | 9.27 ± 4.59 | 14.07 ± 3.53 | 9.11 ± 4.43 | 15.56 ± 3.45 |
| **2017** | 9.67 ± 5.05 | 9.40 ± 1.58 | 9.23 ± 4.54 | 11.65 ± 2.50 | 9.20 ± 4.45 | 12.39 ± 2.61 |
| **2018** | 10.54 ±**6.62** | 8.76 ± 1.16 | 9.24 ± **5.41** | 11.58 ±3.23 | 9.16 ± **5.27** | 12.56 ± 3.56 |
| **2019** | 10.34 ±5.25 | 9.57 ± 1.89 | 9.83 ± 4.65 | 12.50 ±2.95 | 9.83 ± 4.50 | 13.41 ± 3.07 |
| **2020** | **10.75** ±4.56 | 9.68 ± 1.59 | **10.39** ± 4.25 | 11.75 ±2.95 | **10.28** ±4.11 | 12.44 ± 2.59 |
| **2021** | 9.79 ± 5.32 | 9.23 ± 1.36 | 9.23 ± 5.01 | 12.75 ± 2.67 | 8.97 ± 4.62 | 13.18 ± 3.02 |
| **2022** | 10.01 ± 4.96 | 9.67 ± 1.56 | 9.69 ± 4.39 | 12.19 ± 1.99 | 9.55 ± 4.28 | 13.27 ± 2.62 |

*Table 5: Amplitude (K) and phase (converted into months) of the yearly cycle of temperature measured at the Darss Sill in different depths. Phase corresponds to the time lag between temperature maximum in summer and the end of the year. Maxima in boldface.*

| | 7 m depth | | 17 m depth | | 19 m depth | |
|---|---|---|---|---|---|---|
| | Amplitude | Phase | Amplitude | Phase | Amplitude | Phase |
| Year | K | Month | K | Month | K | Month |
| **1992** | 7.43 | 4.65 | 6.84 | 4.44 | 6.66 | 4.37 |
| **1993** | 6.48 | 4.79 | 5.88 | **4.54** | 5.84 | **4.41** |
| **1994** | 7.87 | 4.42 | 6.55 | 4.06 | 6.32 | 4.00 |
| **1995** | 7.46 | 4.36 | 6.36 | 4.12 | – | – |
| **1996** | 7.54 | 4.17 | 6.97 | 3.89 | 6.96 | 3.85 |
| **1997** | 8.60 | **4.83** | – | – | 6.42 | 3.95 |
| **1998** | 6.39 | 4.79 | 5.52 | 4.46 | – | – |
| **1999** | 7.19 | 4.52 | 5.93 | 4.00 | 5.70 | 3.83 |
| **2000** | 5.72 | 4.50 | 5.02 | 4.11 | 5.09 | 4.01 |
| **2001** | 6.96 | 4.46 | 5.35 | 4.01 | 5.11 | 3.94 |
| **2002** | 7.87 | 4.53 | 6.91 | 4.32 | 6.80 | 4.27 |
| **2003** | 8.09 | 4.56 | 7.06 | 4.30 | **7.24** | 4.19 |
| **2004** | 7.11 | 4.48 | 6.01 | 4.21 | 5.90 | 4.18 |
| **2005** | 6.94 | 4.40 | 6.23 | 4.03 | 6.21 | 3.93 |
| **2006** | **8.92** | 4.32 | 7.02 | 3.80 | 6.75 | 3.72 |
| **2007** | 6.01 | 4.69 | 5.53 | 4.40 | 5.51 | 4.36 |
| **2008** | 6.84 | 4.60 | 6.23 | 4.31 | 6.08 | 4.24 |
| **2009** | 7.55 | 4.57 | 7.09 | 4.37 | 7.03 | 4.32 |
| **2010** | 8.20 | 4.52 | 6.54 | 4.20 | 6.19 | 4.08 |
| **2011** | 7.70 | 4.64 | 6.98 | 4.21 | 7.04 | 4.14 |
| **2012** | – | – | – | – | – | – |
| **2013** | – | – | – | – | – | – |
| **2014** | 7.72 | 4.43 | 6.86 | 4.17 | 6.77 | 4.13 |
| **2015** | – | – | – | – | – | – |
| **2016** | 7.79 | 4.65 | 6.33 | 4.33 | 6.11 | 4.23 |
| **2017** | 7.00 | 4.56 | 6.20 | 4.31 | 6.15 | 4.28 |
| **2018** | 8.82 | 4.53 | **7.31** | 4.08 | 7.18 | 4.01 |
| **2019** | 7.29 | 4.47 | 6.42 | 4.21 | 6.22 | 4.18 |
| **2020** | 6.29 | 4.36 | 5.85 | 4.17 | 5.66 | 4.07 |
| **2021** | 7.22 | 4.37 | 6.60 | 4.01 | 6.38 | 3.81 |
| **2022** | 6.63 | 4.54 | 6.03 | 4.21 | 5.80 | 4.01 |

The amplitude and phase shift of the annual cycle were determined from a Fourier analysis of the temperature time series at 7 m depth (surface layer) and at the two lowermost sensors (17 m and 19 m depth). This method finds the optimal fit of a single Fourier mode (a sinusoidal function) to the data, from which amplitude and phase can easily be inferred as the characteristic parameters of the annual cycle.

Table 4 shows that the annual mean temperatures of 2022 were slightly below the long-term average, which is surprising in view of the mild winter conditions and near-surface temperatures that were significantly above the long-term average for the winter, spring and fall seasons (Fig. 10). We attribute this to the strong and unusual upwelling-induced reduction of peak temperatures in August that are also clearly visible in Fig. 10. As discussed in more detail below, the annual mean temperature for 2022 is therefore not a reliable indicator for the average heat content of the Western Baltic Sea. The mild winter conditions are also mirrored in the unusually high minimum temperature of 3.37 °C in January, constituting the second largest value since the beginning of the record (Table 6). Also the maximum temperature of 20.98 °C, observed on 24 August, is clearly above the average of our record, but still significantly below the value of 23.1 °C found in the record-setting year 2018. As emphasized above, the interpretation of the peak temperature in August 2022, and its comparison with other years, should be done with caution due to the unusually frequent upwelling events that strongly effected surface temperatures at the Darss Sill.

Annual near-bottom salinities (Table 4) are far below those of the record years 2003, 2006, 2014, and 2016, which is surprising in view of the small inflow activity in 2022.

*Table 6: Listing of the minimum and maximum temperature measured at 7 m water depth at Darss Sill. Time indicates the date of occurrence. The column "Range" provides the difference between minimum and maximum temperature. Minima and maxima are highlighted in bold face.*

| | Minimum | | Maximum | | |
|---|---|---|---|---|---|
| Year | Temperature °C | Time | Temperature °C | Time | Range °C |
| **1995** | 0.98 | 30.12 | 20.54 | 05.08 | 19.56 |
| **1996** | 0.37 | 27.01 | 17.65 | 09.08 | 17.28 |
| **1997** | 0.16 | 21.01 | 22.50 | 19.08 | 22.34 |
| **1998** | 2.59 | 16.12 | 16.61 | 10.08 | 14.02 |
| **1999** | 1.55 | 18.02 | 19.84 | 31.07 | 18.29 |
| **2000** | 2.65 | 25.01 | 17.87 | 14.08 | 15.22 |
| **2001** | 2.33 | 28.03 | 20.65 | 29.07 | 18.32 |
| **2002** | 2.03 | 13.01 | 20.24 | 30.08 | 18.21 |
| **2003** | 0.09 | 11.01 | 21.92 | 13.08 | 21.83 |
| **2004** | 1.45 | 28.02 | 19.11 | 20.08 | 17.66 |
| **2005** | 1.50 | 13.03 | 19.79 | 13.07 | 18.29 |
| **2006** | 0.40 | 30.01 | 22.80 | 21.07 | **22.40** |
| **2007** | 3.36 | 25.02 | 18.70 | 14.08 | 15.34 |

| | | | | | |
|---|---|---|---|---|---|
| **2008** | 3.12 | 17.02 | 19.67 | 29.07 | 16.55 |
| **2009** | 1.65 | 25.02 | 19.62 | 10.08 | 17.97 |
| **2010** | **-0.44** | 05.02 | 20.33 | 21.07 | 20.77 |
| **2011** | -0.12 | 05.01 | 17.94 | 12.07 | 18.06 |
| **2012** | – | – | – | – | - |
| **2013** | – | – | – | – | |
| **2014** | 1.54 | 09.02 | 21.61 | 09.08 | 20.07 |
| **2015** | 2.95 | 04.02 | 20.97 | 13.08 | 15.19 |
| **2016** | 1.81 | 23.01 | 20.42 | 28.07 | 18.61 |
| **2017** | 2.09 | 19.02 | 18.61 | 30.08 | 16.52 |
| **2018** | 1.11 | 18.03 | **23.10** | 04.08 | 21.99 |
| **2019** | 2.82 | 26.01 | 20.91 | 01.09 | 18.09 |
| **2020** | 4.74 | 07.01 | 19.51 | 22.08 | 14.77 |
| **2021** | 1.68 | 17.02 | 20.74 | 28.07 | 19.07 |
| **2022** | 3.37 | 24.01 | 20.98 | 24.08 | 17.61 |

### 3.2.2 Temporal development at Darss Sill

Fig. 9 shows the development of water temperature and salinity in 2022 in the surface layer (7 m depth) and the near-bottom region (19 m depth). As in previous years, the currents observed by the bottom-mounted ADCP in the surface and bottom layers were integrated in time, in order to emphasize the low-frequency baroclinic (depth-variable) component which is plotted in Fig. 11 as a 'progressive vector diagram' (pseudo-trajectory). This integrated view of the velocity data filters short-term fluctuations and allows long-term phenomena such as inflow and outflow events to be identified more clearly. According to this definition, the average current velocity corresponds to the slope of the curves shown in Fig. 11, using the convention that positive slopes reflect inflow events.

The first two months of the year 2022 were characterized by nearly stagnant water temperatures of 4-5 °C (Fig. 9), approximately 1-2 K above the climatological average as shown in Fig. 10. The velocity data in Fig. 11 suggest an alternation between weak inflow and outflow periods with a vanishing net transport across the Darss Sill. Combined with a slight outflow tendency across the Öresund (Fig. 7), this suggests that the gradual sea level increase observed during this period at Landsort (Fig. 6a) is largely due to a blocking of river runoff. It is interesting to note that the strong south-westerly winds in January and February (Fig. 6b) were not sufficient to trigger any strong inflow signals against the steadily increasing barotropic pressure gradient caused by this process. Occasional weak inflow pulses were sufficient to maintain stable stratification (Fig. 9) and to keep oxygen levels close to the saturation level (Fig. 12).

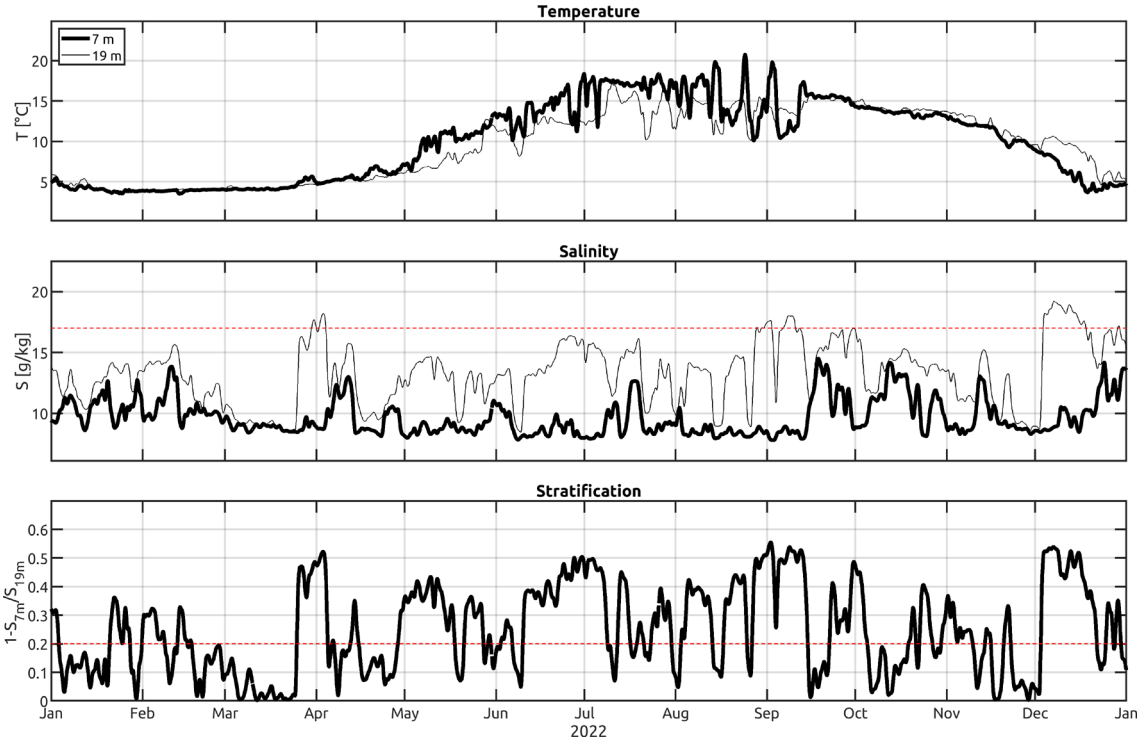


*Fig. 9: Water temperature (upper panel) and salinity (middle panel) measured in the surface layer and the near bottom layer at Darss Sill in 2022. The red dashed line indicates the salinity threshold of 17 g/kg. In the lower panel we show a stratification measure G according to MATTHÄUS & FRANK (1992). Here the red dashed line marks the stratification threshold of 0.2.*

At Landsort, the highest sea level of the year was reached in the last week of February (Fig. 6a), triggering, a four-week period with nearly permanent outflow activity which was supported by a gradual transition from westerly to easterly winds (Fig. 11). Temperatures remained high for this time of the year (Fig. 10), but oxygen concentrations close to saturation until the spring bloom at the end of March became evident from oversaturation in the surface layer and a slight decay near the bottom, pointing at the degeneration of the sinking bloom (Fig. 12).

Low sea levels at the end of March and a shift to increasing winds from westerly directions finally triggered the first of the two significant inflow events in 2022. This event, lasting approximately until mid of April, is clearly identifiable also in the velocity records (Fig. 11), in an increase in surface salinities (Fig. 9), and in a relaxation of oxygen levels back to values close to saturation (Fig. 12). The event ended with decreasing winds and a shift to easterly directions, triggering continued outflow until end of May.

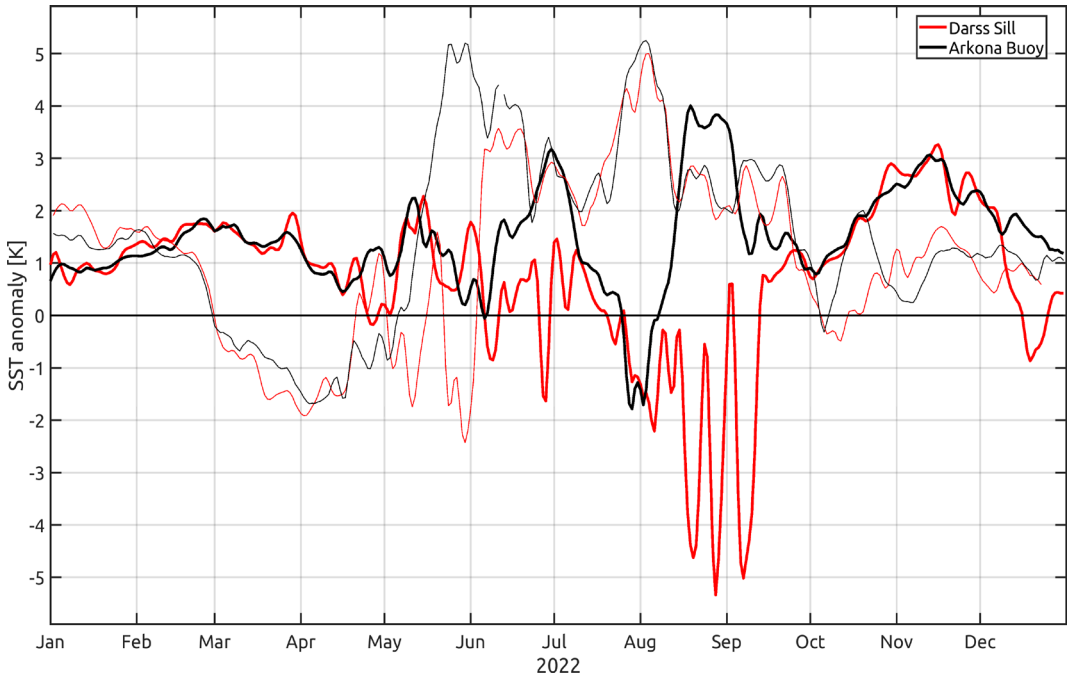


*Fig. 10: Deviation of near surface temperature from the climatology at Darss Sill and Arkona Buoy in 2022. The climatology was build for the national reference period 1982-2011 and is based on the dataset of REYNOLDS et al., 2007. The thin lines show the anomaly from 2018.*

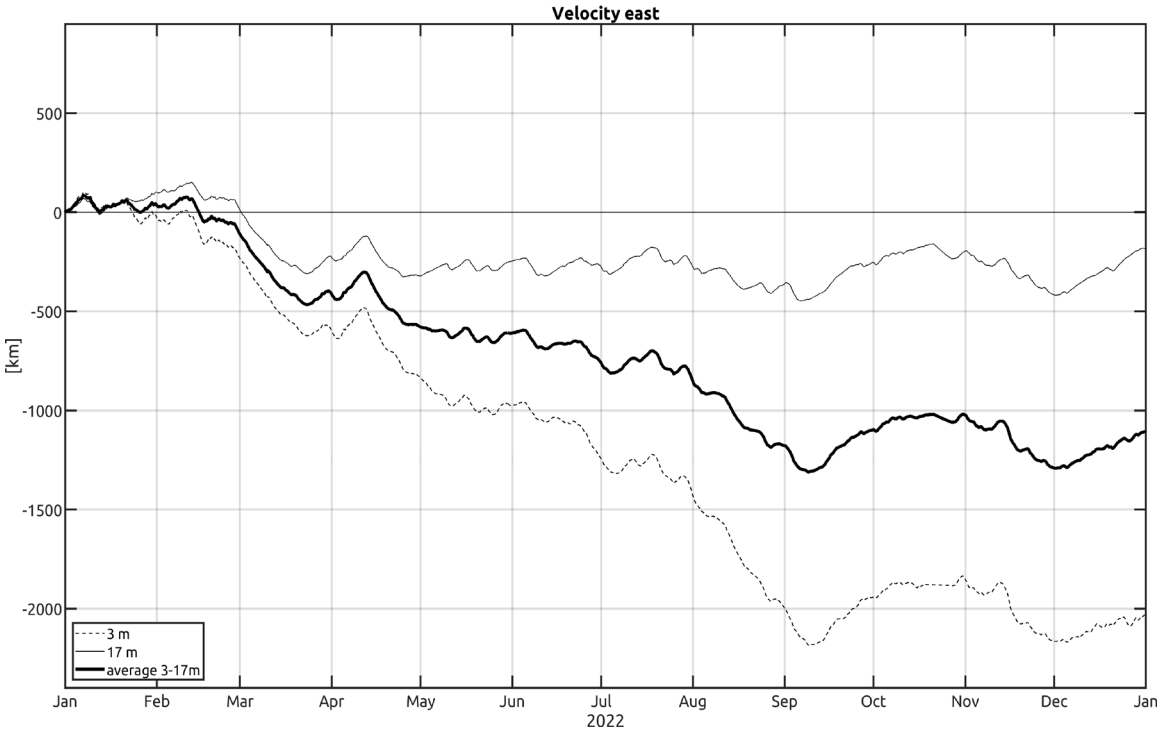


*Fig. 11: East component of the progressive vector diagrams of the current in 3 m depth (dashed line), the vertical averaged current (bold line) and the current in 17 m depth (solid line) at the Darss Sill in 2022.*

The following early summer period until end of June was characterized by an overall outflow tendency at the Darss Sill, interrupted only occasionally by weak inflow pulses that were, however, in their sum strong enough to prevent a dramatic decrease in oxygen concentrations (Fig. 12). Minimum concentrations were reached at the end of this period, in the first week of July,

with saturation values below 60 %. Surface temperatures showed a steady increase up to 18 °C during this warming phase until end of June (Fig. 9), and remained overall close to the climatological average (Fig. 10). Quasi-permanent salinity stratification (Fig. 9) lead to an effective vertical decoupling of the water column, and thus, to a weaker and delayed warming response in the near-bottom region that was largely determined by the intrusion of warm inflow waters. The velocity records in Fig. 11 revealed several weak inflow events with a strong baroclinic component in May and mid of June that left a well-defined imprint in oxygen concentrations (Fig. 12).

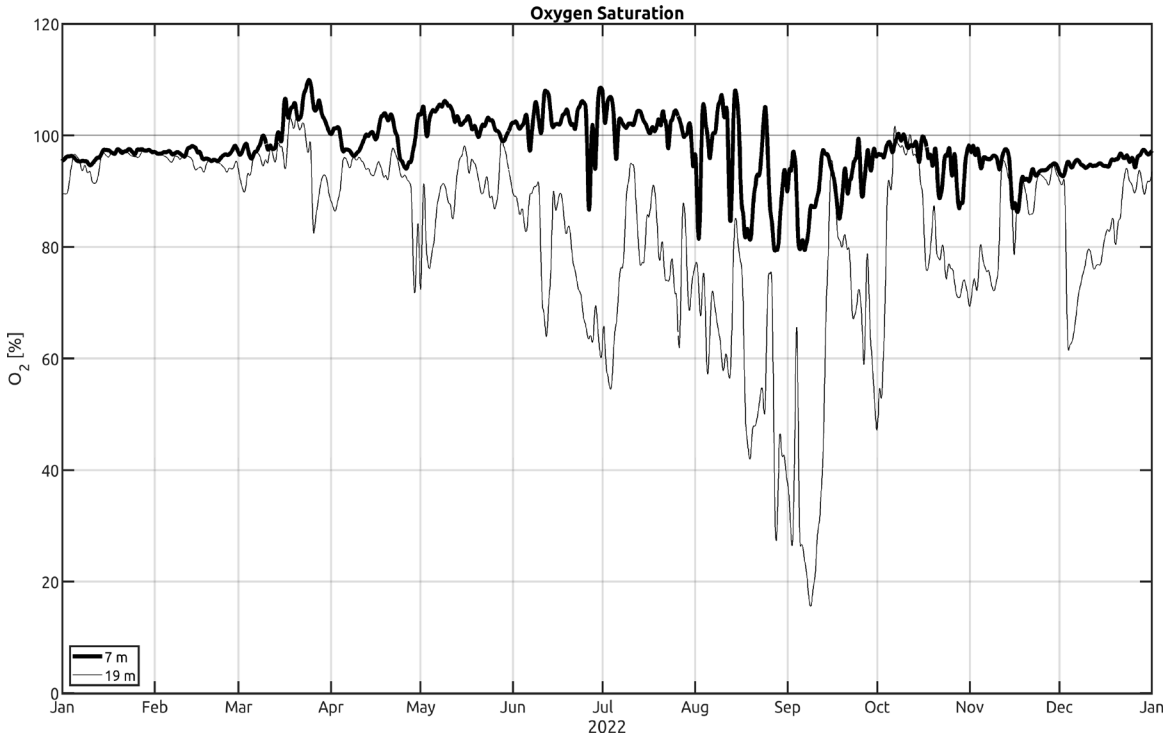


*Fig. 12: Oxygen saturation measured in the surface and bottom layer at the Darss Sill in 2022.*

Unusually strong winds in July stopped this early-summer warming trend, weakened the vertical stratification and resulted in nearly stagnant surface temperatures around 17-18°C throughout the month (Fig. 9), again close to the climatological mean (Fig. 10). The strong westerly winds also triggered a small barotropic summer inflow (Fig. 11) that lead to a strong increase of the near-bottom temperatures (Fig. 9) and a quick recovery of the near-bottom oxygen concentrations (Fig. 12).

The rest of the summer period until the first week of September was characterized by weak winds with a long-term trend towards more easterly directions (Fig. 6b), a general tendency for outflow (Fig. 6a, Fig. 11), and gradually deteriorating oxygen concentrations, reaching the smallest values of the year with less than 20 % saturation in the first week of September. Surface temperatures during this period remained significantly below the climatological average and showed pronounced but largely reversible fluctuations with a duration of a few days and amplitudes larger than 5 K during a number of cooling events (Fig. 10). These unusual cooling events were correlated with short easterly wind events (Fig. 4b), suggesting local upwelling as one possible reason. To substantiate this hypothesis, we analyzed results of a realistic numerical model of

the Western Baltic Sea with 600 m spatial resolution (GRÄWE et al. 2015). A snapshot of the surface temperature is shown in Fig. 13 (right panel) for the peak of the second cooling event on 28 Aug 2022. The model results indicate that at this time, indeed, a local upwelling cell had developed north of the Darss/Zingst peninsula, extending northward up to the position of the corresponding MARNET station. Partly owing to these cooling events and the relatively strong winds, the daily surface temperatures exceeded the threshold of 20 °C only once, in the second half of August, during the year 2022. The important role of the cooling events is further corroborated by a comparison with the significantly higher surface temperatures at the Arkona Station (Fig. 14), which is discussed in more detail in the following chapter. Temperatures at that station (Fig. 10) were up to 4 K above the climatological average, consistent with the unusually high air temperature of this month (see chapter 2), whereas those at the Darss Sill remained significantly below the climatology for this month.

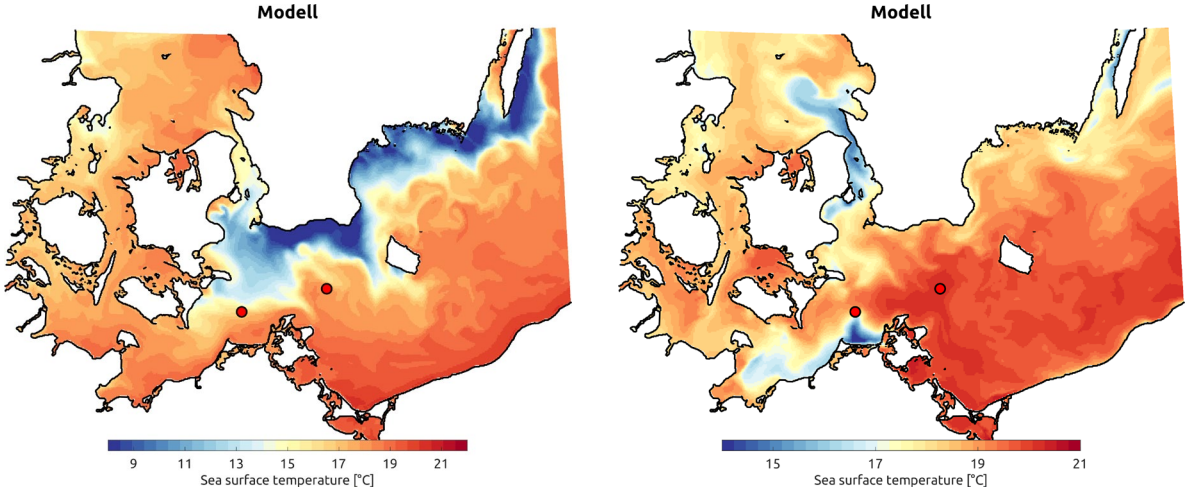


*Fig. 13: Seasurface temperature on (left) 28 Jul 2022 and (right) 28 Aug 2022 from a high-resolution numerical simulation of the Western Baltic Sea. Red markers indicate the MARNET stations at the Darss Sill and the Arkona Basin.*

The lowest water level of the year at Landsort and a strong peak of north-westerly winds in the second week of September finally triggered the strongest inflow event of the year 2022 (Fig. 6), importing a volume of slightly less than 160 km³ and 0.56 Gt of salt into the western Baltic Sea. This event lead to a quick recovery of oxygen concentration to more than 90 % saturation. However, it had no lasting effect: concentrations dropped again to less than 50 % already by the end of September already (Fig. 12). A second smaller inflow at the beginning of October brought additional oxygen and concentrations close to saturation.

The following fall season until beginning of December showed a permanent tendency for outflow (Fig. 11), first weak, approximately balancing the freshwater runoff as indicated by the stagnant sea level at Landsort (Fig. 6a), and finally, starting from the second week of November, intense due the increasing easterly winds (Fig. 6b). In the first week of December, water levels had almost reached the yearly minimum levels found in September, and oxygen saturation values had dropped to 60 %, which is unusually low for this time of the year. Due to the unusually mild

weather conditions, surface temperatures remained above 10 °C until mid of November, and partly exceeded the climatological average by more than 3 K (Fig. 9 and Fig. 10).

Weak but continuous inflow characterized the final month of December (Fig. 9, Fig. 11). This was first purely driven by barotropic pressure differences and later supported by increasing westerly winds towards the end of the year (Fig. 6). Oxygen concentrations gradually increased to the saturation level during this period (Fig. 12), and temperatures varied around the climatological mean (Fig. 10). The parameters at the end of the year therefore very much corresponded to the climatological situation.

## 3.3 Observations at the MARNET monitoring buoy "Arkona Basin"

The AB monitoring station described in this chapter is located almost 20 nm north-east of Arkona in 46 m water depth. The monitoring station in the AB supplied complete records during the year 2022. As described in chapter 3, the optode-based oxygen measurements at the monitoring station were corrected by oxygen data from chemical measurements with the Winkler method, using water samples collected and analysed during the regular MARNET maintenance cruises.

### 3.3.1 Temporal development until summer

Fig. 14 shows time series of water temperature and salinity at depths of 7 m and 40 m, representing the surface and bottom layer properties. Corresponding oxygen concentrations, plotted as saturation values as in the previous chapter, are shown in Fig. 15.

Similar to the measurements at the Darss Sill, the first three months of the year were characterized by an anomalous warm surface layer also at station AB (Fig. 10). The lowest daily mean temperature was only slightly lower than that observed at the Darss Sill, but about four weeks later in mid of February (Fig. 9 and Fig. 14). While surface temperatures in the AB are largely determined by the local atmospheric fluxes, those at the Darss Sill are more strongly affected by lateral advection, which may explain the observed differences.

Surface salinities remained inside a narrow range of 7-9 g $kg^{-1}$ during this period (and, in fact, during the entire year), again pointing at the lack of any major inflow event in 2022. Bottom salinities reached a narrow peak of 20 g $kg^{-1}$ in the second week of January, which is likely the signature of a small inflow event observed in December 2021 at the Darss Sill. It is to note, that the large peak salinities in the AB indicate a significant contribution from the Drogden Sill. Oxygen concentrations at the bottom generally remained above 80 % saturation until mid of March (Fig. 15).

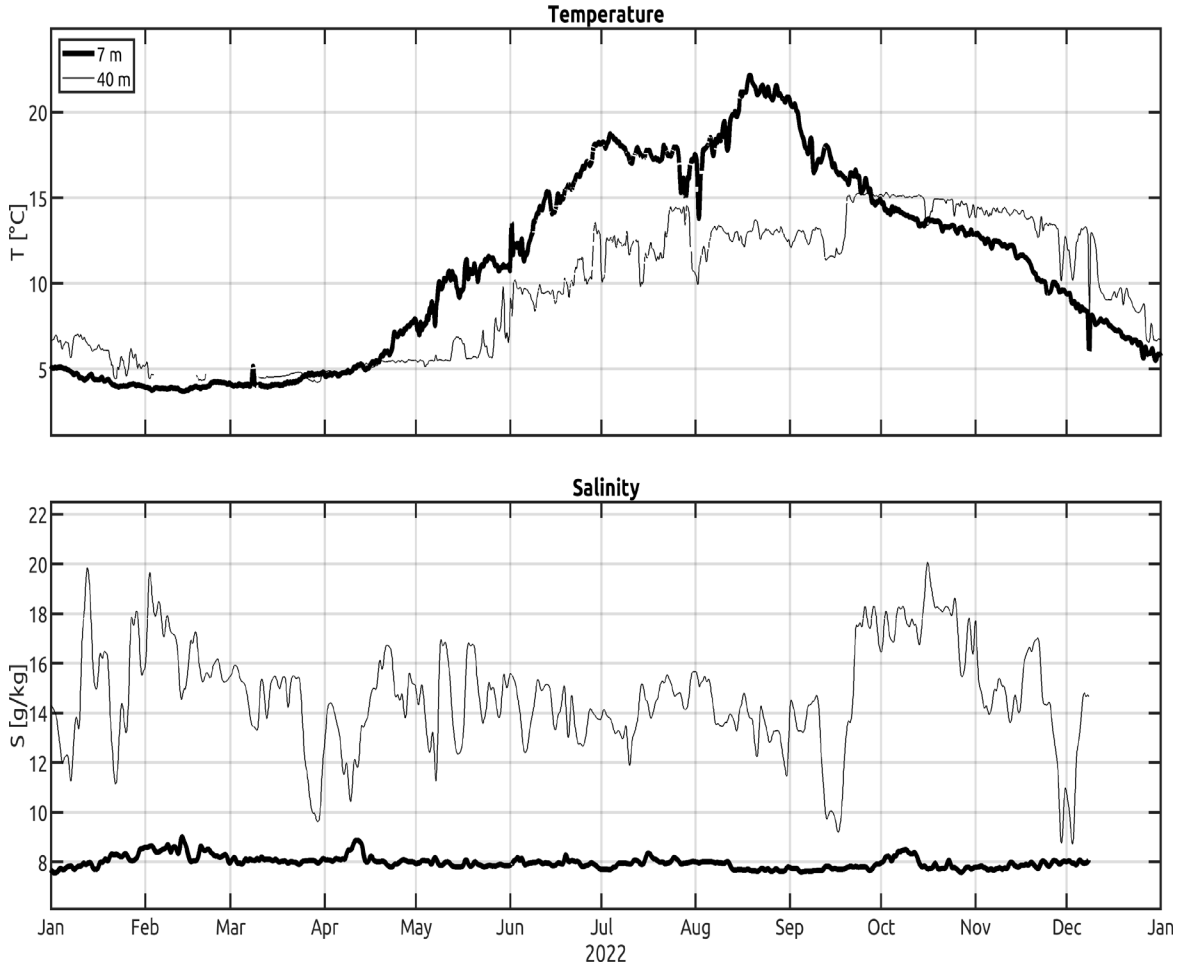


*Fig. 14: Water temperature (above) and salinity (below) measured in the surface layer and near-bottom layer at the station AB in the Arkona Basin in 2022.*

It is interesting to note that the two unusual low-salinity peaks observed at the end of March and around 10 April correlated well with high-oxygen peaks (Fig. 15) and an alternating pattern of strong westerly-easterly-westerly winds that is most clearly evident in the unfiltered wind data in Fig. 6. As the observed salinity and oxygen signals are largely reversible, they likely reflect a basin-scale response to these wind events, transiently advecting less salty and more oxygenated waters from shallower depths past the lowest sensors of the station.

The relaxation from the last event in April occurred in parallel with the arrival of the salty and oxic waters from a weak inflow event that had crossed the Darss Sill at the beginning of April (see Chapter 3). Following this event, no more significant barotropic inflows reached the Arkona Basin until September, which is reflected in gradually decaying oxygen concentrations down to the annual minimum of less than 15% saturation in the first week of September (Fig. 15). Nevertheless, the stepwise increases of near-bottom temperatures during the summer period (for example, end of May, end of June, and in the third week of July) nevertheless point at the arrival of waters from sporadic mixed barotropic/baroclinic inflows (see Chapter 3). These inflows left no clear footprint in the salinities but, as suggested by Fig. 15, they likely helped to maintain oxygen concentrations above 60% saturation until the second week of July.

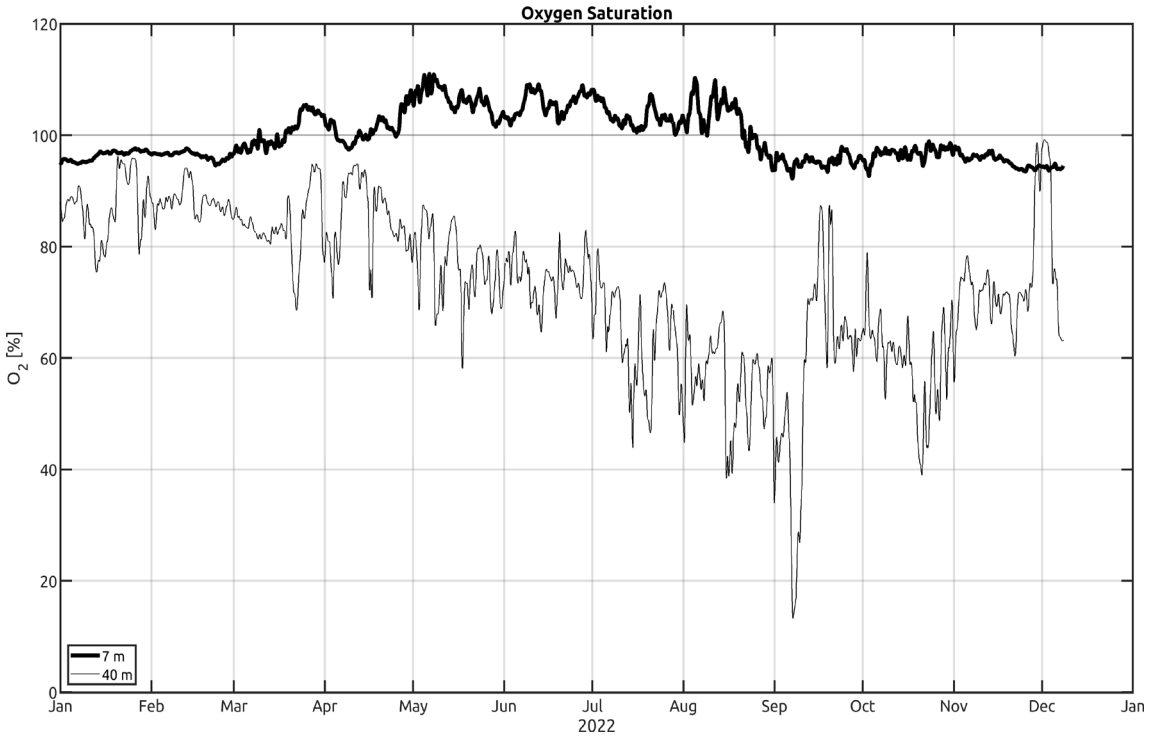


*Fig. 15: Oxygen saturation measured in the surface and bottom layer at the station AB in the Arkona Basin in 2022.*

Similar to the Darss Sill, also at station AB the cool and windy weather conditions in July stopped the warming trend of the surface waters. Numerical model simulations (see Chapter 3) resulted in quasi-permanent upwelling at the Swedish coast and the evolution of upwelling filaments that reached far south into the central Arkona Basin by end of July (Fig. 13, left panel). Due the non-linearity of the processes determining the evolution of the upwelling front and filaments, the predictability of their exact locations and shapes in a numerical model is limited. Therefore, while none of the individual upwelling filaments reached the position of the Arkona Buoy in our simulations, it seems plausible that the rapid cooling events that can be identified in the temperature records at the end of July and beginning of August at both Darss Sill and Arkona (Fig. 9 and Fig. 14) were triggered by the passage of cold upwelling waters.

The unusually hot weather conditions in August finally resulted in a rapid warming of the surface waters up to the annual peak temperature of more than 23 °C at mid of the month (Fig. 14). Fig. 10 shows that the temperatures in the second half of August were far beyond (3.5–4 K) the values expected from the climatology, underlining the exceptional character of this summer heat period. Starting from beginning of September, surface waters show a clear cooling trend with no significant interruptions until the end of the year.

The most important event in the deep layers during the summer period was the arrival of waters from the barotropic inflow passing the Darss Sill at beginning of September. The signatures of this inflow included a rapid increase in near-bottom temperature and salinity (Fig. 14), and a quick recovery of oxygen concentrations to more than 80 % saturation (Fig. 15). It is interesting to note that immediately before this event, in the second week of September, oxygen concentrations already showed a strong increase while salinities rapidly dropped, which can obviously not be attributed to the arrival of inflow waters. We interpret this signal as the large-

scale downwelling response of the basin to the onset of strong westerly winds, advecting waters with high oxygen concentrations and low salinities down the southern slope of the basin to station AB.

An interesting anomaly in the oxygen concentrations was observed at the end of November and beginning of December (Fig. 15). In the last week of November, near-bottom oxygen concentrations started to increase rapidly towards the saturation level. This increase is correlated with a strong decrease in near-bottom salinities (Fig. 14), and therefore cannot be attributed to any inflow activity. Also, no inflow signatures can be detected during this period in the water levels at Landsort Norra (Fig. 6a) and the current records in the Öresund (Fig. 7). A more likely explanation seems to be the following: After a long outflow period in November (Fig. 6a), the pool low-oxygen bottom waters in the Arkona Basin had largely drained through the Bornholm channel, and the halocline and oxycline had descended to a position close to the bottom. Pressure gradients set up by the strong south-easterly winds observed at the end of November and beginning of December (Fig. 6b) resulted in a lateral displacement of this thin near-bottom pool with salty low-oxygen waters away from station AB. Well oxygenated and less salty waters from the layers above the halocline thus appeared at the sensor locations. This situation lasted until the salty inflow waters that had already been recorded at the Darss Sill (Section 3.2) arrived in the Arkona Basin at the beginning of December. It is interesting to note that these inflow waters initially carried relatively low oxygen concentrations (Fig. 12), resulting in an unusual decrease of the deep-water oxygen concentrations during this inflow event (Fig. 15).

## 3.4 Observations at the MARNET monitoring buoy “Oder Bank”

The water mass distribution and circulation in the Pomeranian Bight have been investigated in the past as part of the TRUMP project (TRansport und UMsatzprozesse in der Pommerschen Bucht) (v. BODUNGEN et al. 1995; TRUMP 1998), and were described in detail by SIEGEL et al. (1996), MOHRHOLZ (1998) and LASS, MOHRHOLZ & SEIFERT (2001). For westerly winds (i.e., during downwelling favourable conditions), well-mixed water is observed in the Pomeranian Bight with a small amount of surface water from the Arkona Basin admixed to it. For easterly winds (i.e., upwelling-favourable conditions), water from the Oder Lagoon flows via the rivers Świna and Peenestrom into the Pomeranian Bight, where it stratifies on top of the bay water off the coast of Usedom. As shown below, these processes have an important influence on primary production and vertical oxygen structure in the Pomeranian Bight.

The Oder Bank monitoring station (OB) is located approximately 5 nm north-east of Koserow /Usedom at a water depth of 15 m, recording temperature, salinity, and oxygen at depths of 3 m and 12 m. The oxygen measurements were validated using oxygen data from chemical analysis of water samples taken during the regular maintenance cruises using the Winkler method. After the winter break, the monitoring station OB was brought back to service early in the year, on 12 April 2022. Starting from that date, the station provided continuous time series of all parameters until the end of 2022. While temperature was recorded throughout the year, conductivity and thus salinity observations as well as oxygen observations are not available after 12 December.

Temperatures and salinity at OB are plotted in Fig. 14; associated oxygen readings are presented in Fig. 15. Similar to the other MARNET stations, the maximum temperatures that were reached

during the summer period were lower than in 2018 (maximum temperature at OB 24.8 °C), but comparable to the years 2010, 2013, 2014 and 2021, when temperatures of up to 23 °C were observed at station OB. In 2022, the maximum hourly mean temperature, reached more than 22.5 °C in mid August similar to 2020. As in previous years, surface temperatures at the monitoring station OB were significantly higher compared to those at the deeper and more energetic stations in the Arkona Basin and the Darss Sill (Fig. 9 and Fig. 14), reflecting the shallower and more protected location of this station.

In average years, there is also a dynamical reason for the stronger warming of the surface layer at station OB, related to the suppression of vertical mixing due to the transport of less saline (i.e., less dense) waters from the Odra Lagoon on top of the saltier bottom waters (e.g. Lass et al., 2001) during easterly winds. In 2022, such easterly winds prevailed in August (Fig. 4), which, along with the exceptionally large air temperatures, explains the annual temperature maximum of 22.98 °C (hourly mean value, observed on 17 August). Model simulations (Fig. 13) show that even during one of the stronger easterly wind events, upwelling as characterised by decreased surface temperature and increased surface salinity did not occur at OB.

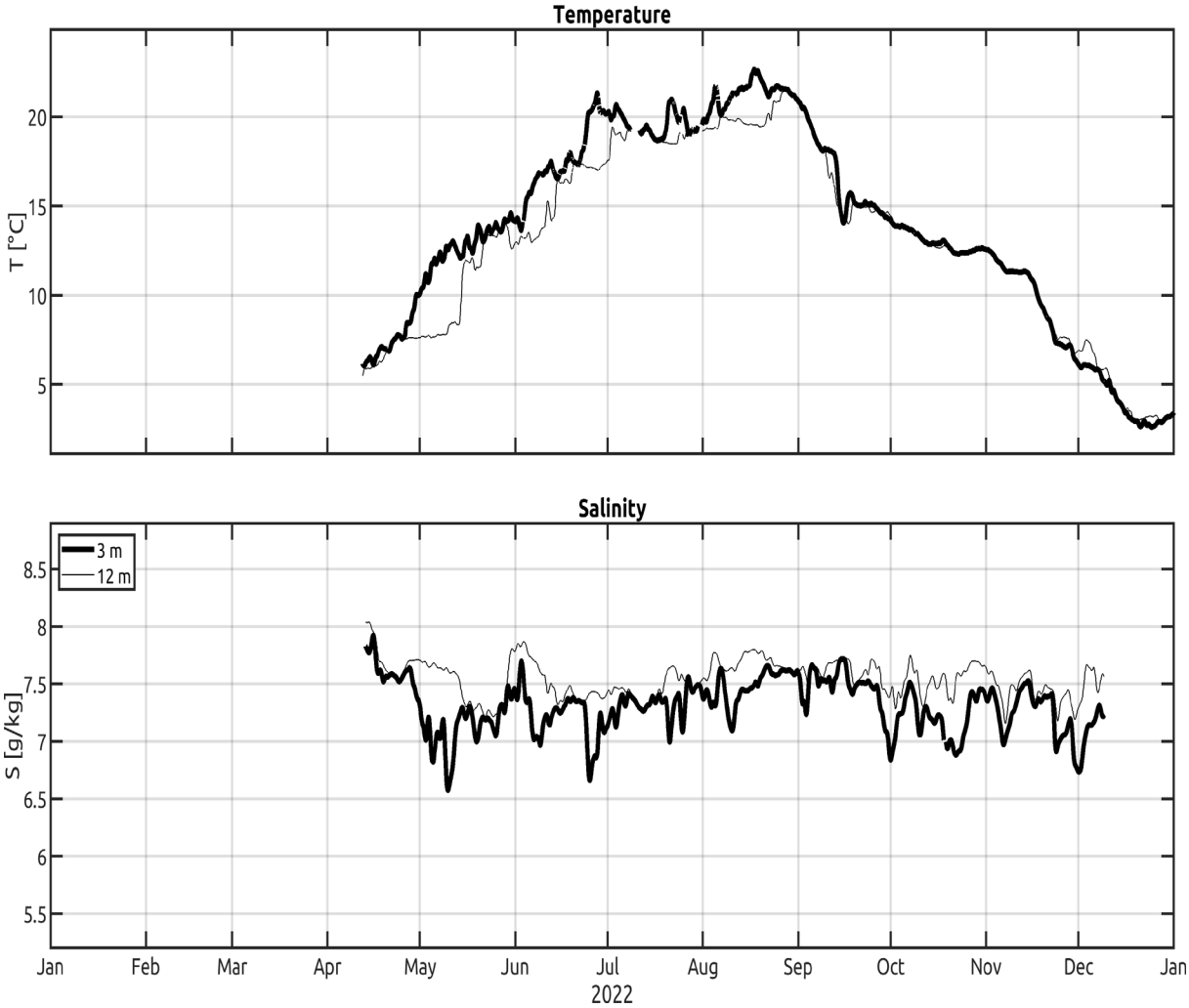


*Fig. 16: Water temperature (above) and salinity (below) measured in the surface layer and near-bottom layer at the station OB in the Pomeranian Bight in 2022.*

At the end of April and probably also before (no data), the water column was well mixed in salinity and temperature. From beginning of May onwards, a temperature and haline stratification developed that was episodically interrupted by shorter well-mixed periods. Four major stratification periods can be identified: early May, early June, late June and mid August. While temperature is vertically homogeneous from end of August until the end of the year, most of the time, salinity remains stratified, with short episodic interruptions. Significant haline stratification is generally associated with distinct minima in surface salinity, which are often below 7 g $kg^{-1}$ (as in early May, late June, beginning of October, late October, and beginning of December). These events are associated with easterly wind directions (Fig. 4), except for October, when winds were almost exclusively from westerly directions (due to a data gap in the DWD wind data for October, this conclusion is based on meteorological data from station AB). A dynamical explanation for the unusual stratification event in October is therefore lacking. Maximum surface to bottom temperature differences during the other stratification events were: 5 K (in early May) and approximately of 3-4 K in late June and mid August. Maximum salinity differences were up to 1 g $kg^{-1}$, during periods when easterly winds push the Odra river plume sufficiently off-shore to reach the OB buoy (e.g. during early May).

From an ecological perspective, the most important consequence of the build-up of stratification and the suppression of turbulent mixing, from May on, was the decrease in near-bottom oxygen concentrations due to the de-coupling of the bottom layer from direct atmospheric ventilation. Their impact on the oxygen budget of the Pomeranian Bight becomes evident from Fig. 17, showing oxygen concentrations at depths of 3 m and 12 m. During four stratification events, well-defined local minima in the near-bottom oxygen concentrations can be identified. These events are characterised by subsequently decreasing oxygen saturation, with minimum values of below 40 % during August. After the end of August, bottom oxygen saturation stayed at values above 85-90 % (Fig. 17), indicating sufficient ventilation by vertical mixing and reduced oxygen consumption rate due to decreasing water temperatures.

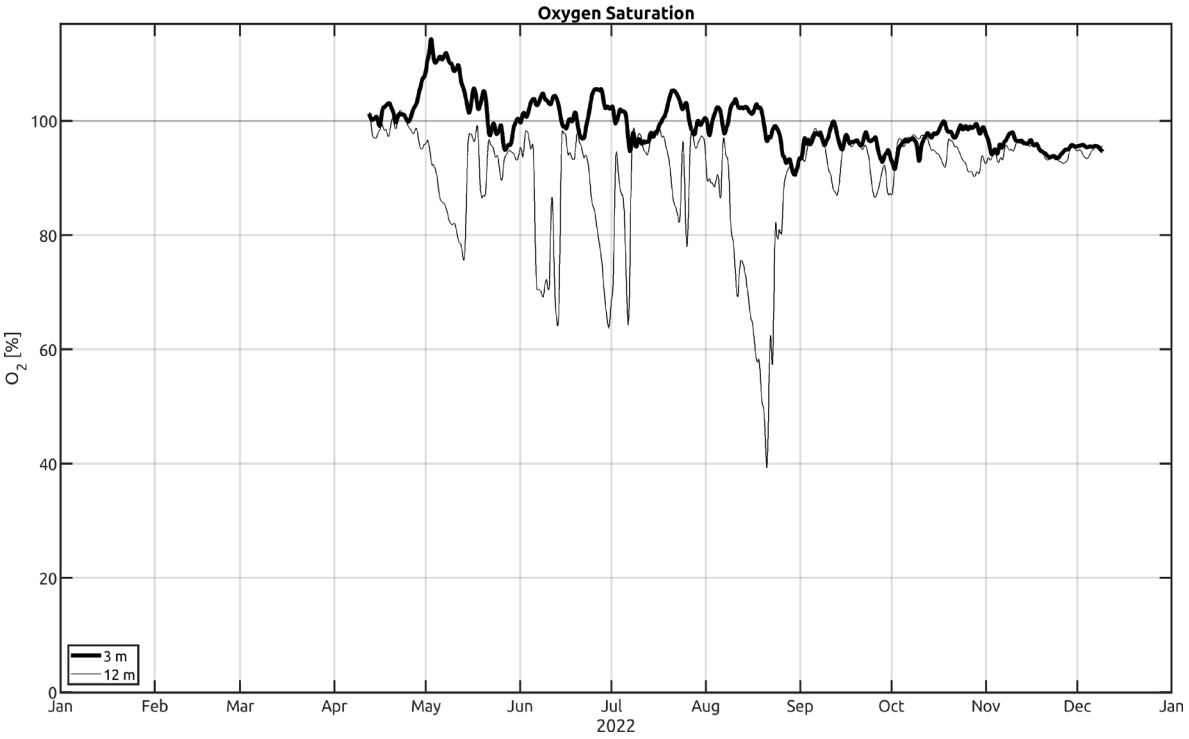


*Fig. 17: Oxygen saturation measured in the surface and bottom layer at the station OB in the Pomeranian Bight in 2022.*

Finally, it is worth noting that the increase in primary production of biomass in the Pomeranian Bight, induced by the lateral transport of nutrient-rich lagoon water to station OB during upwelling-favourable winds, is likely to have supported the generation of super-saturated oxygen concentrations that were observed in the surface-layer during all of the above stratification events (Fig. 16). Highest near-surface oxygen concentrations approximately 15 % above the saturation level were found during the spring bloom in early May. The correlation between the oxygen increase in the surface layer and the decrease in the near-bottom layer points at increased oxygen consumption rates induced by the decay of freshly deposited biomass (“fluff”).

# 4 Results of the routine monitoring cruises: Hydrographic and hydrochemical conditions along the thalweg

The routine monitoring cruises carried out by IOW provide the basic data for the assessments of hydrographic conditions in the western and central Baltic Sea. In 2022, monitoring cruises were performed in February, March, May, August and November. Snapshots of the temperature distribution along the Baltic thalweg transect obtained during each cruise are depicted in Fig. 18 and Fig. 19. This data set is complemented by monthly observations at central stations in each of the Baltic basins carried out by Sweden's SMHI (SMHI 2023c). Additionally, continuous time series data are collected in the Eastern Gotland Basin. Here the IOW operates three long-term moorings that monitor the hydrographic conditions in the deep-water layer. The results of these observations are given in Fig. 20 and Fig. 23.

## 4.1 Water temperature

The sea surface temperature (SST) of the Baltic Sea is mainly determined by local heat flux between the sea surface and the atmosphere. In contrast, the temperature signal below the halocline is detached from the surface and the intermediate winter water layer and reflects the lateral heat flows due to salt-water inflows from the North Sea and diapycnal mixing. The temperature of the intermediate winter water layer conserves the late winter surface conditions of the Baltic till the early autumn, when the surface cooling leads to deeper mixing of the upper layer.

In the central Baltic, the development of vertical temperature distribution above the halocline follows with some delay the annual cycle of atmospheric temperature. The winter of 2021/2022 was again warmer than during the 30 years reference period 1961-1990, and significantly warmer than the previous winter 2020/2021. The January, February and March 2021 depicted moderate to strong positive temperature anomalies of between 0.8 K to 2.5 K. Thus, the surface cooling of the Baltic was lower than in the reference period. The sea surface temperatures remained above the density maximum, except of the Gulf Bothnia and the Gulf of Finland.

During April the mean air temperature was slightly cooler (-0.4 K) than the long term mean. The most extreme air temperature anomalies were observed in February and August 2022 with 2.5 K and 2.0 K above the reference values, respectively. The air temperatures remained at higher than normal level throughout the year, except of April, September and December 2022. During these months the air temperature anomaly was about 0.5 K below the long term mean. The deep-water conditions in the central Baltic were stagnant since 2019, when the actual temperature in deep water was established by subsequent minor inflow events (MOHRHOLZ 2018).

Due to the higher than normal air temperature, the SST in the Baltic in February 2022 was relatively high at 3.5 °C to 4 °C. Unfortunately, bad weather conditions hampered the planned observations during the February cruise. Only in the western and southern part of the Baltic observations could be performed (Fig. 18). The lowest surface temperature was observed in the Slupsk Furrow with 3.25 °C. This exceeded the climatological mean of 1.8 °C by 1.5 K. At the central station of the AB (TF0113) the SST of about 3.9 °C (climatological mean 1.9 °C) was slightly lower than in the Belt Sea. As in the previous years the surface temperatures were well above the temperature of maximum density- in the entire western and southern Baltic. Therefore, the

temperature driven convection was still ongoing, and no shallow temperature stratification was observed in the beginning of February. The upper layer was homogenized down to 40 m to 60 m depth.

The temperature distribution below the halocline is governed by the inflow of saline water from the North Sea. In the second half of 2021 baroclic inflows and a minor barotropic inflow transported warm water into the western Baltic. This is visible as warm halocline layer in the eastern Bornholm Basin and as deep water in the Slupsk Furrow. In January 2022 a minor barotropic inflow event carried about 54 km³ of cool saline water into the western Baltic. In February 2022 the bottom layer in the AB was covered with this cool water, forming a bottom layer in the western and central part of the AB. The temperature in the bottom water of 4.5 °C was only 0.5 K warmer than the surface water. In the eastern AB remains of the warm autumn inflows are still present. The major part of the warm autumn inflows covered the upper halocline of the Bornholm Basin and the Slupsk Furrow. The maximum temperature in the halocline of the Bornholm Basin was 10.2 °C. Below 65 m depth the temperature decreased towards the bottom to about 8.4 °C. The bottom water temperature was 9.0 °C in the Slupsk Furrow.

The exceptional high temperatures in February 2022 caused only weak surface cooling during the late winter. End of March the sea surface temperatures were rising and a weak seasonal thermocline was developing in the western Baltic. Here the surface temperatures ranged between to 4.5 °C and 5.2 °C from the Fehmarn Belt to the Arkona Basin, which was about 2 K above the climatological mean. At the central station of the Bornholm Basin TF213 the SST was 4.4 °C. The SST decreased to the further east and reached 3.3 °C in the Eastern Gotland Basin, 3.1 °C in the Farö Deep, and 2.8 °C in the Northern Gotland Basin. Below the thin warming surface layer the cold winter water becomes enclosed. The eastward advection of saline water from minor inflows in autumn and winter control the temperature distribution below the surface layer. The bottom water in the Arkona Basin is covered by cold waters from the January inflow event, which is only slightly warmer than the intermediate winter water layer. The cold inflow has reached the western Bornholm Basin where it pushes the warm halocline water eastward. However, the major part of the halocline water in the Bornholm Basin still consists of the warm autumn inflow. The temperature maximum in the Bornholm Basin was found at station TF0213 with 9.5 °C at 66 m depth. The bottom water temperature in the Bornholm Basin was 7.82 °C, slightly cooler than in February. A part of the cold water from the Bornholm Basin upper halocline water crossed the Slupsk Sill and formed the new cooler bottom water layer in the Slupsk Furrow. Here the bottom water temperature decreased significantly from 8.6 °C to 8.1 °C. At the entrance of the Eastern Gotland Basin small warmer patches of inflow water were observed. They move northward and will be sandwiched in the halocline of the Eastern Gotland Basin. The temperature maximum in the Eastern Gotland Basin was found at 150m depth with 7.26 °C. The bottom temperatures at station TF 0271 (Gotland Deep) and in the Farö Deep did not change significantly and were still at 7.22 °C and 7.21 °C respectively.

In the first half of May the seasonal thermocline was established also in the central Baltic. The sea surface temperatures ranged from 10.8 °C in the Kiel Bight, 9.0 °C in the Arkona Basin, and 6.0 °C in the Eastern Gotland Basin. This was 2 K above the climatological mean values for the western Baltic, but close to the long term mean in the central Baltic. A strong SST gradient was observed from the Arkona Basin to the Bornholm basin. The thermocline depth in the western

Baltic was at shallow depth of 15 m to 20 m. It increases east ward to about 30 m depth in the central Baltic. Below the thermocline the winter water layer was well pronounced even in the western Baltic. In the Bornholm Basin the core temperature of winter water was 4.6 °C. It decreased slightly to 4.5 °C in the Slupsk Furrow. In the Eastern Gotland Basin the winter water layer was somewhat cooler with 3.7 °C.

Below the intermediate layer the temperatures increase with depth. In the halocline of the Bornholm Basin the remains of the warm inflow waters from autumn 2021 were mixed up with the colder water from January inflow. This led to an increase in the bottom water temperature in the Bornholm Basin to 8.1 °C. In the Slupsk Furrow the deep-water conditions did not change significantly. Here the bottom water temperature was about 8.0 °C. At the eastern sill of the Slupsk Furrow a small overflow of warm deep water towards the Gotland Basin is visibly. The warm water patch observed in the Southern Gotland Basin in March was mostly mixed up the upper deep-water layer of the Gotland Basin. There was no significant change observed in the deep water and bottom water layer of the Eastern Gotland Basin. The maximum temperature of deep water (7.26 °C) was found at 160 m. The bottom water temperature was found unchanged at 7.22 °C. This indicates that none of the inflowing warm plumes was dense enough to reach the bottom of the basin. The bottom water temperature in the Farö Deep was 7.21 °C.

In the early August 2022 the surface temperature in the Baltic has reached its annual maximum. A strong summer thermal stratification has developed throughout the Baltic Sea. The seasonal thermocline, which separated the warm layer of surface water from the cooler intermediate water, was found at relatively shallow depths of about 15 m in the western Baltic. In the Fehmarn Belt the surface temperature reached 21.2 °C. In the Arkona Basin 18.8 °C were measured in the surface layer. Below the thermocline a cool layer with remains of former winter water was still present, with a minimum temperature of 8.6 °C. The bottom layer in the Arkona Basin was covered with warmer waters from baroclic inflows, which led to an increase in deep water temperature to 13.6 °C. At the Darss Sill a patch of extreme warm bottom water from an active baroclic overflow is visible. Here the bottom water temperature was 15.6 °C.

In the Bornholm Basin an SST of 18.5 °C was observed, which was 1.5 K above the long-term mean. The thermocline in the Bornholm Basin was located at 24m depth. Towards the central Baltic the SST increased. In the Eastern Gotland Basin the SST amounted to 19.9 °C in a very thin surface layer of 13 m thickness at station TF271. For this location the climatological mean value for August is 17.0 °C. Generally, in the central Baltic the SST was extreme high, but it did not reach the temperatures observed in July 2018, when SST of 23.9 °C was recorded in the Eastern Gotland Basin.

Despite of the high SSTs throughout the Baltic, below the thermocline the winter water layer depicted normal temperature values. Minimum temperatures in this intermediate water layer were about 3.9 °C in the Eastern Gotland Basin, and 3.6 °C in the Northern Gotland Basin, which caused a strong vertical temperature gradient between 15 m and 25 m. In the Bornholm Basin and the Slupsk Furrow the winter water layer was slightly warmer with core temperatures of about 5.0 °C. In the western Bornholm Basin the tip of the warm baroclic inflow water is spreading along the bottom. This plume depicted a core temperature of 12.3 °C at 55 m depth. The bottom water in the basin was still covered with mixed water from the previous autumn/winter inflows. The

stagnation in the deep basins of the central Baltic is ongoing. The bottom temperature in the Eastern Gotland Basin remains unchanged and was still at 7.22 °C. The weak diapycnal mixing in the Basin smoothed the vertical temperature gradients in the deep water so that there is almost no vertical temperature gradient below 120m.

The general temperature distribution in November depicted the autumnal cooling and the erosion of the seasonal thermocline in the surface layer. The seasonal surface cooling has deepened the surface mixed layer to 30 m to 35 m. However, the surface temperatures were still high. In the Arkona Basin surface temperatures of about 11.7 °C were observed, which are 2.5 K higher than the climatological mean. In the Bornholm Basin at station TF213 the SST of 12.7 °C was about 4 K higher than normal. Towards east the SST decreased only slightly. In the Slupsk Furrow the SST was 12.3 °C. In the Eastern Gotland Basin the SST was 10.8 °C at station TF0271, still 2.4K above the long term mean. The deepening of the seasonal thermocline reduced the vertical extend of the winter water layer to about 35 m thickness, with minimum temperatures of 4.3 °C in the Eastern Gotland Basin. In the Bornholm Basin only smaller patches of intermediate winter water were found above the halocline. From the Belt Sea to the Arkona Basin the bottom water is significantly warmer than the surface water layer. In September 2022 an unusual minor barotropic inflow transported 26 km³ saline water into the western Baltic. This water filled the bottom layer of the Arkona Basin that depicted a maximum deep-water temperature of 14.1 °C. Parts of this warm water have reached the western Bornholm Basin and flushed the bottom layer there. The temperature distribution in the Bornholm Basin was quite patchy. Warm summer inflows and former cold bottom water were concurrently present. In the central part warm waters from summer inflows dominating. The maximum temperature in this water body was 12.6 °C. The Slupsk Furrow was flushed with warm halocline water from the Bornholm Basin. The bottom temperature in the Slupsk Furrow increased to about 8 °C. The deep-water temperature conditions in the Gotland Basin remained still unchanged, with bottom temperature of 7.22 °C at station TF0271. In November 2022 a number of planned stations in the Northern Gotland Basin could not be performed due to bad weather conditions.

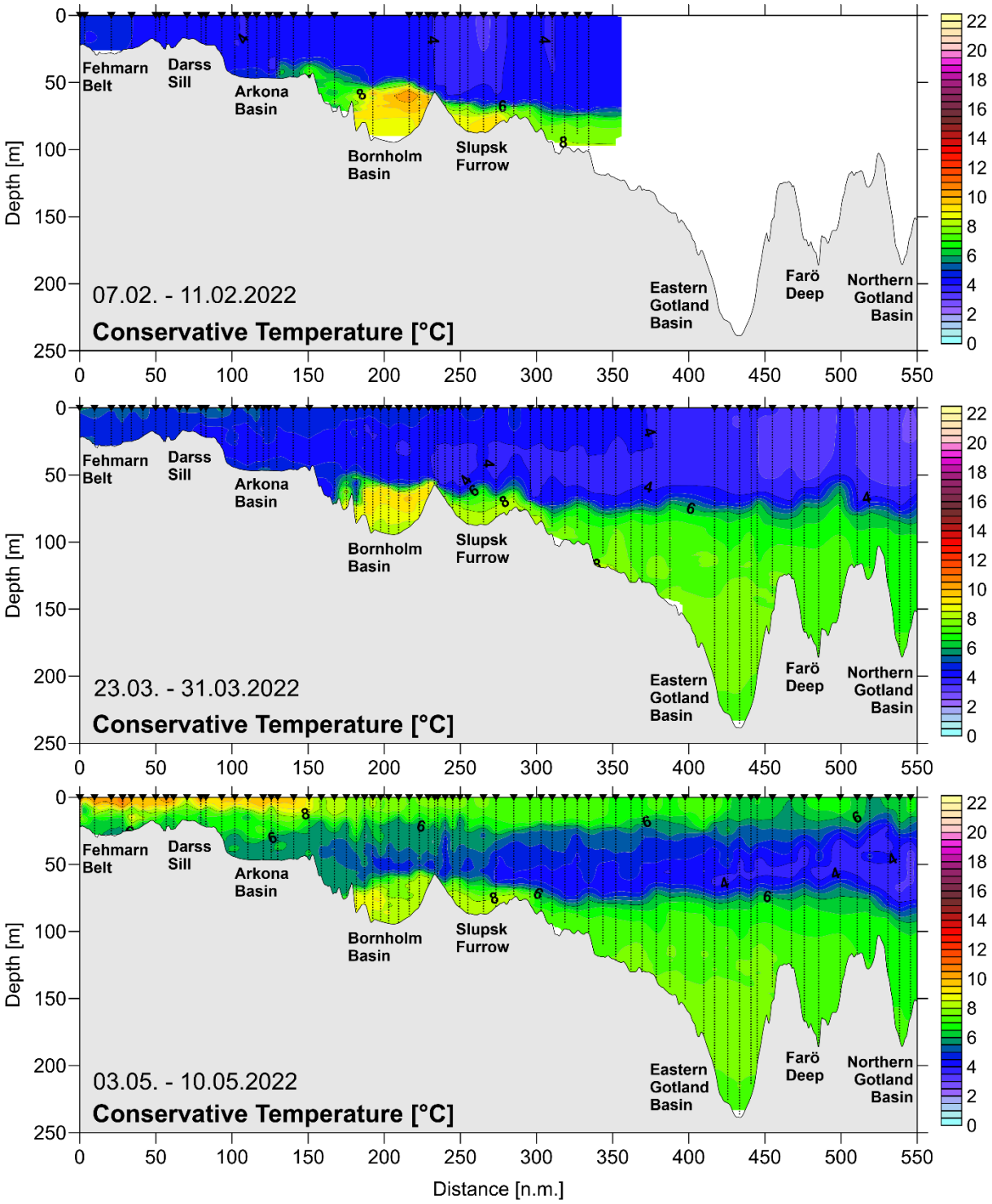


*Fig. 18: Temperature distribution along the thalweg transect through the Baltic Sea between Darss Sill and Northern Gotland Basin for February, March, and May 2022.*

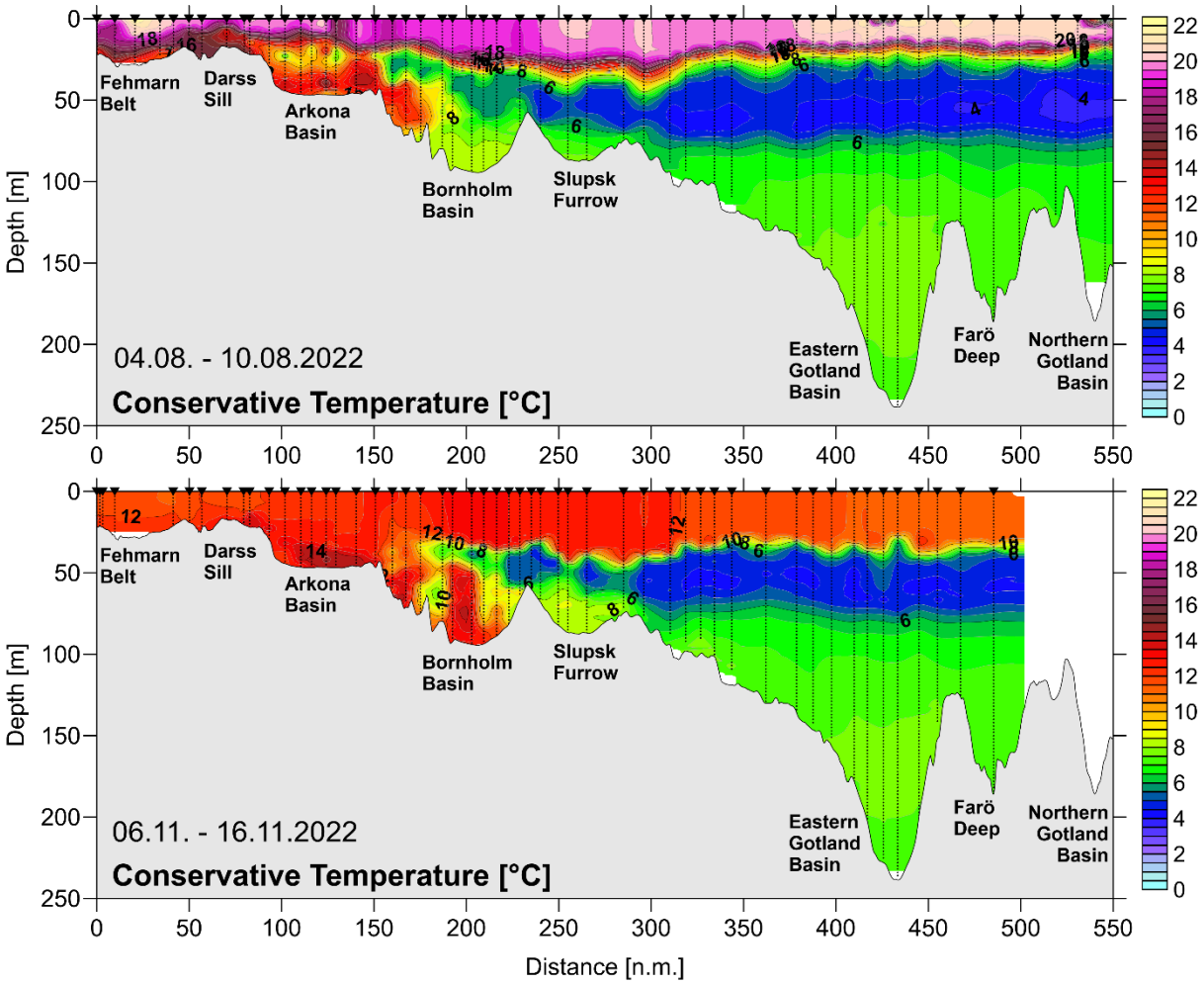


*Fig. 19: Temperature distribution along the thalweg transect through the Baltic Sea between Darss Sill and Northern Gotland Basin for August and November 2022.*

As part of its long-term monitoring programme, IOW operates hydrographic moorings near station TF271 in the Eastern Gotland Basin since October 2010. In contrast to the Gotland Northeast mooring, operational since 1998 and from where the well-known 'Hagen Curve' (FEISTEL et al. 2006, NAUMANN et al. 2017) is derived, the mooring at TF271 also collects salinity and oxygen data. The gathered time series data allow the description of the development of hydrographic conditions in the deep water of the Gotland Basin in high temporal resolution. This time series greatly enhances the IOW's ship-based monitoring programme. Figure 20 shows the temperature time series at five depths in the deep water of the Eastern Gotland Basin between January 2021 and December 2022. In the year 2021 the temperature stratification in the deep water is characterized by a downward decreasing temperature, although the vertical temperature gradient of 1 mK $m^{-1}$ is rather weak. This gradient is stable till October 2021. Then the vertical temperature gradient is further decreasing and reached only 0.3 mK $m^{-1}$ in February/March 2022. It remained at that level throughout the year 2022. The reduction of the temperature gradient between October 2021 and February 2022 was most probably caused by the enhanced forcing and the higher level of eddy kinetic energy during the winter months. During that time, the shallow seasonal thermocline in the upper layer vanished and allowed the atmospheric forcing to act directly down to the halocline. The increase in dynamic forcing enhances also the short-term variability in the temperature time series, especially between November and February. The

recent inflow events were not dense enough to reach the deep layers of the Eastern Gotland Basin. Thus, the period of relatively warm deep-water conditions is continued in 2022.

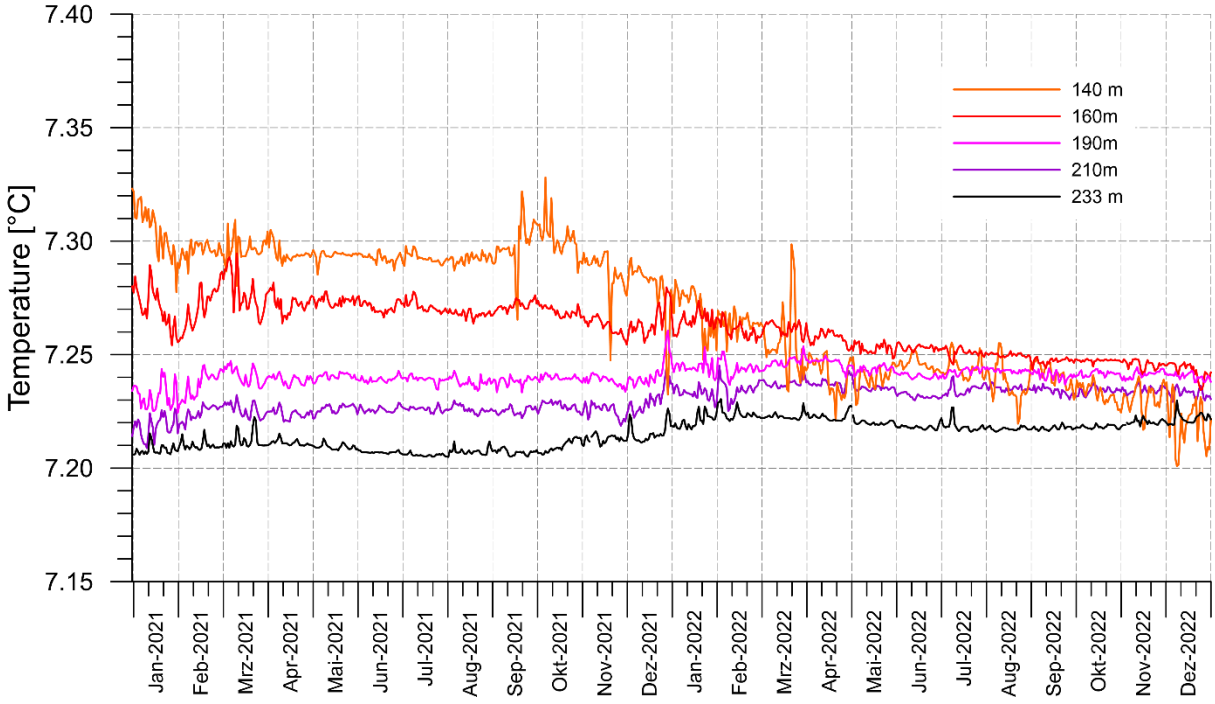


*Fig. 20: Temporal development of deep-water temperature in the Eastern Gotland Basin (station TF271) from January 2021 to December 2022 (daily averages of original data with 10 min sampling interval).*

Table 7.1 summarises the annual means and standard deviations of temperature in the deep water of the central Baltic based on CTD measurements over the past five years. The deep water temperatures in the entire Baltic remained at nearly the same level as in 2021, with the exception of slightly decrease in the Farö Deep and the Landsort Deep. This stopped the generally increasing trend that was previously observed since the extreme Christmas MBI in 2014. However, the absolute decrease in deep water temperatures was extremely weak. The tiny increase of 0.01 K at 200 m depth in the Eastern Gotland Basin can be attributed to vertical mixing processes with the warmer water above this layer. In the Farö Deep the temperature at 150 m depth was decreasing by 0.06 K with an extreme low standard deviation. The weak decrease in the Landsort deep and the Karlsö Deep might be caused by the ongoing slow spreading of the halocline water of the northern Baltic. In the Bornholm Basin the deep-water temperature was constant, but depicted a high standard deviation of 0.94 K caused by the active inflow dynamic of baroclic and minor barotropic inflows.

*Table 7: Annual means and standard deviations of temperature, salinity and oxygen concentration in the central Baltic Sea: IOW- and SMHI data (n= 14-24).*

*Table 7.1: Deep water temperature (°C; maximum in bold).*

| Station | Depth m | 2018 | 2019 | 2020 | 2021 | 2022 |
|---|---|---|---|---|---|---|
| **213** (Bornholm Deep) | 80 | 7.81 ±1.49 | **8.65 ±0.12** | 8.45 ±0.29 | 8.42 ±0.39 | 8.43 ±0.94 |
| **271** (Gotland Deep) | 200 | 6.89 ±0.01 | 7.20 ±0.07 | 7.21 ±0.01 | 7.23 ±0.00 | **7.24 ±0.00** |
| **286** (Fårö Deep) | 150 | 6.70 ±0.04 | 7.05 ±0.18 | 7.24 ±007 | **7.24 ±001** | 7.18 ±0.01 |
| **284** (Landsort Deep) | 400 | 6.27 ±0.03 | 6.37 ±0.15 | 6.60 ±0.27 | **6.67 ±0.02** | 6.57 ±0.02 |
| **245** (Karlsö Deep) | 100 | 5.67 ±0.12 | 5.64 ±0.12 | 5.83 ±0.11 | **6.05 ±0.11** | 6.04 ±0.09 |

*Table 7.2: Deep water salinity (maximum in bold).*

| Station | Depth m | 2018 | 2019 | 2020 | 2021 | 2022 |
|---|---|---|---|---|---|---|
| **213** (Bornholm Deep) | 80 | **16.64 ±0.32** | 16.63 ±0.27 | 16.34 ±0.34 | 15.84 ±0.26 | 15.03 ±0.36 |
| **271** (Gotland Deep) | 200 | **13.17 ±0.03** | 13.16 ±0.03 | 13.03 ±0.03 | 12.93 ±0.03 | 12.77 ±0.03 |
| **286** (Fårö Deep) | 150 | **12.50 ±0.12** | 12.46 ±0.08 | 12.39 ±0.03 | 12.24 ±0.08 | 12.02 ±0.03 |
| **284** (Landsort Deep) | 400 | **11.41 ±0.05** | 11.33 ±0.06 | 11.34 ±0.16 | 11.24 ±0.06 | 10.94 ±0.02 |
| **245** (Karlsö Deep) | 100 | **10.44 ±0.21** | 10.35 ±0.24 | 10.40 ±0.18 | 10.36 ±0.18 | 10.26 ±0.12 |

## 4.2 Salinity

The vertical distribution of salinity in the western and central Baltic Sea during IOW's five monitoring cruises is shown in Fig. 21 and Fig. 22. The salinity distribution is markedly less variable than temperature distribution, and a west-to-east decreasing gradient in the surface and the bottom water is typical. Greater fluctuations in salinity are observed particularly in the western Baltic Sea where the influence of salt-water inflows from the North Sea is strongest. The duration and influence of minor inflow events is usually too small to be reflected in the overall

salinity distribution. Only combined, they can lead to slow, long-term changes in salinity. The salinity distributions shown in Fig. 21 and Fig. 22 are mere 'snapshots' that cannot provide a complete picture of inflow activity. In 2022 the evolution of salinity distribution was mainly controlled by the minor barotropic inflows in autumn and winter 2021/2022, the baroclinic inflows in late summer and the minor barotropic inflow in September 2022. However, the IOW monitoring cruises covered the inflows only partly. The salinity at the Darss Sill was below 17 g $kg^{-1}$ during all cruises, although there were significant volumes of high saline water observed in the Fehmarn Belt. It is not possible to produce meaningful statistics on inflow events, by using only the monitoring cruises. The analyses of the sea level changes and the salinity observations in the western Baltic revealed a moderate barotropic inflow activity in the winter season 2021/2022. Weak barotropic inflows were detected in October 2021 (0.72 Gt salt) and in January/February/March 2022 (in total 1.86 Gt salt), which transported together about 2.6 Gt salt into the western Baltic. Another minor inflow was observed in September 2022 (0.56 Gt salt). During summer and autumn 2022 baroclic inflows dominated the water exchange with the North Sea.

The first monitoring cruise in 2022 was performed shortly after the moderate inflow in January. The salinity in the Fehmarn Belt was relatively high with 21.3 g $kg^{-1}$ throughout the water column. At the Darss Sill bottom salinity of 14.4 g $kg^{-1}$ was observed. The saline layer covered here the water column from 7m depth downward. The major part of the inflow water was found in the Arkona Basin, where it formed a saline bottom layer up to 20 m thickness. Its maximum salinity was 18.0 g $kg^{-1}$. Above the bottom water the basin was filled with the brackish Baltic surface water with a salinity of 8.0 g $kg^{-1}$ to 8.5 g $kg^{-1}$. The eastern AB and the Bornholmgat were already filled with warmer saline water from autumn inflows. In the Bornholm Basin the halocline depth was at 49 m, 5 m above the sill depth of the Slupsk Sill. In the deep water layer the salinity increased continuously to a bottom salinity of 15.4 g $kg^{-1}$. The Slupsk Furrow depicted relatively low saline waters in the deep layer. The bottom salinity was only 12.1 g $kg^{-1}$. Due to bad weather conditions during the February cruise no data could be gathered in the Gotland Basin.

In March 2022 the salinity distribution in the western Baltic was still affected by the minor barotropic inflows, although no active inflow was covered during that cruise. The bottom salinity in the Fehmarn Belt was 21.1 g $kg^{-1}$. The surface layer depicted an outflow of brackish water of about 9.1 g $kg^{-1}$. At the Darss Sill no saline bottom layer was found. Here the brackish surface water covered the entire water column. In the Arkona Basin the total volume of the saline bottom pool from the winter inflows has strongly decreased. Here a maximum bottom salinity of 15.8 g $kg^{-1}$ was detected. The halocline depth increased considerably to 37 m. The major part of the inflow waters has left the AB and reached the western Bornholm Basin as seen in the temperature distribution. The changes in the stratification were weak. The bottom salinity in the Bornholm Basin was 15.6 g $kg^{-1}$. Parts of the inflowing saline waters have crossed the Bornholm Basin in the halocline layer and reached the Slupsk Furrow. At station TF0222 the bottom salinity increased by about 1.4 g $kg^{-1}$ to 13.5 g $kg^{-1}$ since February. Due to the lack of larger inflow events in the recent years the salinity in the deep water of the central Baltic Sea decreased continuously since 2016. The bottom salinity in the Gotland Deep was of 12.90 g $kg^{-1}$. The 12 g $kg^{-1}$ isohaline was at a depth of around 132 m, nearly 20 m deeper as observed one year before, pointing to a continuous salt loss of the deep water by weak vertical mixing. The 13 g $kg^{-1}$ isohaline vanished.

In the previous year it was found at 205 m depth. Further north in the Farö Deep the bottom salinity in the was 12.16 g $kg^{-1}$, nearly 0.3 g $kg^{-1}$ less than one year before. The stagnation in the bottom waters of the central Baltic was still ongoing.

During the spring monitoring cruise in May the salt distribution in the Fehmarn Belt and at the Darss Sill depicted a strong stratification. The bottom salinity in the Kiel Bight was 26.9 g $kg^{-1}$ and dropped strongly to 18.1 g $kg^{-1}$ in the Fehmarn Belt. However, the surface layer was covered by brackish Baltic surface water of about 9 g $kg^{-1}$ salinity. At the Darss Sill the bottom salinity was only 14.0 g $kg^{-1}$. The saline bottom water pool in the AB has not changed its volume significantly. The halocline was found at 37 m depth in the centre of the basin. The bottom salinity of amounted to 17.5 g $kg^{-1}$, 1.5 g $kg^{-1}$ above the March value. In the Bornholm Basin the halocline depth was found at 57 m depth, close to the sill depth of the Slupsk Sill. The bottom salinity in the Bornholm Basin was further decreased to 15.2 g $kg^{-1}$ at station TF0213. The saline deep-water pool in the Slupsk was slightly increased. Here the bottom salinity was 13.6 g $kg^{-1}$. A small patch of saline water has left the Slupsk Furrow eastward and entered the Southern Gotland Basin. No significant changes of deep-water conditions were observed in the central Baltic. At station TF271 (Gotland Deep) the bottom salinity remained nearly unchanged at 12.90 g $kg^{-1}$. The 12 g $kg^{-1}$ isohaline was at a depth of 138 m. Six metres deeper than in March. A bottom salinity of 12.15 g $kg^{-1}$ was observed in the Farö Deep.

The observations during the summer cruise in August 2022 depicted the ongoing of baroclic inflows through the Belt Sea. A strong continuous salinity gradient of 0.5 g $(kg\ m)^{-1}$ occurred between the surface and the bottom in the Fehmarn Belt and the Darss Sill. In the Fehmarn Belt the surface and bottom salinities amounted to 12 g $kg^{-1}$ and 23.5 g $kg^{-1}$, respectively. At the time of the cruise a patch of extremely warm inflow water with 14.2 g $kg^{-1}$ salinity passed the Darss Sill, but has not reached the Arkona Basin yet. The pool of saline bottom water in the Arkona Basin was moderately filled with warm, but less saline water from a previous baroclic inflow. At Station TF0113 in the centre of the basin this inflow water with a maximum salinity of 15.6 g $kg^{-1}$ formed a 10 m to 15 m thick layer. The tip of this water mass has passed the Bornholmgat, and spreads into the western Bornholm Basin. Here the halocline depth has lifted up by about 10 m. At station TF0213 the bottom salinity remained at 15.1 g $kg^{-1}$. The halocline depth in the eastern Basin was found at 55 m. Further east, in the central Baltic basins, again no significant changes were observed. The depth of the 12 g $kg^{-1}$ isohaline in the Gotland Deep was at 136 m. The bottom salinity in the Gotland Deep and the Farö Deep was 12.87 g $kg^{-1}$ and 12.13 g $kg^{-1}$, respectively, which was 0.03 g $kg^{-1}$ less than in May. The surface salinity in the central Baltic decreased according its usual seasonal cycle, and was at 6.80 g $kg^{-1}$ in the Eastern Gotland Basin.

In September 2022 a weak barotropic inflow transported about 26 $km^3$ saline water into the western Baltic. The results of this inflow were detected during the November cruise. In the Fehmarn Belt the bottom salinity amounted to 23.6 g $kg^{-1}$. However, at the Darss Sill brackish Baltic surface water covered most of the water column. A thin bottom layer of saline water depicted a maximum salinity of 12.8 g $kg^{-1}$. The water of the September inflow was met in the Arkona Basin where it formed warm and bottom layer of 18 m thickness. The maximum bottom salinity of 19.1 g $kg^{-1}$ was about 4 g $kg^{-1}$ higher than in August. The warm saline water from the inflows has also reached deep layers of the Bornholm basin. Here the old bottom water was replaced with warm water of 17.6 g $kg^{-1}$ salinity. The halocline in the Bornholm Basin was lifted

up to 49 m at station TF0213. This enabled an overflow of the Slupsk Sill by halocline water, which increased the salinity in the bottom water pool of the Slupsk Furrow to 13.0 g kg$^{-1}$. The stagnation in the deep water of the central Baltic was still ongoing. The bottom salinity decreased very slowly in the Gotland Deep and the Farö Deep to 12.86 g kg$^{-1}$ and 12.11 g kg$^{-1}$, respectively. Bad weather conditions in November did not allow observations in the Northern Gotland Basin.

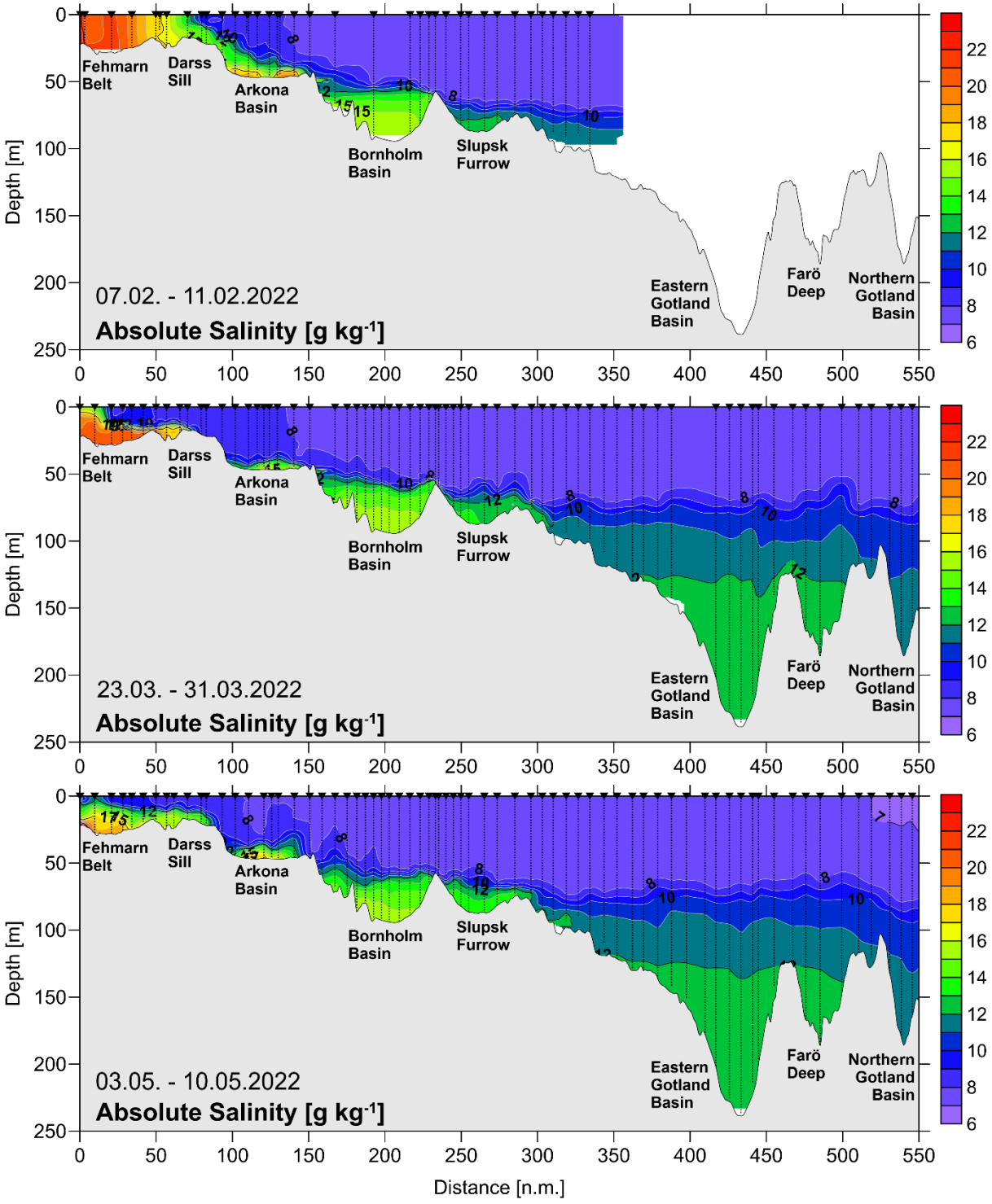


*Fig. 21: Salinity distribution along the thalweg transect through the Baltic Sea between Darss Sill and Northern Gotland Basin for February, March, and May 2022.*

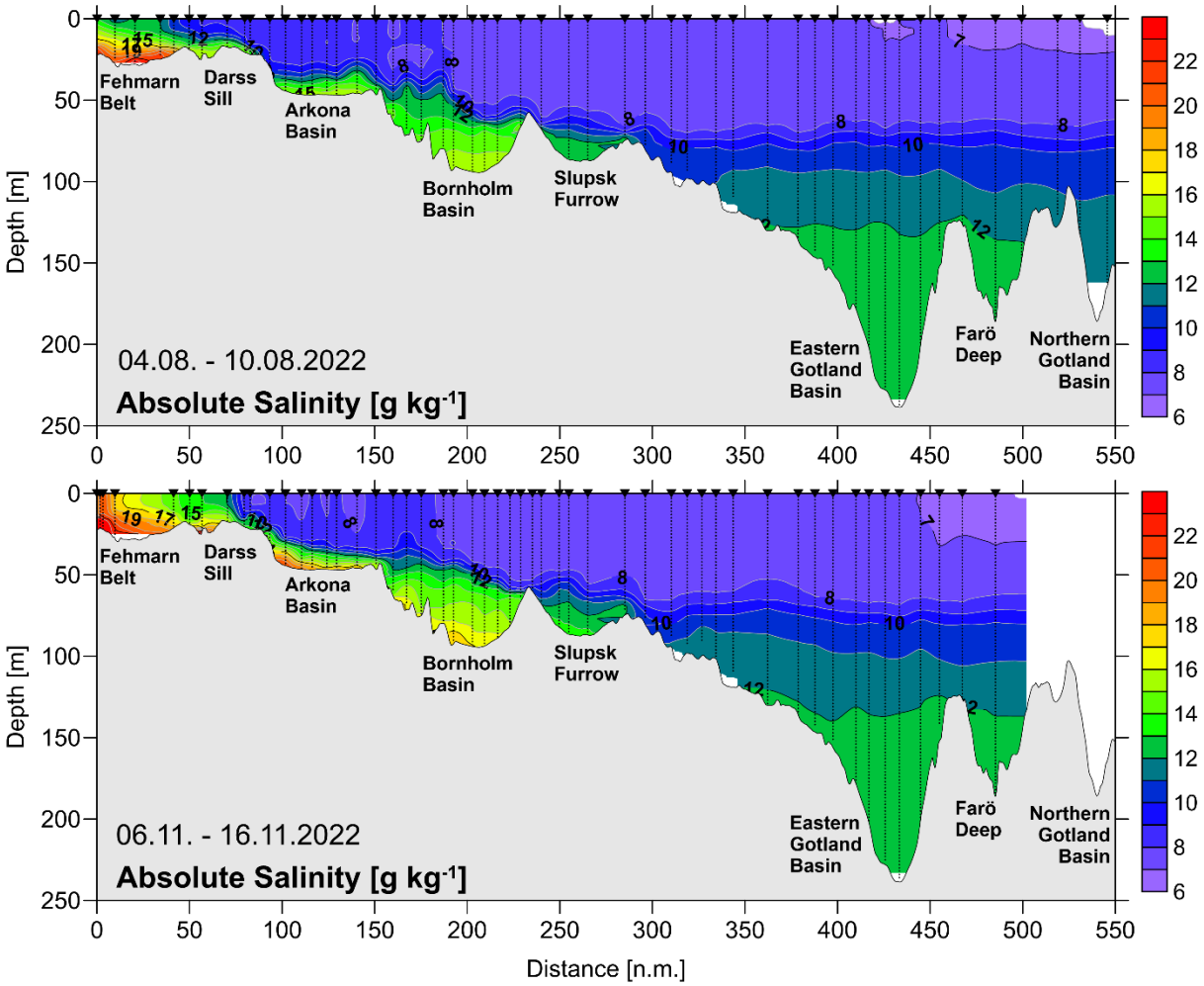


*Fig. 22: Salinity distribution along the thalweg transect through the Baltic Sea between Darss Sill and Northern Gotland Basin for August and November 2022.*

Table 7.2 shows the overall trend of salinity in the deep water of the Baltic in the past five years. After the series of stronger inflow events in 2014 to 2016 the bottom salinity in the Gotland Deep and Farö Deep reached its maximum in 2016 and 2017. Since than only weak changes in salinity stratification were observed in the central Baltic. The deep-water salinity in the Eastern Gotland Basin dropped slightly due to vertical mixing by 0.10 g $kg^{-1}$ to 0.15 g $kg^{-1}$ per year. In the Farö Deep the annual salinity decrease is about 0.08 g $kg^{-1}$ to 0.20 g $kg^{-1}$. Also in the Karlsö Deep and Landsort Deep the slow decrease of deep water salinity has continued. In the Bornholm Basin the mean deep-water salinity decreased also in 2022. However, the high standard deviation of salinity in the Bornholm basin is caused by rapid fluctuations due to particular inflow events. Thus, the drop in deep-water salinity of the Bornholm Basin do not point to an overall trend.

No clear trend was visible in the surface salinity of the Baltic. In the Eastern Gotland Basin and the Farö Deep the surface salinity decreased by about 0.2 g $kg^{-1}$. An opposite behaviour was seen west of Gotland in the Landsort Deep and the Karlsö Deep. Table 7.3 summarises the variations in surface layer salinity.

*Table 7.3: Annual means of 2018 to 2022 and standard deviations of surface water salinity in the central Baltic Sea (minimum values in bold, n= 14-24). The long-term averages of the years 1952-2005 are taken from the BALTIC climate atlas (FEISTEL et al. 2008).*

| Station | 1952-2005 | 2018 | 2019 | 2020 | 2021 | 2022 |
|---|---|---|---|---|---|---|
| **213** (Bornholm Deep) | 7.60 ±0.29 | **7.53 ±0.08** | 7.63 ±0.11 | 7.80 ±0.18 | 7.54 ±0.26 | 7.66 ±0.06 |
| **271** (Gotland Deep) | 7.26 ±0.32 | **7.09 ±0.27** | 7.19 ±0.25 | 7.33 ±0.16 | 7.36 ±0.13 | 7.17 ±0.25 |
| **286** (Fårö Deep) | 6.92 ±0.34 | 6.92 ±0.34 | **6.78 ±0.33** | 7.07 ±0.29 | 7.12 ±0.23 | 6.85 ±0.39 |
| **284** (Landsort Deep) | 6.75 ±0.35 | 6.59 ±0.32 | 6.52 ±0.26 | 6.58 ±0.50 | **6.33 ±0.33** | 6.58 ±0.28 |
| **245** (Karlsö Deep) | 6.99 ±0.32 | 7.06 ±0.18 | 6.89 ±0.24 | 7.16 ±0.12 | **6.86 ±0.25** | 6.98 ±0.31 |

Fig. 23 shows the temporal development of salinity in the deep water of the Eastern Gotland Basin between January 2021 and December 2022, based on data from the hydrographic moorings described above. The stratification in this period was controlled by stagnation and weak vertical mixing. This led to a slowly decreasing salinity in the entire deep-water body, with a nearly constant vertical salinity gradient below 160 m depth. The higher temporal variability in the 140 m depth level was caused by pulse like inflows of saline water plumes into the halocline of the Eastern Gotland Basin.

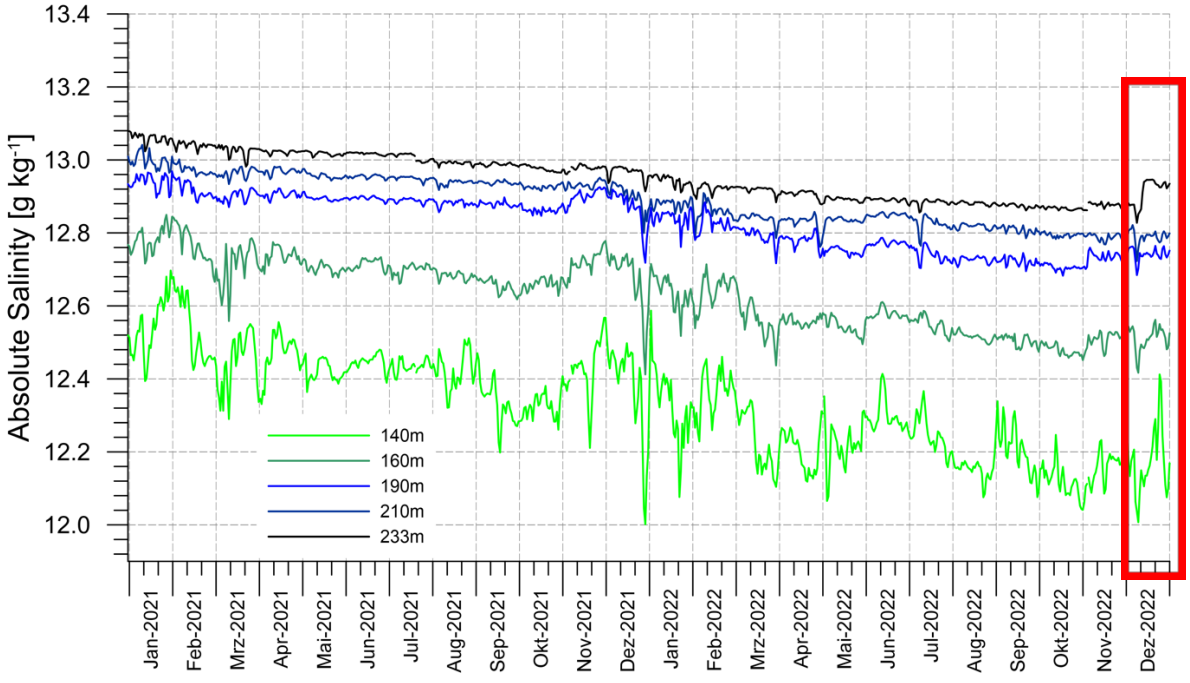


*Fig. 23: Temporal development of deep-water salinity in the Eastern Gotland Basin (station TF271) from January 2021 to December 2022 (daily averages of original data with 10 min sampling interval).*

## 4.3 Oxygen distribution

Availability of sufficient oxygen reflects a precondition for the survival of higher marine life. Low oxygen concentration occurs especially in density gradients and at the sea floor, where the ecosystem is biased at first. For the Baltic Sea, it is a natural phenomenon that oxygen supply to the deep basins is limited by a shallow and narrow transition area between the North Sea and the Baltic Sea. Although an almost permanent slow entrainment of oxygenated waters to the central Baltic Sea happens, only episodic strong inflows of cold and haline oxygenated waters, known as "Major Baltic Inflows" reach the bottom waters of the deep Baltic basins. The improvement is mainly determined by the supplied oxygen and the density of the water. However, the effect of recent strong MBIs only caused a relative short-term improvement, and after a few years of stagnation the water below the permanent halocline turned into anoxic and then to euxinic conditions again. This is in principle caused by the elevated density of the deep water after the MBI, initially hindering further MBIs. But the fast consumption of oxygen by mineralization of unprecedented enormous amounts of accumulated organic matter and reducing chemical species, mainly ammonium and hydrogen sulphide, appears to be a phenomenon of recent times. After oxygen depletion, other oxidants are used. Sulphate, a major constituent of seawater is converted to poisonous hydrogen sulphide that turns Baltic Sea deep waters into dead zones for aerobic life. This process is fostered by eutrophication and subsequent excessive supply of organic matter to the seafloor (DIAZ & ROSENBERG 2008). The lack of oxygen below the halocline of the Baltic Sea areas is evaluated by using the HELCOM oxygen debt indicator for the deep basins to estimate the deviation from a "good environmental status" (HELCOM 2013). However, recently it became obvious that also shallow Baltic Sea areas are more often subjected to temporally low oxygen values. Shallow areas in this context are regions, which are too shallow to establish a permanent halocline, usually shallower than about 60 m. Here, deep winter mixing each year oxygenates the water column down to the bottom. However, during summer the microbial decomposition of large amounts of organic matter requires considerable amounts of the present oxygen. In surface waters as well as in shallow areas, the gas exchange with the atmosphere maintains an oxygen concentration of seawater controlled by the surface water temperature. This includes release of oxygen during primary production in spring as well as uptake of oxygen during elevated remineralisation activity in summer and autumn (KUSS et al. 2006). The disconnection of deeper waters happens, when a stable thermocline develops in addition to the halocline, separating oxygenated surface waters from the waters below. Then, the oxygen concentration clearly declines by respiration in bottom waters that is not replenished during summer. Strong temperature and/or salinity gradients hinder mixing between the bottom and upper waters. So, lasting oxygen consumption during calm weather condition at summer water temperatures could threaten the ecosystem near the seafloor. To observe and finally to recommend measures, the bottom water oxygen concentration in shallow areas is for the first time assessed for test purposes during HOLAS III (HELCOM "Third Holistic Assessment of the Ecosystem Health of the Baltic Sea") by an indicator based on the long-standing application of the "Iltsvind" (Oxygen loss) model for the western Baltic Sea, proposed by the Danish party in HELCOM.

The overall decreasing trend of the oxygen concentration, in fact an accumulation of hydrogen sulphide expressed as negative oxygen concentration, in deep waters of the four Gotland Sea

deeps was basically ongoing (Table 7.4 - Oxygen). The choice of an individual reference depths in the middle of the respective deep waters thereby secures annual averages, basically unbiased from episodic smaller inflows that frequently occur in the depth range of the pycnocline and sediment resuspension in the bottom layer but their influnces disappear soon. At Gotland Deep station, the decline of oxygen continued since 2018 (-38 µmol $l^{-1}$) and showed in 2022 an accumulation of hydrogen sulphide equivalent to -243 µmol $l^{-1}$oxygen at 200 m depth. At Fårö Deep station in 150 m depth, oxygen decreased since 2018 (-33 µmol $l^{-1}$) to -123 µmol $l^{-1}$ oxygen in 2022. In the Western Gotland Basin the worst situations of the last years were in 2020 and 2022 and showed a little improvement in 2021. So, the annual average oxygen concentration in the Landsort Deep decreased from -25 µmol $l^{-1}$ in 2018 to -98 µmol $l^{-1}$ in 2020 and in 2022. In 2021 it was a little better with -74 µmol $l^{-1}$ oxygen equivalents of hydrogen sulphide. Likewise at Karlsö Deep oxygen concentration changed from -84 µmol $l^{-1}$ in 2018 to -102 µmol $l^{-1}$ in 2020 and -109 µmol $l^{-1}$ in 2022 at 100 m depth (Table 7.4). Bornholm Deep more frequently receives oxygenated waters from the Arkona Basin. Even in summer and autumn at higher temperatures, the density is often high enough to reach the deep waters. So the annual and interannual changes are more pronounced. Bornholm Deep station showed a change of the annual average oxygen concentration between almost 43 µmol $l^{-1}$ in 2019 and 2020, and 8 µmol $l^{-1}$ and hardly detectable 1 µmol $l^{-1}$ in 2021 and 2022, respectively, with a standard deviation of up to ±67 µmol $l^{-1}$ oxygen equivalents (Table 7.4).

*Table 7.4: Annual means and standard deviations of deep water oxygen concentration from 2018 to 2022 (µmol $l^{-1}$, hydrogen sulphide is expressed as negative oxygen equivalents; maximum in bold).*

| Station | Depth (m) | 2018 | 2019 | 2020 | 2021 | 2022 |
|---|---|---|---|---|---|---|
| **213** (Bornholm D.) | 80 | 7.1 ±16.5 | **43.3 ±67.0** | 39.7 ±59.8 | 7.6 ±41.1 | 1.3 ±46.1 |
| **271** (Gotland D.) | 200 | **-38.0 ±22.3** | -110.8 ±52.7 | -184.4 ±58.1 | -188.8 ±17.2 | -242.4 ±30.6 |
| **286** (Fårö D.) | 150 | **-32.6 ±18.8** | -77.7 ±18.3 | -63.4 ±28.6 | -94.6 ±17.8 | -122.9 ±74.8 |
| **284** (Landsort D.) | 400 | **-25.5 ±17.9** | -66.5 ±11.2 | -97.8 ±20.1 | -74.0 ±4.2 | -98.2 ±16.7 |
| **245** (Karlsö D.) | 100 | **-84.4 ±32.2** | -87.1 ±55.8 | -101.8 ±29.0 | -92.4 ±38.2 | -108.5 ±39.4 |

The oxygen concentration in surface water of respective areas from the Belt Sea to the western Gotland Sea is basically controlled by the seasonal changing temperature and primary production (Fig. 24a). The highest average oxygen concentrations measured during the monitoring campaigns were consequently observed in February, March and May between about 335 µmol $l^{-1}$ and 440 µmol $l^{-1}$ oxygen in 2022. The spring bloom may also significantly contribute to the oxygen concentration in March and May. Thereby, the maxima were mostly measured in

March, as this month usually shows the lowest water temperature. Except for the central eastern Gotland Sea, where oxygen was highest in May, likely supported by the spring bloom. For the Odra Bight, no mean oxygen concentration for March could be calculated from regular monitoring data. After the summer minimum in July between 265 µmol $l^{-1}$ and 315 µmol $l^{-1}$ oxygen in 2022, the concentration of oxygen was then higher in November likely caused by cooling and wind mixing at autumn weather conditions.

The bottom water of the shallow Belt Sea, Mecklenburg Bight and the Arkona Sea (Fig. 24b) showed a similar seasonal pattern as the surface water (Fig. 24a), however at a slightly lower concentration level. The maximum oxygen concentrations were between 320 µmol $l^{-1}$ and 380 µmol $l^{-1}$ in March 2022. The corresponding lowest average oxygen concentration in bottom waters in the western Baltic Sea were 80 µmol $l^{-1}$ and 170 µmol $l^{-1}$ recorded in the Mecklenburg Bight, and the Arkona Sea, respectively in August 2022. Until November, the oxygen concentration improved to almost 135 µmol $l^{-1}$ and more than 180 µmol $l^{-1}$, respectively, for these areas. The sampling schedule with five monitoring cruises annually, is relatively coarse and insufficient to record the annual oxygen minima at the respective sites. Thus, the summer monitoring measurements give only a rough impression of oxygen deficit in summer/early autumn of shallow Baltic Sea waters. The average oxygen concentration in the bottom water of the Bornholm Sea showed only a slight variability in 2022 between weak oxic of 7 µmol $l^{-1}$ oxygen in May and presence of some hydrogen sulphide in February, August and November. The worst average concentration of -50 µmol $l^{-1}$ hydrogen sulphide equivalents of oxygen was measured in August. In the relatively shallow south-eastern Gotland Sea an average weak oxic situation was measured during all campaigns in 2022 with 18 µmol $l^{-1}$ to 63 µmol $l^{-1}$ oxygen. The passage of oxygen bearing filaments is also apparent in the Fig. 25 and Fig. 26. The deep water usually reflects a more stable environment that is decoupled from processes in the halocline range and above. So during the year 2022 in the deep water layer of the eastern Gotland Sea the oxygen equivalent concentration of hydrogen sulphide reached record low concentrations of -313 µmol $l^{-1}$ and -470 µmol $l^{-1}$, in the northern Gotland Sea between -112 µmol $l^{-1}$ and -130 µmol $l^{-1}$, and in the western Gotland Sea between -90 µmol $l^{-1}$ and -135 µmol $l^{-1}$ oxygen equivalents, respectively. This shows an overall worsening trend with regard to the oxygen deficit compared to the last year.

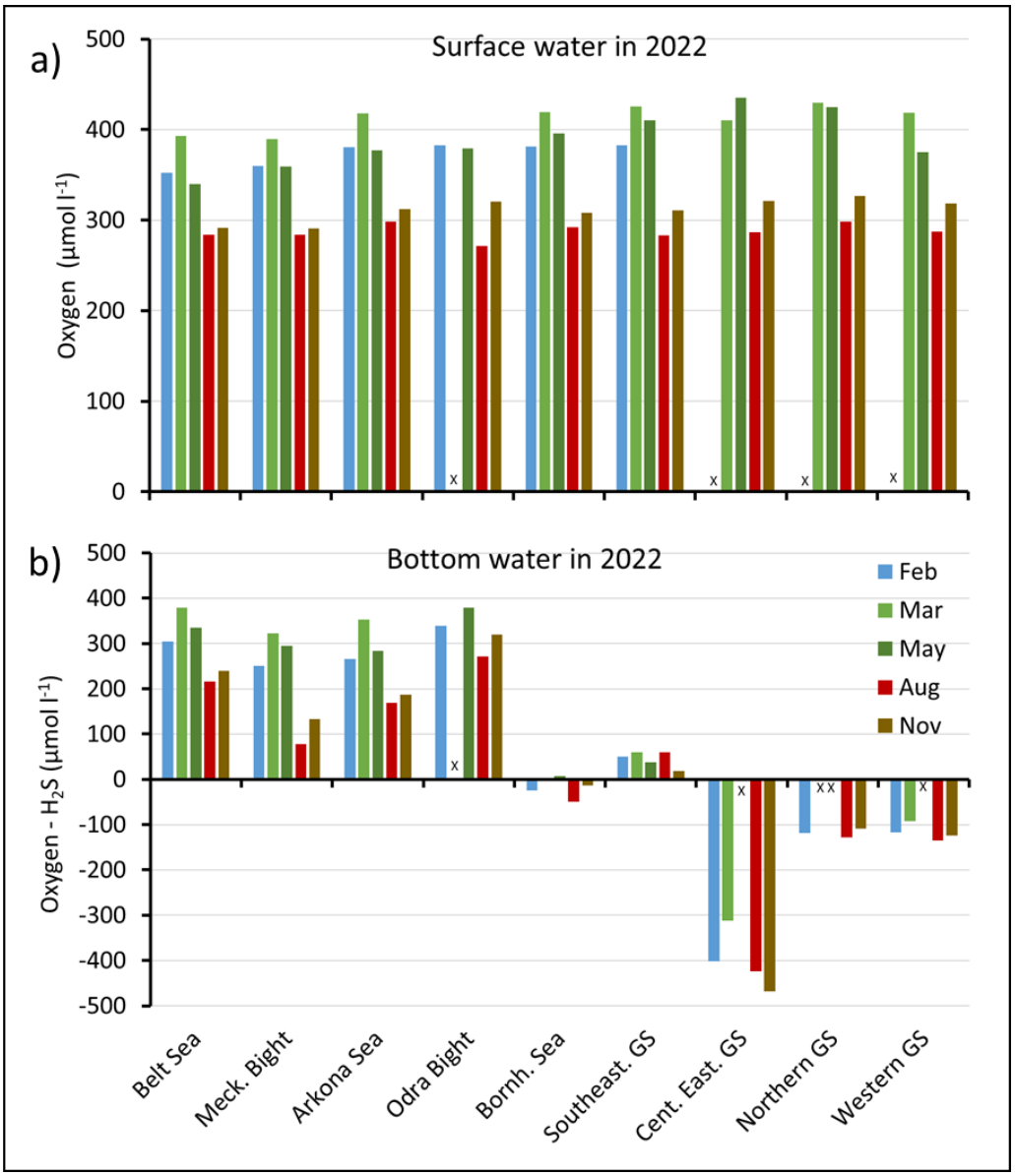


*Fig. 24: Comparison of average oxygen concentrations a) in surface waters (with O2-sensor data) and b) average oxygen/hydrogen sulphide concentrations in bottom waters (without sensor data) of the studied Baltic Sea areas of February to November: Belt Sea, Mecklenburg Bight, Arkona Sea, Odra Bight, Bornholm Sea, southern Gotland Sea, central eastern Gotland Sea, northern Gotland Sea, and western Gotland Sea.*

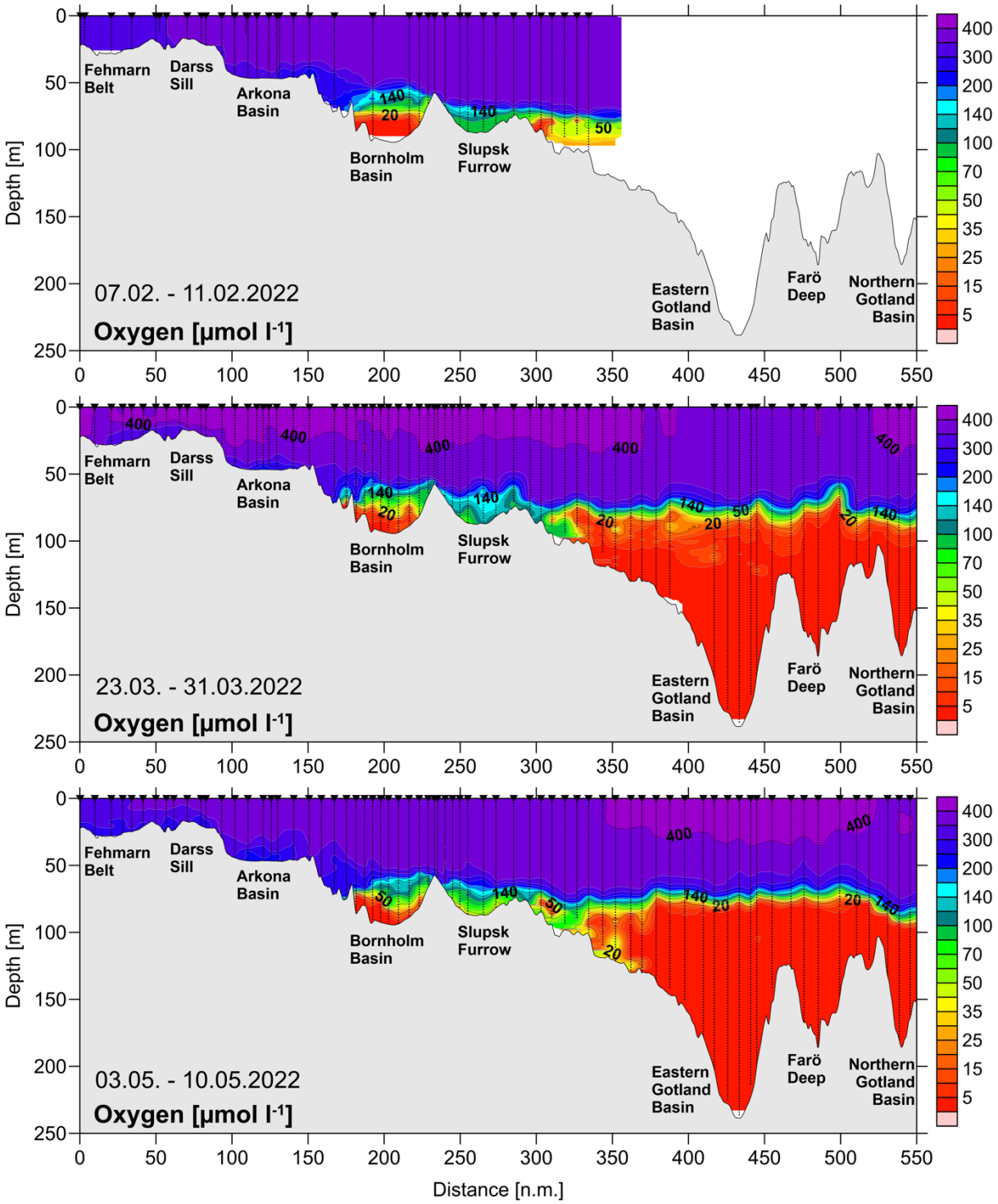


*Fig. 25: Vertical distribution of oxygen (without $H_2S$) during the February, March and May cruises in 2022 between the Darss Sill and the Northern Gotland Basin. Values below 5 µmol $l^{-1}$ could not be distinguished from 0 µmol $l^{-1}$.*

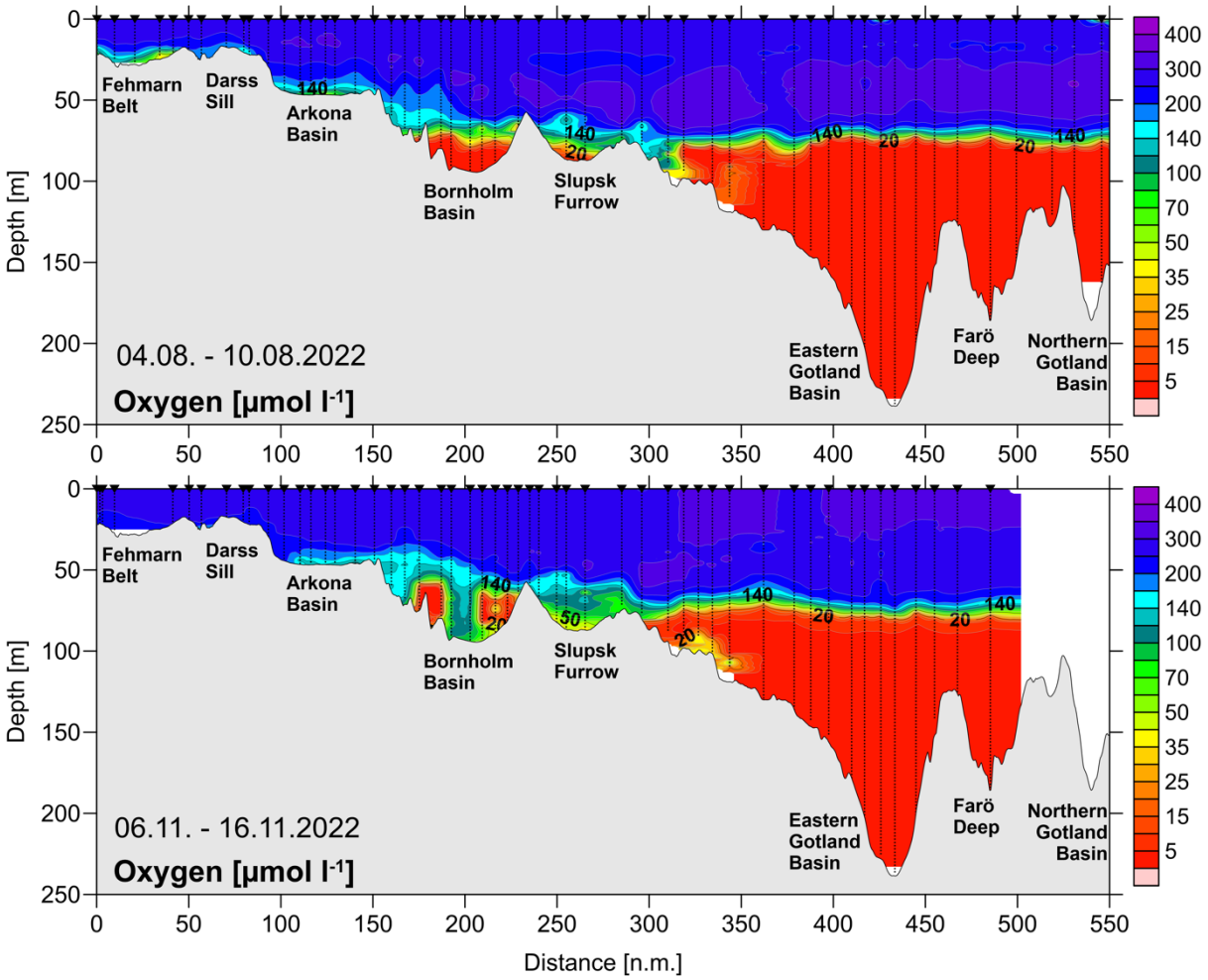


*Fig. 26: Vertical distribution of oxygen (without $H_2S$) during the August and November cruises in 2022 between the Darss Sill and the Northern Gotland Basin. Values below 5 µmol $l^{-1}$ could not be distinguished from 0 µmol $l^{-1}$.*

The oxygen conditon of the deep water of the central Baltic Sea is primarily influenced by the occurrence or absence of moderate and strong barotropic and/or baroclinic inflows. The minor barotropic inflow event of cold saline water in January 2022 seemed to determine oxygen transport during 2022 up to the southern part of the Eastern Gotland Basin (Fig. 25, Fig. 26). In February a bottom layer in the western and central part of the Arkona Basin with a concentration of 315-335 µmol $l^{-1}$ oxygen was formed that flowed via the Bornholmsgatt. Subsequently, it was mixed in the Bornholm Basin with the remains of the warm inflow waters of autumn 2021 resulting in a heterogeneous distribution of oxygen between 180 µmol $l^{-1}$ and 315 µmol $l^{-1}$ above a depth of 70 m in March, and 135-270 µmol $l^{-1}$ above 80 m depth in May. Its further eastward advection is especially visible in the oxygen distribution in March, May and August 2022 when an overflow of oxygenated warm deep water from Slupsk Furrow entered the Gotland Basin above a depth of 100 m with up to about 45 µmol $l^{-1}$ oxygen. A new inflow during the summer likely determined the oxygen concentration in the Arkona and Bornholm Basins in November (Fig. 26).

## 4.4 Nutrients: Inorganic nutrients

Reduction measures of nutrient input that have been implemented in the last decades could not prevent the Baltic Sea from being eutrophied. A drastic description of the consequences of eutrophication is given by DUARTE et al. (2009) "The effects of eutrophication include the development of noxious blooms of opportunistic algae and toxic algae, the development of hypoxia, loss of valuable seagrasses, and in general a deterioration of the ecosystem quality and the services they provide". According to the second "State of the Baltic Sea" report, 97 % of the Baltic Sea area is affected by eutrophication and 12 % is assessed as being in the worst status category (HELCOM 2018a).

In Germany, riverine inputs of total phosphorus declined between 2006 and 2014 by 14 %. In the same time-period, total nitrogen input decreased by 31 % (HELCOM 2018a). Despite this positive development, German territorial waters and bordering sea areas of the Baltic Sea remained hypertrophied by up to 50 % in the western and up to 100 % in the eastern part (HELCOM 2018b). To determine the effects of changes in nutrient inputs and to evaluate the results of reduction measures undertaken, the frequent monitoring of the nutrient situation is mandatory. Nutrients are core parameters since HELCOM established a standardized monitoring programme at the end of the 1970ies. An updated comprehensive overview of the ecosystem health of the Baltic Sea that covers the assessment period 2016-2021 - HOLAS 3 (HELCOM 2023) is in preparation at HELCOM and member states. It appears that only locally slight improvements were observed, but an overall significant shift to a less eutrophied Baltic Sea was so far not seen.

### 4.4.1 Surface water processes

The long-standing observation that nitrate and phosphate concentrations in the surface waters of temperate latitudes exhibit a typical annual cycle with high concentrations in winter, depletion during spring and summer, and recovery in autumn (NAUSCH & NEHRING 1996, NEHRING & MATTHÄUS 1991) seems partly no longer valid. In recent years it appears more and more clear that nitrate is still completely taken up by the spring bloom and is replenished during late autumn and winter, whereas phosphate significantly declines in April/May, but persists at low concentration almost throughout the entire summer. Thus, blooms of diazotrophic cyanobacteria that use dinitrogen gas as nitrogen source for growth are enabled during summer nitrate limitation.

Fig. 27 illustrates the annual cycle of nitrate and phosphate concentrations in surface waters at the stations Gotland Deep and Bornholm Deep in comparison to the surface water temperature development in 2022. For this purpose, the data of five monitoring cruises of the IOW were combined with data of the Swedish Meteorological and Hydrological Institute (SMHI) to get a better resolution of the seasonal patterns. In the central Baltic Sea, a typical phase of elevated nutrient concentrations usually develops during winter, which lasted two to three months (NAUSCH et al, 2008). In 2022, the maximum nitrate concentration was measured in early February of 3.4 µmol $l^{-1}$ in the central Eastern Gotland Basin and in mid-February of 2.9 µmol $l^{-1}$ in the central Bornholm Sea, respectively. The decline of nitrate at the Gotland Deep station reached the detection limit in mid-April at a surface water temperature of 4.5 °C. At Bornholm Deep station nitrate already reached the detection limit (~0.2 µmol $l^{-1}$) end of March at 4.4 °C. A maximum phosphate concentration was determined in early February of 0.71 µmol $l^{-1}$ at Gotland Deep, and of 0.69 µmol/l at Bornholm Deep site that stretched until mid-March, with 0.69 µmol $l^{-1}$ and

0.59 µmol $l^{-1}$ phosphate, respectively. The phosphate reserves lasted at both stations well during the summer of 2022. Only one phosphate measurement appeared to be below the detection limit, in the beginning of August at Gotland Deep station. Thus, the spring bloom in 2022 likely ended in the Bornholm Sea end of March, and at the Gotland Deep station in mid-April, similar as in 2021. A significant replenishment of these basic major nutrients in the surface waters did not take place at the Bornholm Deep station before early December. At that time, cooling to below 8 °C enabled wind induced mixing in autumn weather conditions and a supply of nutrients from deeper layers. Unfortunately, no data were available for the Gotland Deep station after November, when concentrations of nitrate and phosphate were still very low, at a water temperature of above 10 °C.

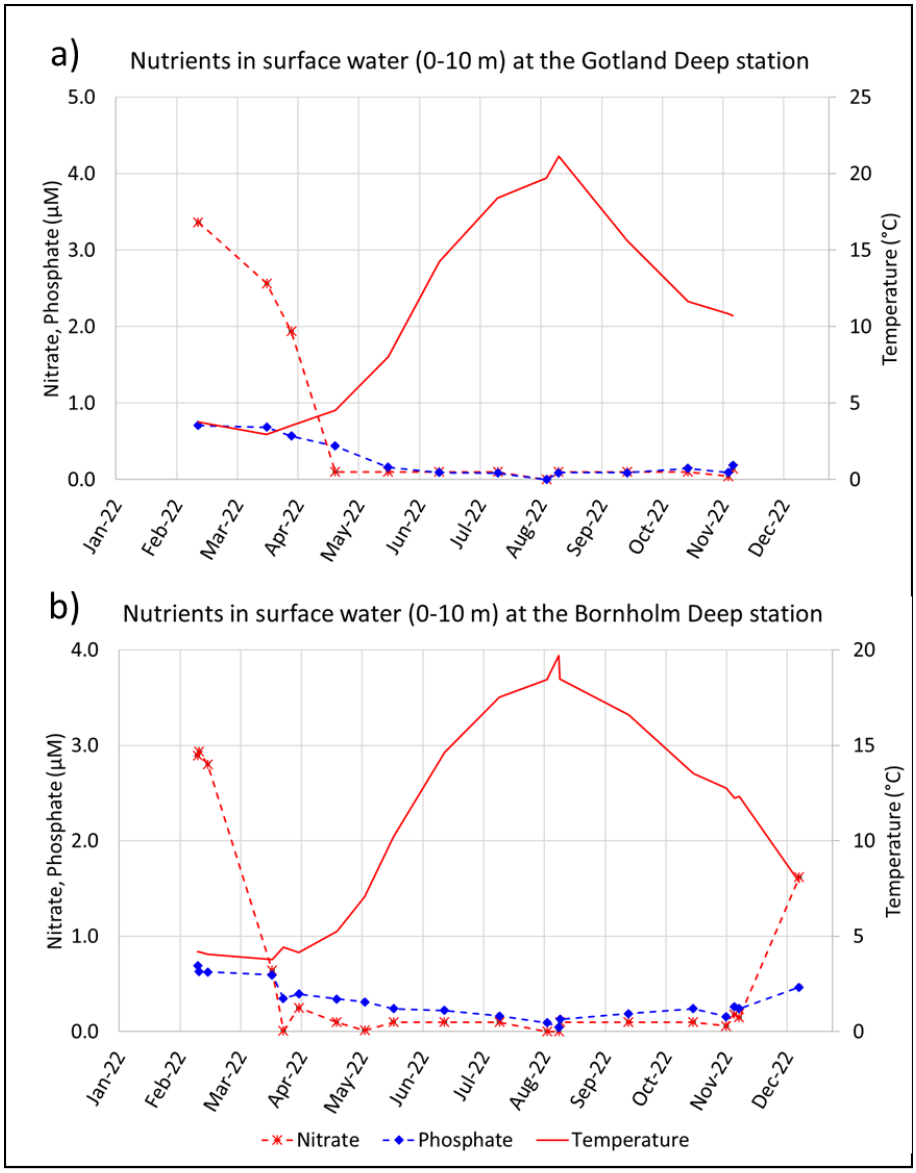


*Fig. 27: Seasonal Cycle of average phosphate and nitrate concentrations in 2022 compared to the temperature development in the surface layer (0-10 m) at the Gotland Deep station (a) and at the Bornholm Deep station (b), respectively, by depicting IOW and SMHI data.*

The relatively low maximum nitrate concentration of 3.4 µmol $l^{-1}$ (4.1 µmol $l^{-1}$ in 2021) at Gotland Deep site and 2.9 µmol $l^{-1}$ (4.1 µmol $l^{-1}$ in 2021) at Bornholm Deep station caused an early exhaustion of nitrate already at low temperatures. This likely enabled availability of phosphate

almost throughout the year 2022. This is seen in a general low dissolved inorganic nitrogen/phosphorus ratio (DIN/DIP) present in the winter surface water of the Baltic Sea (Fig. 28). The favourable uptake ratio of about 16 was already shown by an early study of Redfield (REDFIELD et al. 1963) and was proven to be a valuable approximation many times thereafter. The DIN/DIP ratio (mol/mol) was determined from the sum of ammonium, nitrate, and nitrite concentrations versus the phosphate concentration. The surface water DIN/DIP ratio in the Baltic Sea in winter 2022 ranged between 5.2 mol/mol and 10.9 mol/mol in the investigated sea areas. Because of a bad weather situation in February, no data of the central and northern Gotland Sea were available. Closest to the ideal ratio were the data of the Belt Sea, Mecklenburg Bight and Odra Bight with a ratio between 10 mol/mol and 11 mol/mol in 2022 (Fig. 28). In the other investigated areas the N/P ratio was about 6 mol/mol, Arkona Sea (6.4), Bornholm Sea (5.2) and the southeastern Gotland Sea (5.6). That confirmed again in 2022 that nitrogen was a limiting factor in the Baltic Proper, giving diazotrophic cyanobacteria an advantage compared to primary producers that depend on nitrate.

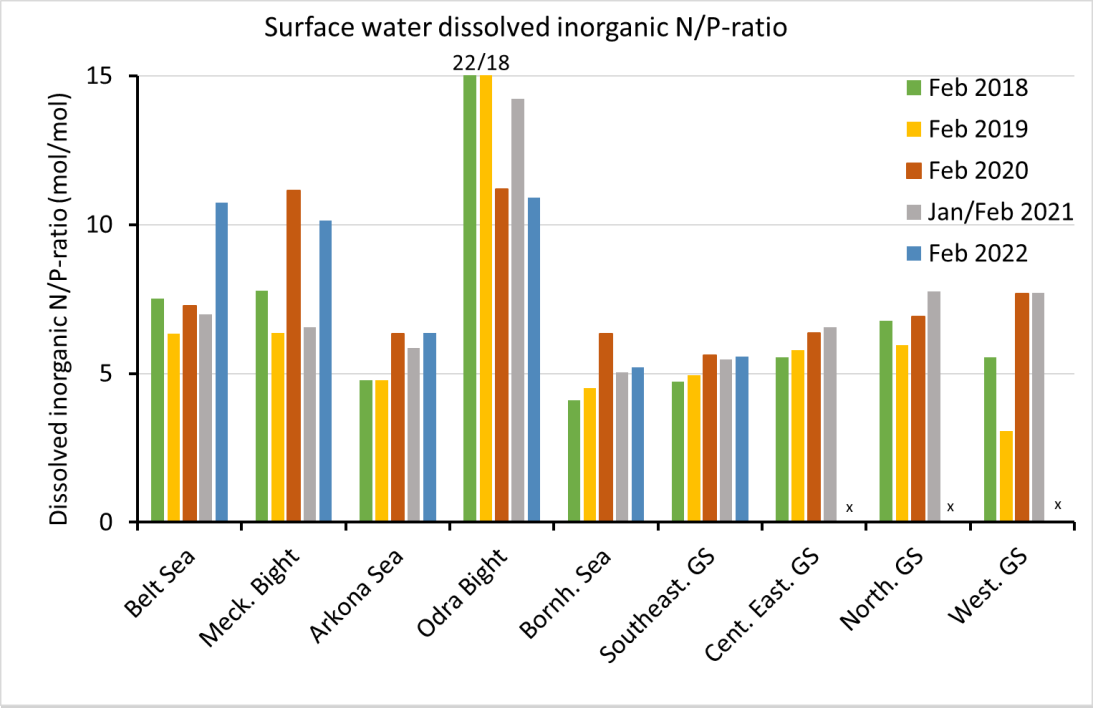


*Fig. 28: Average winter dissolved inorganic nitrogen versus phosphate ratio in surface waters of selected Baltic Sea areas for 2018 to 2022.*

Table 8 shows winter phosphate and nitrate concentrations in surface waters, obtained from measurements in February (or late January) of recent years. Interestingly, the lowest phosphate winter concentrations since 2018 were measured at all stations in 2020, with exception of the Lübeck Bight station with no value for 2022. In the following year 2021, winter phosphate was highest at the reference stations from the Belt Sea to the Bornholm Deep and Karlsö Deep stations. At Gotland Deep station it was the same phosphate value of 0.71 µmol $l^{-1}$ in 2021 and 2022, then Fårö Deep and Landsort Deep stations were clearly higher in 2022.

The winter nitrate concentration in surface water of the selected stations in the regions west of Darss Sill (Fehmarn Belt and Mecklenburg Bight) measured in February 2022 were generally at the higher end of recent years, which might reflect an influence of North Sea water, whereas the

stations in the Baltic Proper were characterized by low nitrate concentration, perhaps originating from an increasing oxygen debt in the deep water body.

After a couple of winters with lower phosphate and nitrate concentrations in western Baltic Sea surface water, the phosphate concentration of the time before was even exceeded in 2021 but decreased to an average in 2022. Fehmarn Belt was an exception in 2022, as 0.76 µmol $l^{-1}$ is still clearly above the average since 2013 of 0.61 µmol $l^{-1}$. Fehmarn Belt and Mecklenburg Bight showed increasing nitrate concentrations since 2020 and 2019, respectively, until 2022. At the Gotland, Fårö, Landsort and Karlsö Deep stations the surface water winter concentration of phosphate and nitrate concentrations remained relatively stable since 2013, at the mean values from 2013 to 2022 for phosphate of 0.64±0.08, 0.65±0.08, 0.69±0.10, and 0.74 ±0.11 µmol $l^{-1}$, and for nitrate of 3.5±0.4, 3.7±0.5, 3.8±0.7, and 3.2±0.11 µmol $l^{-1}$, respectively. However, at Landsort Deep and Karlsö Deep stations the winter nitrate concentration was clearly lower in 2022 with 2.4 µmol $l^{-1}$ nitrate at each. Statistically solid reductions of nutrient concentrations that have already been observed in coastal waters are not reflected in the nutrient concentrations of the central Baltic Sea basins up to now (NAUSCH et al. 2011, NAUSCH et al. 2014). However, a decrease of the nutrient/salinity gradients between coastal and open sea waters were shown for many German Baltic Sea areas since 1995, indicating a decline from the open sea perspective (KUSS et al. 2020). By comparison with nutrient target values elaborated in the TARGEV project (HELCOM 2013), a discrepancy is observed between the phosphate (DIP) and dissolved inorganic nitrogen (DIN), basically nitrate in surface waters, in terms of reaching the targets. The target values of DIN and DIP winter concentrations are for the Kiel Bight 5.45/0.60 µmol $l^{-1}$, Mecklenburg Bight 4.24/0.50 µmol $l^{-1}$, the Arkona Sea 2.90/0.36 µmol $l^{-1}$, for the Bornholm Sea 2.52/0.32 µmol $l^{-1}$, and for the Eastern Gotland Basin 2.59/0.29 µmol/l, respectively. This indicates that the nitrate winter concentration (ammonium and nitrite reflect minor contributions) may reach the respective target values in certain years, but a permanent fulfillment appears unlikely in the near future. For phosphate very likely it may need some more decades to reach the targets that were elaborated.

*Table 8: Mean nutrient concentrations in the surface layer (0-10 m) in winter in the western and central Baltic Sea (IOW and SMHI data).*

*Table 8.1: Surface water **phosphate** concentrations (µmol $l^{-1}$) in February (Minima in bold).*

| Station | 2018 | 2019 | 2020 | 2021 | 2022 |
|---|---|---|---|---|---|
| 360 (Fehmarn Belt) | 0.66 ±0.02 | 0.42 ±0.00 | **0.26 ±0.04** | 0.90 ±0.03 | 0.76 ±0.00 |
| 022 (Lübeck Bight) | **0.69 ±0.00** | - | - | 0.82 ±0.01 | 0.72 ±0.00 |
| 012 (Meckl. Bight) | 0.70 ±0.00 | **0.58 ±0.00** | **0.58 ±0.00** | 0.83 ±0.01 | 0.64 ±0.00 |
| 113 (Arkona Sea) | 0.67 ±0.01 | 0.59 ±0.00 | **0.43 ±0.01** | 0.72 ±0.03 | 0.57 ±0.00 |
| 213 (Bornholm Deep) | 0.65 ±0.01 | 0.61 ±0.02 | **0.51 ±0.03** | 0.81 ±0.02 | 0.66 ±0.01 |
| 271 (Gotland Deep) | **0.67 ±0.01** | 0.68 ±0.02 | **0.67 ±0.00** | 0.71 ±0.03 | 0.71 ±0.00 |
| 286 (Fårö Deep) | 0.64 ±0.01 | 0.71 ±0.01 | **0.57 ±0.01** | 0.64 ±0.01 | 0.73 ±0.01 |
| 284 (Landsort Deep) | **0.59 ±0.01** | 0.70 ±0.01 | **0.59 ±0.00** | 0.64 ±0.00 | 0.74 ±0.01 |
| 245 (Karlsö Deep) | 0.70 ±0.01 | 0.65 ±0.01 | **0.58 ±0.01** | 0.74 ±0.04 | 0.69 ±0.01 |

*Table 8.2: Surface water **nitrate** concentrations (µmol $l^{-1}$) in February (Minima in bold).*

| Station | 2018 | 2019 | 2020 | 2021 | 2022 |
|---|---|---|---|---|---|
| 360 (Fehmarn Belt) | 3.7 ± 0.0 | 1.7 ± 0.1 | **1.1 ± 0.8** | 5.0 ±0.5 | 6.3 ±0.0 |
| 022 (Lübeck Bight) | 6.1 ± 0.0 | - | - | **4.3 ±0.2** | 5.4 ±0.0 |
| 012 (Meckl. Bight) | 4.7 ± 0.3 | **2.8 ± 0.1** | 3.8 ± 0.0 | 4.5 ±0.1 | 5.8 ±0.0 |
| 113 (Arkona Sea) | 2.8 ± 0.0 | 2.6 ± 0.0 | **2.5 ± 0.0** | 3.7 ±0.3 | 2.8 ±0.1 |
| 213 (Bornholm Deep) | **2.5 ± 0.0** | 2.6 ± 0.1 | 2.9 ± 0.0 | 3.8 ±0.1 | 2.9 ±0.1 |
| 271 (Gotland Deep) | **3.4 ±0.0** | 4.0 ±0.0 | **3.4 ±0.1** | 3.9 ±0.2 | **3.4 ±0.2** |
| 286 (Fårö Deep) | 3.9 ± 0.0 | 4.0 ± 0.0 | 3.6 ± 0.1 | 4.2 ±0.1 | **3.5 ±0.0** |
| 284 (Landsort Deep) | 3.9 ±0.0 | 4.0 ±0.0 | 3.8 ±0.0 | 4.8 ±0.0 | **2.4 ±0.1** |
| 245 (Karlsö Deep) | 3.6 ±0.0 | **1.2 ±0.1** | 3.6 ±0.1 | 4.1 ±0.2 | 2.4 ±0.0 |

### 4.4.2 Deep water processes in 2022

In central Baltic Sea deep waters, the nutrient distribution is primarily influenced by the occurrence or absence of strong barotropic and/or baroclinic inflows and, thus, by its oxygen/hydrogen sulphide concentrations in deep waters. Since the MBI 2014/2015 the accumulation of phosphate in the deep water of the central basins has continued, however certain moderate inflows partly lead to lower hydrogen sulphide, ammonium and phosphate concentrations. Nitrate was mostly not detected in deep waters. During locally weak oxic water conditions, phosphate could be bound to iron/manganese particles that subsequently sink to the sediment. During anoxia, the particles are dissolved and then phosphate is released back to the water column. The annual mean phosphate concentration in the Bornholm Deep reflects a considerable interannual variability on a high level of 4.2 ± 0.9 µmol $l^{-1}$ since 2018. Whereas, the Landsort and Karlsö Deeps with 3.7 ± 0.4 µmol $l^{-1}$ and 3.8 ± 0.3 µmol $l^{-1}$ in the selected reference depths, respectively, were more stable. Gotland Deep significantly accumulated phosphate in recent years to 6.1 µmol $l^{-1}$ in 2022. In Farö Deep, phosphate concentration smoothly increased to 4.7 µmol $l^{-1}$ in 2022, with a lower value in 2020 of 3.4 µmol $l^{-1}$ phosphate at the reference depth (Table 9).

The fading of the MBI impact (NAUMANN et al. 2018) is also reflected in the depletion of nitrate in deep waters. Only the Bornholm Deep showed intermittend a high nitrate concentration in deep waters of an annual average of 6.8 µmol $l^{-1}$ in 2019 and 7.7 µmol $l^{-1}$ in 2020. In 2021 nitrate concentration declined to 2.9 µmol $l^{-1}$, but increased again in 2022 to 4.1 µmol $l^{-1}$. On Gotland Deep, Fårö Deep, Landsort Deep and Karlsö Deep stations no significant amounts of nitrate were detected since 2018, except the 0.3 µmol $l^{-1}$ nitrate found at depth in the Fårö Deep in 2020 (Table 9). An explanation is that anoxic conditions prevent mineralization of organic matter to nitrate. Instead, ammonium is formed and represents the end product of the degradation of biogenic material. Therefore in general, ongoing accumulation of ammonium in deep waters was recorded in Baltic Sea deep waters, in the Gotland Deep from 12.2 µmol $l^{-1}$ in 2019 to 27.9 µmol $l^{-1}$ in 2022. Similarly, in the Fårö Deep, ammonium increased from 9.1 µmol $l^{-1}$ in 2019 to 15.9 µmol $l^{-1}$ in 2022. Only in 2020 the increase was interrupted in Fårö Deep by a lower ammonium concentration of 7.3 µmol $l^{-1}$ annual average ammonium in the 150 m reference depth. The Landsort Deep showed a moderate increase of ammonium since 2018 from 5.0 µmol $l^{-1}$ to 12.6 µmol $l^{-1}$ in 2022, and the ammonium concentration at Karlsö Deep station in 100 m depth changed from ~ 10 µmol $l^{-1}$ 2018/2019 to 16 µmol $l^{-1}$ in 2022. In the Bornholm Deep annual average ammonium varied between a minimum of 0.4 µmol $l^{-1}$ in 2020 and a maximum of 4 µmol $l^{-1}$ in 2021 in the last 5 years (Table 9).

*Table 9: Annual means and standard deviations for phosphate (Tab. 9.1), nitrate (Tab. 9.2) and ammonium (Tab. 9.3) in the deep water of the central Baltic Sea (IOW and SMHI data).*

*Table 9.1: Annual mean deep water **phosphate** concentration (µmol $l^{-1}$; Maxima in bold).*

| Station | depth/m | 2018 | 2019 | 2020 | 2021 | 2022 |
|---|---|---|---|---|---|---|
| 213 (Bornholm Deep) | 80 | 4.73 ±1.56 | 3.78 ±1.40 | 2.88 ±1.03 | 4.49 ±2.65 | **5.15 ±4.02** |
| 271 (Gotland Deep) | 200 | 4.08 ±0.13 | 4.38 ±0.25 | 5.14 ±0.34 | 5.39 ±0.16 | **6.14 ±1.03** |
| 286 (Fårö Deep) | 150 | 3.55 ±0.68 | 4.02 ±0.45 | 3.36 ±0.42 | 4.37 ±0.17 | **4.66 ±0.32** |
| 284 (Landsort Deep) | 400 | 3.12 ±0.22 | 3.64 ±0.57 | 3.98 ±0.24 | 3.69 ±0.14 | **4.06 ±0.21** |
| 245 (Karlsö Deep) | 100 | 3.63 ±0.34 | 3.51 ±0.29 | 3.89 ±0.25 | 3.98 ±0.32 | **4.17 ±0.29** |

*Table 9.2: Annual mean deep-water **nitrate** concentration (µmol $l^{-1}$; Minima in bold).*

| Station | depth/m | 2018 | 2019 | 2020 | 2021 | 2022 |
|---|---|---|---|---|---|---|
| 213 (Bornholm Deep) | 80 | **1.6 ±1.5** | 6.8 ±2.9 | 7.7 ±4.1 | 2.9 ±4.5 | 4.1 ±5.0 |
| 271 (Gotland Deep) | 200 | **0.0 ±0.0** | **0.0 ±0.0** | 0.1 ±0.1 | 0.1 ±0.0 | 0.2 ±0.4 |
| 286 (Fårö Deep) | 150 | **0.0 ±0.0** | **0.0 ±0.0** | 0.3 ±0.6 | 0.1 ±0.0 | 0.2 ±0.4 |
| 284 (Landsort Deep) | 400 | **0.0 ±0.0** | **0.0 ±0.0** | 0.1 ±0.0 | **0.0 ±0.1** | **0.0 ±0.0** |
| 245 (Karlsö Deep) | 100 | **0.0 ±0.0** | **0.0 ±0.0** | 0.1 ±0.0 | 0.1 ±0.1 | 0.1 ±0.1 |

*Table 9.3: Annual mean deep-water **ammonium** concentration (µmol $l^{-1}$; Maxima in bold).*

| Station | depth/m | 2018 | 2019 | 2020 | 2021 | 2022 |
|---|---|---|---|---|---|---|
| 213 (Bornholm Deep) | 80 | 1.9 ±2.4 | 1.5 ±3.1 | 0.4 ±0.7 | **4.0 ±4.9** | 3.2 ±6.6 |
| 271 (Gotland Deep) | 200 | 6.0 ±2.3 | 12.2 ±3.8 | 20.1 ±5.0 | 22.8 ±0.9 | **27.9 ±7.5** |
| 286 (Fårö Deep) | 150 | 3.6 ±1.7 | 9.1 ±1.2 | 7.3 ±3.6 | 12.2 ±1.6 | **15.9 ±3.0** |
| 284 (Landsort Deep) | 400 | 5.0 ±2.2 | 8.0 ±1.0 | 9.4 ±2.2 | 10.3 ±0.3 | **12.6 ±1.5** |
| 245 (Karlsö Deep) | 100 | 10.4 ±2.9 | 9.4 ±5.1 | 12.8 ±2.9 | 12.1 ±3.8 | **16.0 ±3.9** |

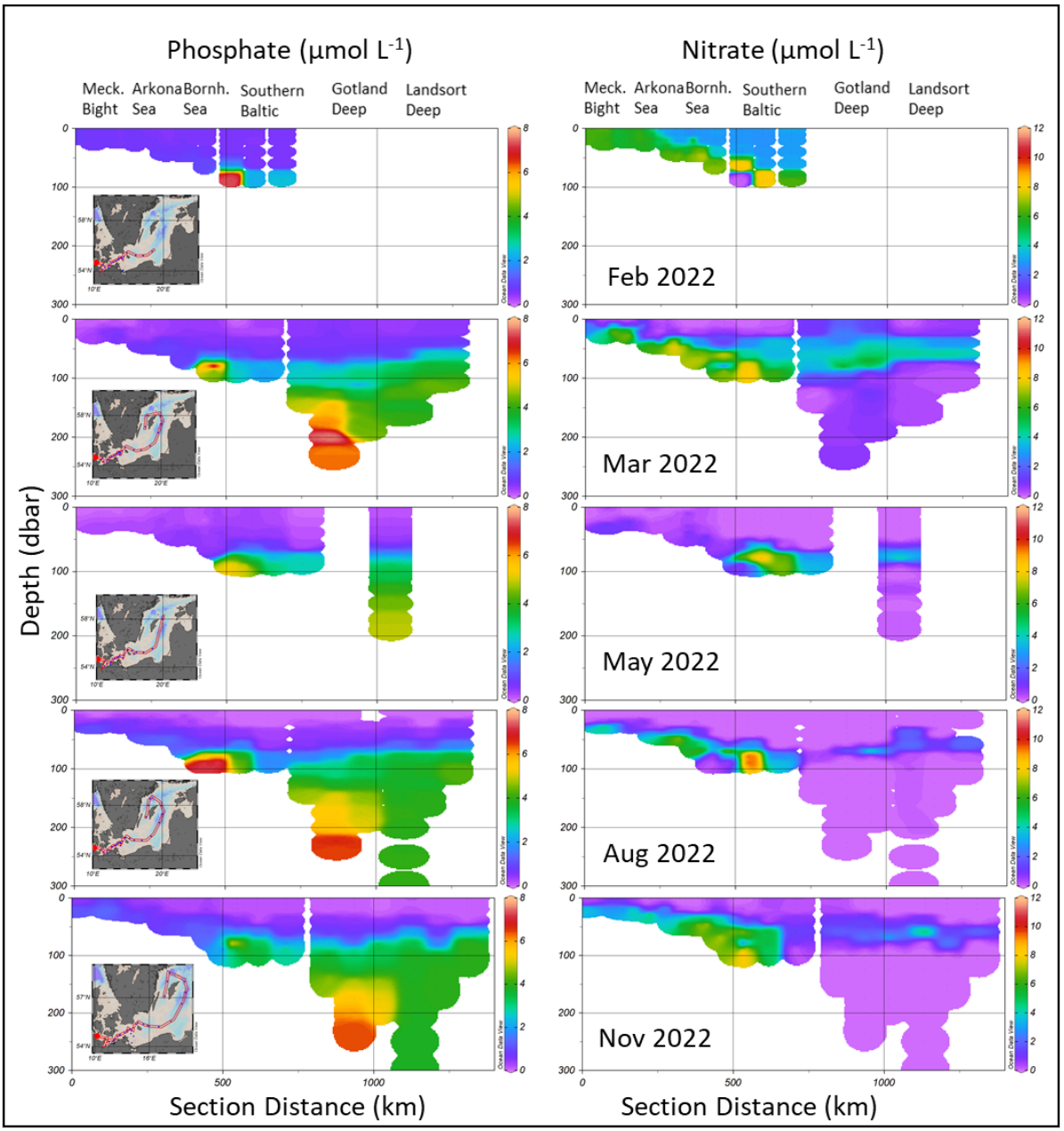


*Fig. 29: Vertical distribution of phosphate (left column) and nitrate (right column) in 2022 between the Mecklenburg Bight and the Western Gotland Basin measured on the monitoring cruises in February, March, May, August and November; in Aug and Nov 2022, a 300 m deep station near Landsort Deep was investigated. Figure panels were prepared by using ODV 5, (SCHLITZER 2018).*

Fig. 29 illustrates the nutrient distributions in the water column on transects between the Mecklenburg Bight and the western Gotland Sea in February, March, May, August and November 2022 (small maps on the left side of Fig. 29 indicate the available stations for each transect). Thereby, point measurements at their respective depth were enlarged on the basis of weighted-average gridding to give an impression of spatial nutrient concentration distributions of phosphate and nitrate along the thalweg transect. To show the concentration range of nitrate and phosphate and their occurrence, a few features are mentioned in advance. The large areas of purple shading corresponds to relatively low concentrations of below ~1 µmol $l^{-1}$ nitrate and ~0.2 µmol $l^{-1}$ phophate. Below the halocline, phosphate increased to a maximum of 7.4 µmol $l^{-}$

$^{1}$ in the Bornholm Deep, 6.5 µmol $l^{-1}$ in the Gotland Deep, 5 µmol $l^{-1}$ in the Fårö Deep and of about 4 µmol $l^{-1}$ in the deep water of the Landsort area at nitrate depletion in August 2022. Elevated nitrate concentrations were determined in the first half of the thalweg above a depth of 100 m from 6 µmol $l^{-1}$ (greenish) up to 10 µmol $l^{-1}$ nitrate (redish) in Fig. 29.

During the **February** campaign (Fig. 29, panels Feb 2022), nitrate showed a maximum of 8 µmol $l^{-1}$ in the ventilated western Baltic Sea, Arkona Sea bottom water (Fig. 29, yellow greenish zone) at moderate phosphate concentration of 1 µmol $l^{-1}$. A high phosphate concentration of up to 7.3 µmol $l^{-1}$ has been measured in the bottom water of the Bornholm Deep at nitrate depletion. Further east along the thalweg, the bottom water was oxygenated at that time and phosphate declined to 2.2 µmol $l^{-1}$ in the Slupsk Furrow and 2.5 µmol $l^{-1}$ in the southern Gotland Sea. Nitrate showed a maximum in the bottom water of Slupsk Furrow of ~8 µmol $l^{-1}$ and was 6.5 µmol $l^{-1}$ at the slope of the Eastern Gotland Basin. The central eastern and western Gotland Sea could not be investigated in February 2022 because of bad weather. In **March** (panels Mar 2022), the situation had changed slightly, the phosphate maxima in the Bornholm und Gotland Deeps were pushed upwards and narrowed, but were still around 7.5 µmol $l^{-1}$. In **May** supply of oxygenated water reduced phosphate concentration in the Bornholm Sea deep water to 5.5 µmol $l^{-1}$ that further declined in eastern direction along the thalweg to 2.7 µmol $l^{-1}$. Nitrate showed a maximum of 9 µmol $l^{-1}$ in the Bornholm Sea deep water and declined eastwards to 3.0 µmol $l^{-1}$. The phosphate concentration in the Fårö Deep bottom water was 4.9 µmol $l^{-1}$ and nitrate could not be detected. The nitrate maximum in May of 4.6 µmol $l^{-1}$ at Fårö Deep site was measured at 70 m depth, above the redoxcline between the nitrate depleted deep water and exhausted surface water.

In **August** (panels Aug 2022), the bottom water concentration of phosphate in the Bornholm Basin was again 7.4 µmol $l^{-1}$ and nitrate was not detected at oxygen depletion. In the Gotland Deep bottom water, phosphate was 6.5 µmol $l^{-1}$ at undetectable nitrate concentration. The nitrate maximum in the Eastern Gotland Basin was in the range from 0.5-4.6 µmol $l^{-1}$ in the 70 m range. The Western Gotland Basin showed a relative homogeneous distribution of phosphate of about 4 µmol $l^{-1}$ below 70 m. In **November** (panels Nov 2022) the Bornholm Deep reflected a maximum phosphate concentration of 6.6 µmol $l^{-1}$ at 80 m depth, as extracted from the profile, that declined further east to about 2 µmol $l^{-1}$ in the Slupsk Furrow. Below the phosphate maximum, nitrate concentration was almost 10 µmol $l^{-1}$ and decreased eastward to 4.8 µmol $l^{-1}$ and 3.2 µmol $l^{-1}$.

## 4.5 Nutrients: Particulate organic carbon and nitrogen (POC, PON)

POM includes biomass from living microbial cells, detrital material including dead cells, fecal pellets, other aggregated material, and terrestrially-derived organic matter (KHARBUSH et al. 2020). It constitutes the main pathway by which organic matter is channeled through the biological pump to depths (LE MOIGNE 2019). In the photic surface waters of the Baltic Sea, particulate organic carbon (POC) and nitrogen (PON) concentrations are mainly controlled by the presence, growth, and degradation of biologically produced material (SZYMCZYCHA et al. 2017, WINOGRADOW et al. 2019). Although terrestrial inputs are a significant source of organic matter to the Baltic Sea regarding the dissolved fraction (NAUSCH et al. 2008, SEIDEL et al. 2017), the weak correlation of salinity and POC (Pearson's $r=0.06$, $p<0.01$, $n=2683$) indicated that terrestrial particulate organic matter (POM) played a negligible role at the sampled stations.

In 2022, POC and PON concentrations were elevated in the surface water of the Baltic Sea in March, July and partially May, likely induced by primary production during spring and summer blooms. In the deep water of the Fehmarn Belt at Station TF0360, increased concentrations of POC and PON in March and July likely resulted from sinking bloom material, while the extremely high values in November were presumably produced from sediment resuspension during windy conditions (POC=134.7 µmol $l^{-1}$, PON=15.2 µmol $l^{-1}$). Generally, POC and PON concentrations were highly correlated (1995 to 2022, Pearson's r=0.93, p<0.001, n=3069), indicating common production and transport pathways. Surface and deep POC and PON or particulate C/N ratios were not significantly different from long term means (Table 10, Fig. 30). Particulate C/N ratios were slightly below long-term mean (7.4±1.4) with the overall 2022 C/N ratio of 6.9±1,2 being higher than the ratio for living plankton of 6.6 (REDFIELD 1934), indicating a combined effect of higher terrigenous input of usually higher C/N ratio, primary production, and enhanced heterotrophic biomass contribution during the summer (ZIMMERMANN et al. 2014).

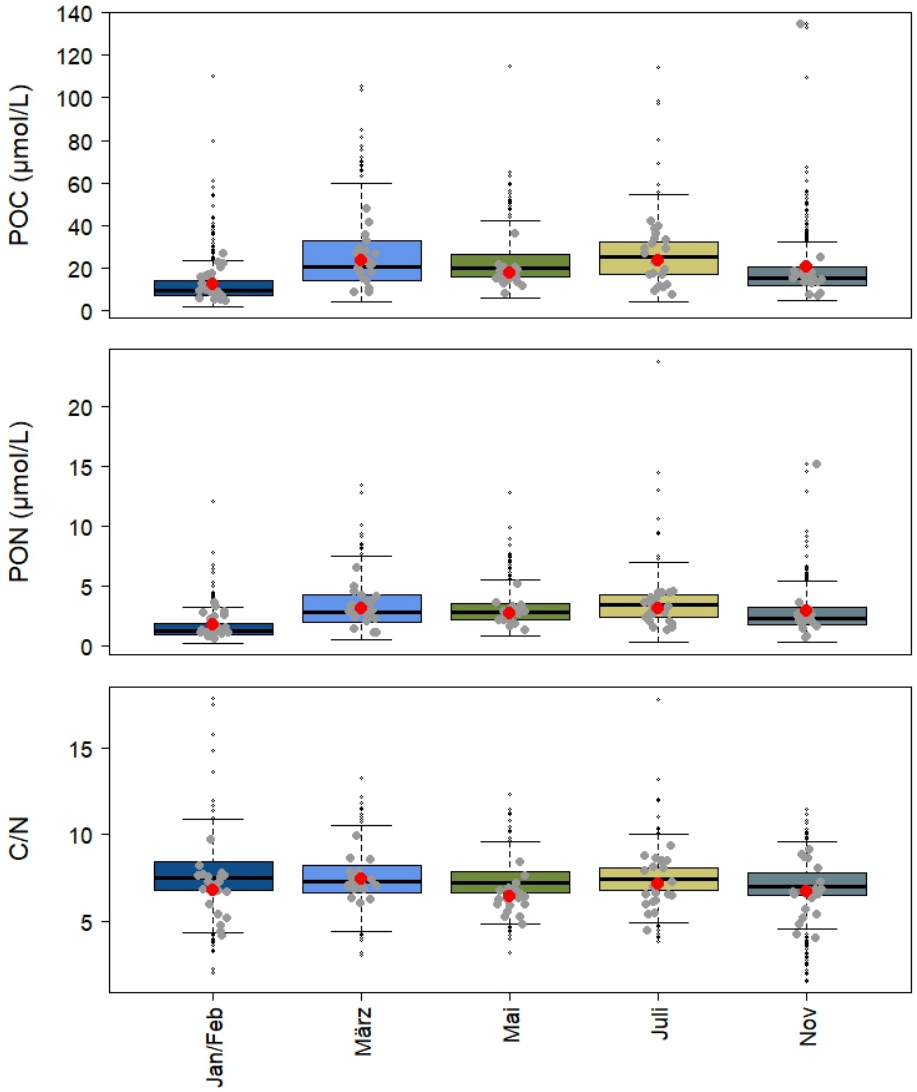


*Fig. 30: Boxplots show POC and PON concentrations as well as particulate C/N ratios over the whole water column from 1995 to 2021 by month, with minimum, first quartile, median, third quartile, maximum, and outliers. Boxplots are overlaid by all 2022 values (gray circles) and means (red circles).*

*Table 10: Average concentrations and C/N ratio of POC and PON in the surface and bottom waters in 2022 in comparison to historic data (1995-2021), as well as analysis including all depths. Differences in means were analyzed via Welch test, significance and degrees of freedom (df) are provided.*

| | Surface water POM | | | Bottom water POM | | | All depths POM | | |
|---|---|---|---|---|---|---|---|---|---|
| | 2022 | before 2022 | Welch-Test | 2022 | before 2022 | Welch-Test | 2022 | before 2022 | Welch-Test |
| POC (µmol/L) | 22.2 ±11.3 | 24.6 ±14.6 | p=0.27, df=31.4 | 22.9 ±23.2 | 19.4 ±12.2 | p=0.44, df=27.6 | 19.5 ±14.4 | 20.5 ±12.8 | p=0.49, df=113.1 |
| PON (µmol/L) | 3.0 ±1.2 | 3.3 ±1.8 | p=0.29, df=32.4 | 3.0 ±2.6 | 2.6 ±1.7 | p=0.37, df=27.9 | 2.8 ±1.6 | 2.8 ±1.7 | p=0.76, df=115.1 |
| C/N | 7.1 ±1.4 | 7.4 ±1.4 | p=0.19, df=30.0 | 7.4 ±1.2 | 7.7 ±1.4 | p<0.22, df=30.2 | 6.9 ±1.2 | 7.4 ±1.4 | p<0.001, df=117.3 |

## 4.6 Organic hazardous substances in surface water and sediment of the Baltic Sea in February 2022

The Baltic Sea is largely affected by contamination since the onset of the industrialization in the late 19$^{th}$ century. Riverine transport and atmospheric deposition are the main transport pathways of organic hazardous substances from land-based sources in the catchment area into the Baltic Sea (HELCOM 2018c). This report summarizes data for organic contaminants for the year 2022 (for an overview see Fig. 31) and time series data for the Mecklenburg Bight, Arkona Sea and the Pomeranian Bight in surface water as well as in surface sediments. The results are assessed based on criteria of HELCOM as well as the Marine Strategy Framework Directive (MSFD) and the Water Framework Directive (WFD).

Samples were taken during the winter season when the Baltic Sea water is most unaffected by biological processes such as algal blooms. Thus, during the expedition in February 2022 with RV Elisabeth Mann Borgese (EMB286) Baltic Sea surface water and sediment were sampled; the sediment sample for the eastern Arkona Basin was obtained during the cruise EMB293 in May 2022. The surface seawater samples were obtained through transect sampling as shown inFig. 32. During the transect route, a pump/filtration system was used to continuously pump surface water from 5 m below the surface through a GF/F filter and subsequently through an XAD-2 resin packed column with a flow rate of about 1.1 l min$^{-1}$ for 4 to 6 hours. The surface sediment samples were taken using a multi corer.

The samples were analyzed for chlorinated hydrocarbons (CHC) and polycyclic aromatic hydrocarbons (PAH); the surface sediment samples additionally analyzed for organotin compounds (OT) (Table 11). Chemical analysis of the CHC and PAH in the dissolved and particulate water fractions as well as in in sediment was conducted as described before (e.g., SCHULZ-BULL et al. 2011; KANWISCHER et al. 2020). Organotin compounds were analyzed by GALAB Laboratories GmbH.

However, due to the occurrence of technical problems during the sample preparation procedure the PAH data for the surface water samples cannot be reported.

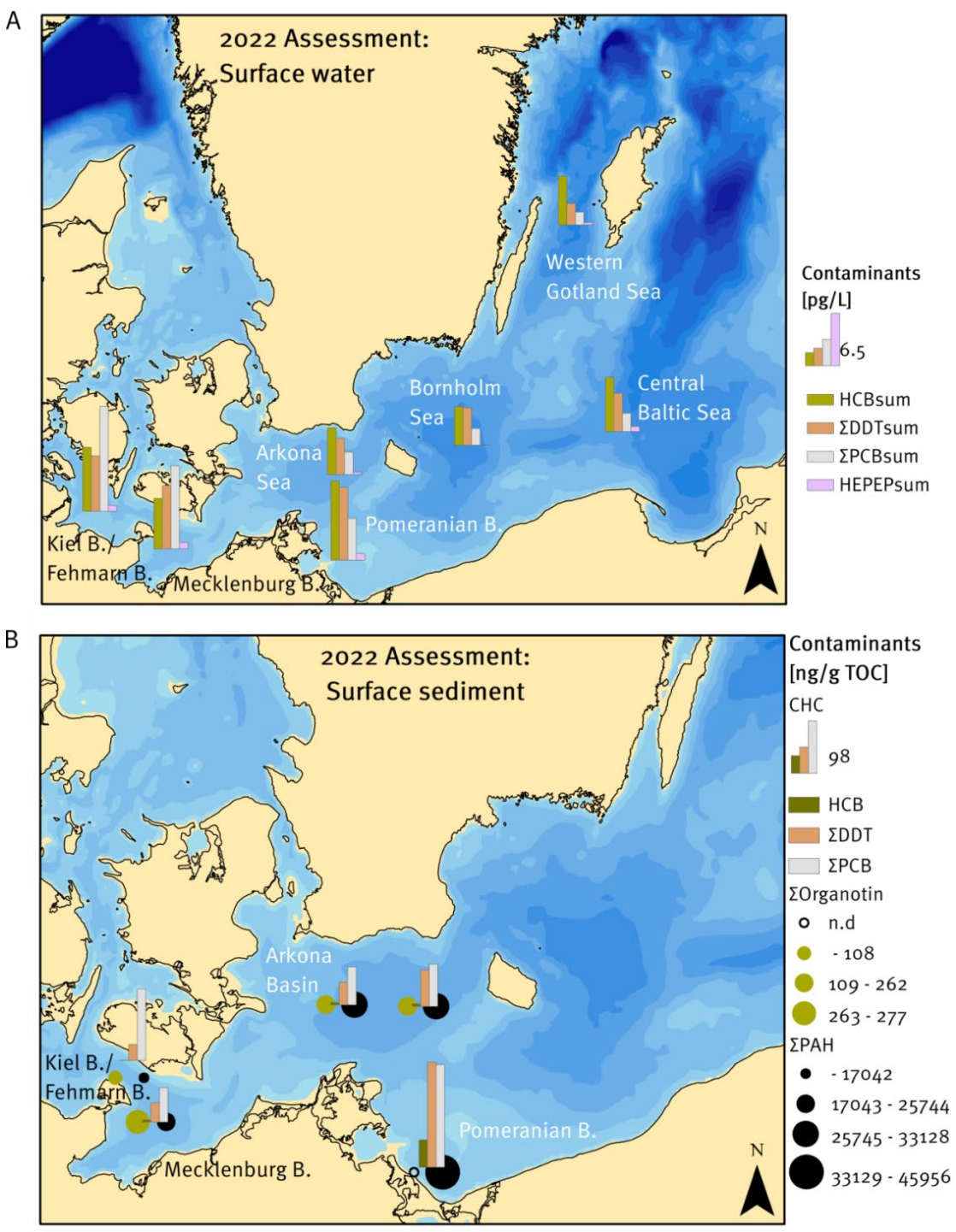


*Fig. 31: Summary of obtained contaminant data for the Baltic Sea study areas in (A) surface water and (B) surface sediment in February 2022. A: summarized concentrations for dissolved and particulate water fraction for HCB (HCBsum), DDT and metabolites (ΣDDTsum), PCB$_{ICES}$ congeners (ΣPCBsum) and HEPEP (HEPEPsum), B: summarized sediment contents of U.S. EPA PAH compounds (ΣPAH, without Naph), HCB, DDT and metabolites (ΣDDT), PCB$_{ICES}$ congeners (ΣPCB) and the organotin compounds MBT, DBT, TBT and TPhT (ΣOrganotin).*

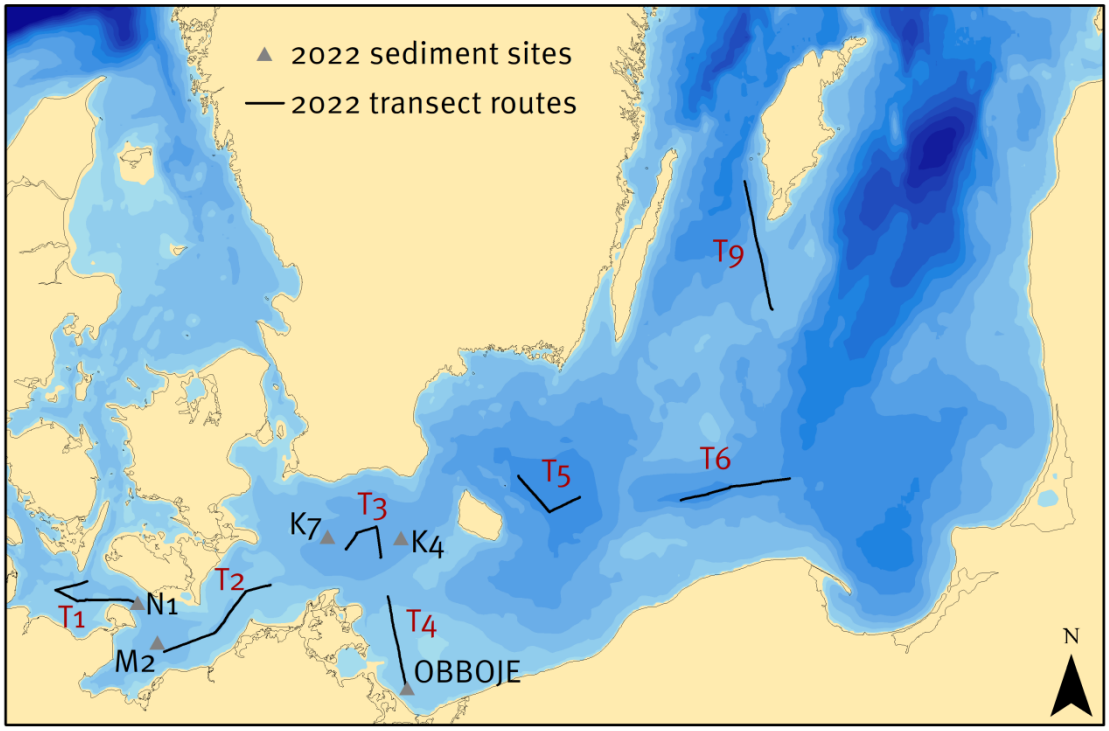


*Fig. 32: Surface water sampling transect routes of the research vessel as well as sediment sampling sites during the February 2022 monitoring campaign. T1: Kiel Bight/Fehmarn Belt, T2: Mecklenburg Bight, T3: Arkona Sea, T4: Pomeranian Bight, T5: Bornholm Sea, T6: central Baltic Sea, T9: western Gotland Sea*

*Table 11: Analyzed compounds in Baltic Sea surface water and sediment samples during the February 2022 observation. *) in surface water samples only, **) in sediment samples only*

| Compound group | Determined substances |
|---|---|
| Chlorinated hydrocarbons | ICES-polychlorinated biphenyls ($PCB_{ICES}$):<br>PCB28/31, PCB52, PCB101, PCB118, PCB153, PCB138, PCB180 |
| | dichlorodiphenyl-trichloroethane (DDT) and metabolites:<br>*p,p'*-DDT, *o,p'*-DDT<br>dichlorodiphenyldichloroethylene (DDE): *p,p'*-DDE<br>dichlorodiphenyldichloroethane (DDD): *p,p'*-DDD |
| | hexachlorobenzene (HCB) |
| | heptachlor (HEP) *)<br>heptachlor epoxide (cis-heptachlor-exo-epoxide (isomer B) (HEPEP) *) |
| Polycyclic aromatic hydrocarbons (PAH) | U.S. EPA PAH indicator compounds except naphthalene **):<br>acenaphthylene (ACNLE), acenaphthene (ACNE), fluorine (FLE), pheanthrene (PA), anthracene (ANT), fluoranthene (FLU), pyrene (PYR), benzo(*a*)anthracene (BAA), chrysene (CHR), benzo(*b*)fluoranthene (BBF), benzo(*k*)fluoranthene (BKF), benzo(*a*)pyrene (BAP), indeno(1,2,3-*cd*)pyrene (ICDP), dibenzo(*a,h*)anthracene (DBAH), benzo(*g,h,i*)perylene (BGHIP) |
| Organo-tins | organotin compounds **):<br>monobutyltin (MBT), dibutyltin (DBT), tributyltin (TBT), triphenyltin (TPhT) |

The insecticide **DDT** has been used as a contact and feeding poison in agriculture and forestry since the 1940s. DDT technical formulations were mixtures of o,p' and p,p' congeners with p,p'-DDT as the predominant one. In the environment, DDT degrades to the stable metabolites DDE and DDD. Due to their chemical stability and lipophilic properties, these contaminants accumulate in the tissues of animals and humans via the food chain.

**HCB** is a fungicide which was mainly used for seed treatment and as wood preservative. It is persistent and toxic to aquatic organisms.

Since the 1930s, **PCBs** have been used as fluids in hydraulic systems, as lubricants, and as insulating or cooling fluids in transformers and electrical capacitors. Commercial PCB formulations usually consisted of a wide range of PCB congeners which differ in the number and position of substituted chlorine on the biphenyl rings. Seven PCB congeners were suggested as indicators for environmental monitoring by the International Council of the Exploration of the Sea (ICES, $PCB_{ICES}$).

The insecticide **heptachlor** (HEP) has been used in agriculture, for wood protection and also for household insect control since 1945. Heptachlor rapidly converts to mainly **heptachlor epoxide (HEPEP)**, which is more toxic, bioaccumulative and persistent than the parent compound (EFSA 2007). The cis-isomer of heptachlorepoxide is the main metabolite of abiotic and biotic oxidation of heptachlor (MÜLLER et al. 1997).

Production and use of DDT, HCB, PCBs and HEP is internally restricted or banned by the Stockholm Convention of 2004.

**Organotin compounds** (OT) are organometallic compounds with one or more tin-carbon bonds and are mostly of anthropogenic origin. Since the 1950s, triorganotin compounds such as tributyltin (TBT) have been widely used as biocides, including as an effective agent in antifouling paints for marine vessels (e.g., ANTIZAR-LADISLAO 2008). TBT degrades to the mono- and dibutyl organotin compounds (MBT, DBT) and, thus, detected organotin in the marine environment mainly originates from the application of TBT in antifouling paints. The occurrence of imposex in marine organisms is linked to intensive TBT usage which had severe consequences on the population level of effected species (ALZIEU 1998). An international convention on the ban of the use of TBT in antifouling paints from 2008 was put into force by the International Maritime Organization. However, due to the intensive use of TBT in the past, high levels of TBT can still be detected, especially in harbor sediments (HOCH 2001).

### 4.6.1 Chlorinated Hydrocarbons in the Baltic Sea surface water

Results for DDT and metabolites

In February 2022 concentrations for DDT and its metabolites ($\Sigma DDT_{sum}$ [1]) ranged from 2.7 pg/L in the western Gotland Sea (T9) to 9.1 pg/L in the Pomeranian Bight (T4) (median: 4.8 pg/L, Fig. 33, Appendix 1). Among the study sites $\Sigma DDT_{sum}$ concentrations were highest in the areas Kiel Bight/Fehmarn Belt (T1), Mecklenburg Bight (T2) and Pomeranian Bight (T4).

Higher DDT/met. load of the particulate water fraction ($\Sigma DDT_{part}$ [2]) is accompanied by higher suspended matter (SPM) loads (Fig. 33) of these sites. High SPM loads might have derived from the beginning spring bloom or increasing load of sediment particles in the water column due to stormy weather conditions at these shallow study sites. Severe storm events were recorded for the period from January to February 2022 (see chapter 2 "General meteorological conditions"). At the Pomeranian Bight, the high load of SPM might have additionally derived from the riverine inflow of the river Odra. Thus, in the areas Kiel Bight/Fehmarn Belt (T1), Mecklenburg Bight (T2) and Pomeranian Bight (T4) particulate DDT/met. contribute more to the overall DDT load ($\Sigma DDT_{sum}$) than at the other sites.

Similar to previous years, higher concentrations of the long-lived degradation products *p,p'*-DDE and *p,p'*-DDD as compared to *p,p'*-DDT were observed (Table 12). This implies no recent fresh inputs of DDT which is also reflected by *p,p'*-DDT/*p,p'*-DDE ratios below 0.5 (STRANDBERG et al. 1998) (Table 12).

*Table 12: Ratios of p,p'-DDT/p,p'-DDE for the determined concentrations of DDT and metabolites in Baltic Sea surface water. [a] ratios were determined from summed particulate and dissolved concentrations.*

| | T1 | T2 | T3 | T4 | T5 | T6 | T9 |
|---|---|---|---|---|---|---|---|
| ***p,p'*-DDT/*p,p'*-DDE** [a] | 0.18 | 0.20 | 0.38 | 0.30 | 0.28 | 0.38 | 0.41 |

[1] $\Sigma DDT_{sum}$: summarized concentration of DDT congeners and metabolites in particulate and dissolved water fraction

[2] $\Sigma DDT_{part}$: summarized concentration of DDT congeners and metabolites in particulate water fraction

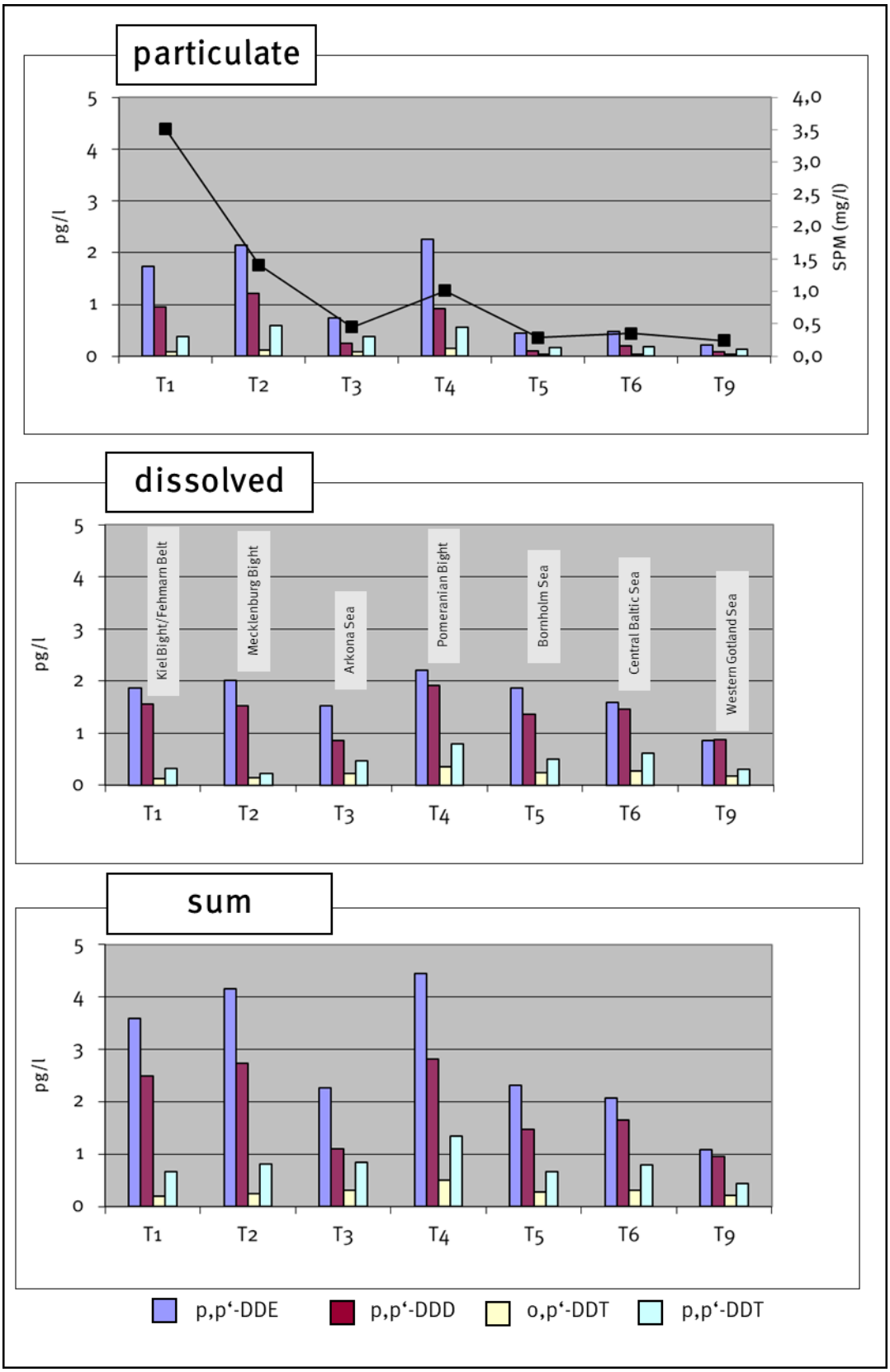


*Fig. 33: Concentrations of DDT and its metabolites in the dissolved and particulate fractions of the Baltic Sea surface water samples from the February 2022 observations. Black squares: SPM contents.*

Concentrations of p,p‘-DDT and the metabolite p,p‘-DDE of past winter observations for the study areas Mecklenburg Bight, Arkona Sea and Pomeranian Bight are shown in Fig. 34. The 2022 data continue the decreasing trends for both compounds at these sites. Higher interannual variations of p,p‘-$DDE_{sum}$ are more pronounced for the Pomeranian Bight which mainly derives from particulate DDE at this site and reflects the particulate transport of DDE by the river Odra into the Baltic Sea.

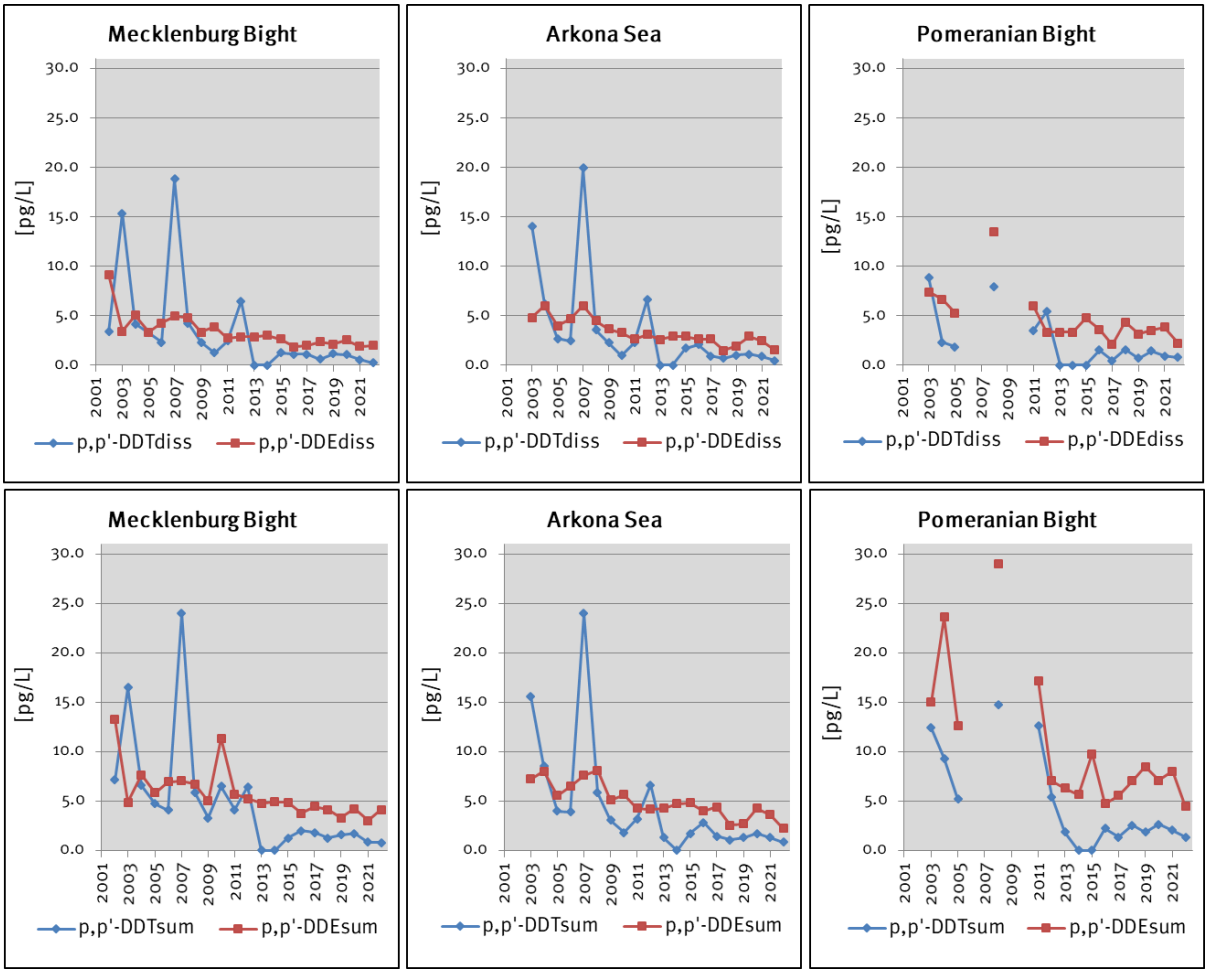


*Fig. 34: Time series of p,p’-DDT and p,p’-DDE concentrations in surface water of the Mecklenburg Bight, Arkona Sea and Pomeranian Bight. Upper panel: dissolved water fraction, lower panel: summed dissolved and suspended water fraction. Gaps in the time line indicate no sampling in the respective year; concentrations at “0 ng/L” mean that the compound was not detected in the sample.*

## Results for HCB

Observed concentrations for $HCB_{sum}$[3] ranged from 4.8 pg $l^{-1}$ in the Bornholm Sea to 9.9 pg $l^{-1}$ in the Pomeranian Bight (median: 6.3 pg $l^{-1}$). HCB was mainly found in the dissolved water fractions (Appendix 3). The highest $HCB_{part}$[4] concentration of 0.58 pg $l^{-1}$ was determined for the site Pomeranian Bight.

[3] $HCB_{sum}$: summarized HCB concentrations of particulate and dissolved water fraction
[4] $HCB_{part}$: HCB concentrations in the particulate water fractions

Fig. 35 depicts long-term observations of HCB concentrations for the study areas Mecklenburg Bight, Arkona Sea and Pomeranian Bight since 2001. Declining trends of HCB concentrations are marginal comparing to DDT and PCB reflecting the persistence of HCB in the marine environment.

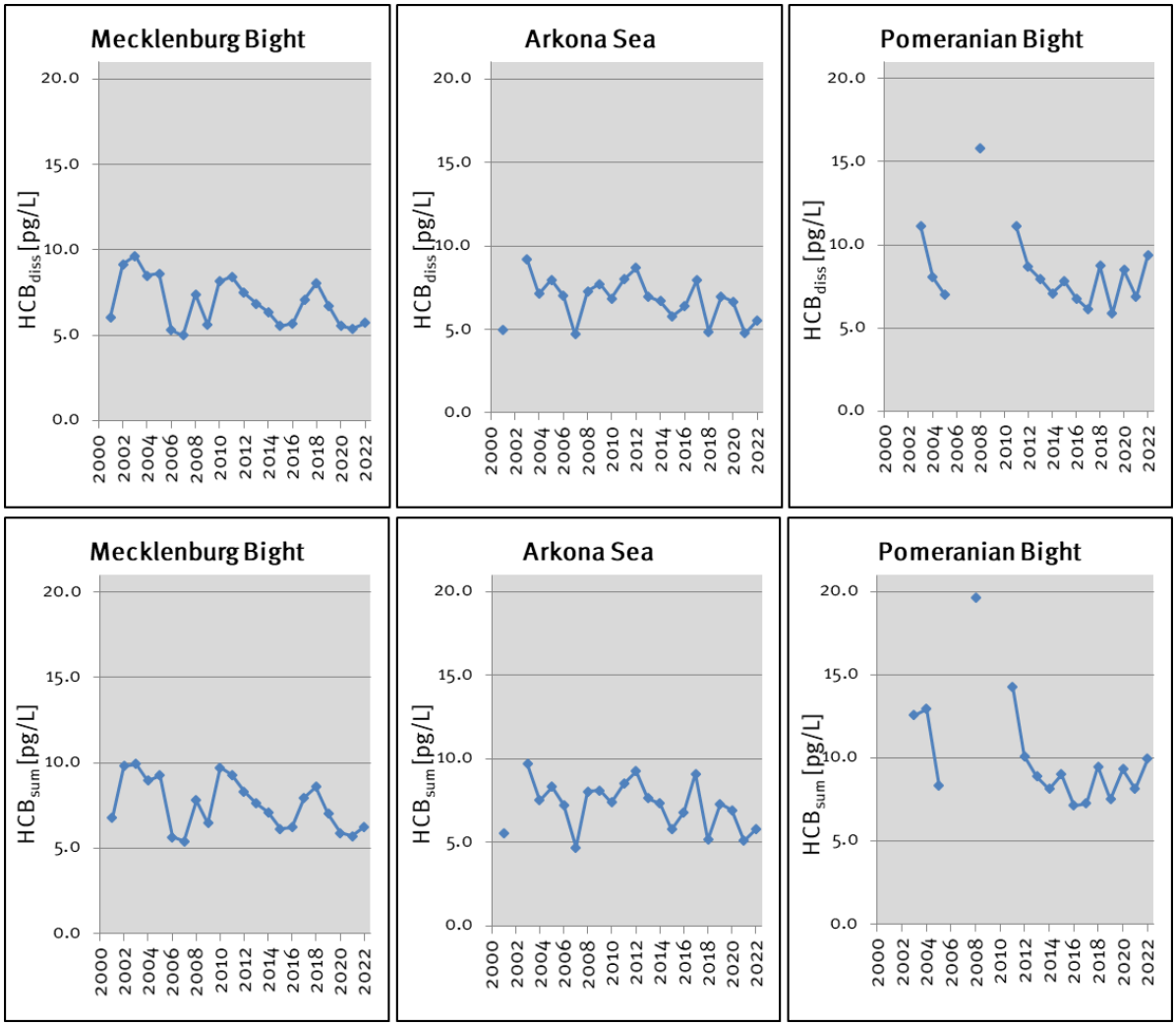


*Fig. 35: Concentrations of HCB in Baltic Sea surface water of Mecklenburg Bight, Arkona Sea and Pomeranian Bight. Upper panel: dissolved water fraction, lower panel: summarized dissolved and suspended water fraction. Gaps in the time line indicate no sampling in the respective year.*

Results for $PCB_{ICES}$

Concentrations for $PCB_{ICES}$ ranged from 1.6 pg $l^{-1}$ $\Sigma PCB_{sum}$[5] in the western Gotland Sea (T9) to 13.1 pg $l^{-1}$ $\Sigma PCB_{sum}$ in the Kiel Bight/Fehmarn Belt (T1) (median: 2.8 pg $l^{-1}$, Fig. 36, Appendix 2). In 2022, highest concentrations of $\Sigma PCB_{sum}$ were found in the Kiel Bight/Fehmarn Belt (T1, 13.1 pg $l^{-1}$) and Mecklenburg Bight (T2, 10.4 pg $l^{-1}$). In these areas and in the Pomeranian Bight particulate PCB ($\Sigma PCB_{part}$[6]) have a noticeably higher share of total PCB ($\Sigma PCB_{sum}$) than at the other sites with particulate PCB contributing more to the overall PCB load at T1 (7.1 pg $l^{-1}$ $\Sigma PCB_{part}$), T2 (6.7 pg $l^{-1}$

[5] $\Sigma PCB_{SUM}$: summarized concentrations of $PCB_{ICES}$ congeners of the dissolved and particulate water fraction
[6] $\Sigma PCB_{part}$: summarized concentrations of $PCB_{ICES}$ congeners in the particulate water fraction

$\Sigma PCB_{part}$) and T4 (2.9 pg $l^{-1}$ $\Sigma PCB_{part}$) than at the other investigated sites. Similar to the observations for DDT/met., the higher PCB load of the particulate water fraction is accompanied by higher SPM loads and might have derived from sediment resuspension due to storm events or in case of the Pomeranian Bight from Odra river inflow.

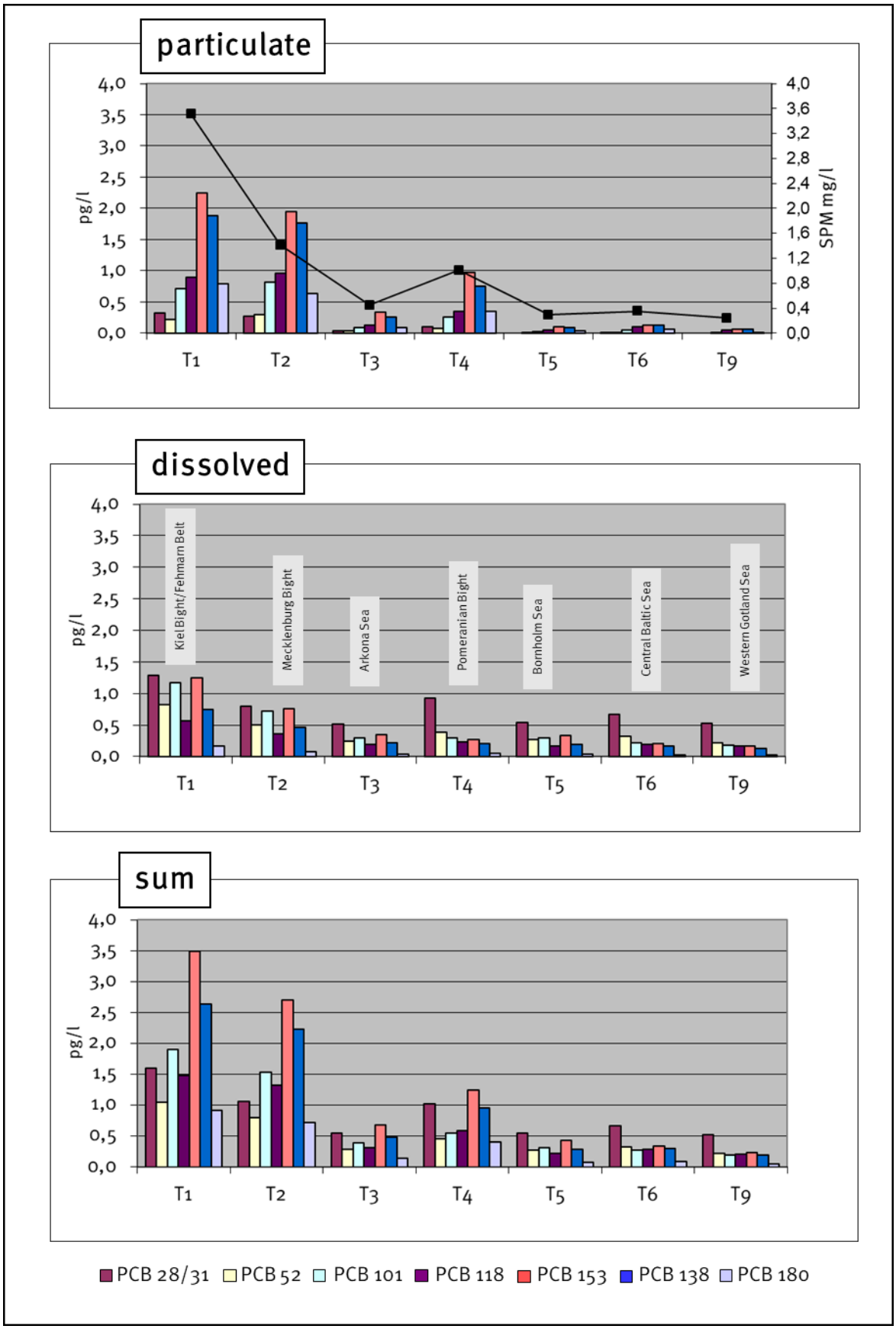


*Fig. 36: Concentrations of PCB$_{ICES}$ in the particulate and dissolved water fractions of Baltic Sea surface water in February 2022. Black squares: SPM contents.*

Concentrations for $PCB_{ICES}$ in surface water for the areas Mecklenburg Bight, Arkona Sea and Pomeranian Bight of past winter observations are shown in Fig. 37. The 2022 data continue the decreasing trends these sites. The increase of $\Sigma PCB_{sum}$ in the Mecklenburg Bight for 2022 results from the noticeable contribution of particulate PCB in 2022.

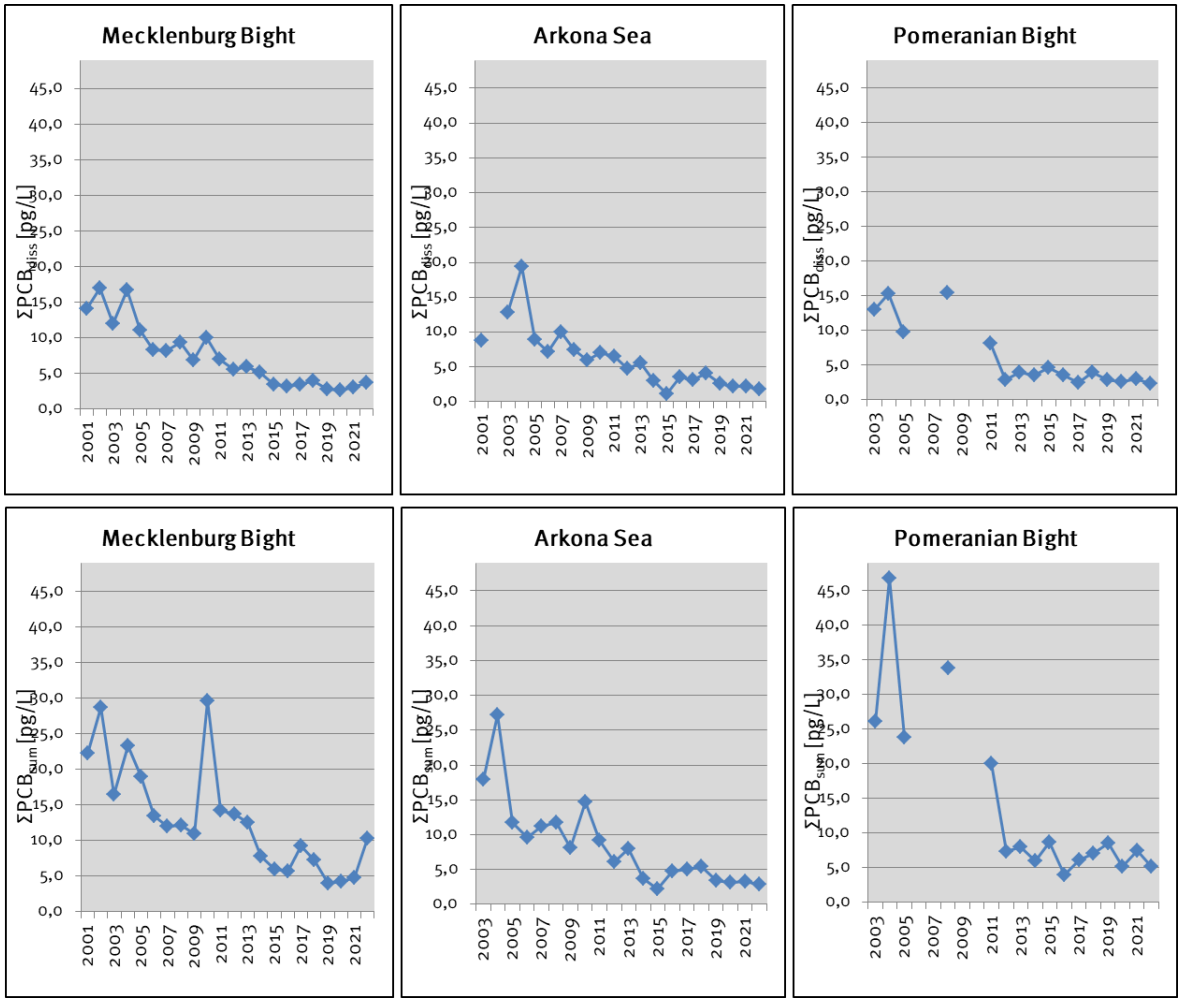


*Fig. 37: Time series of $\Sigma PCB_{ICES}$ concentrations in Baltic Sea surface water of the Mecklenburg Bight, the Arkona Sea and the Pomeranian Bight. Upper panel: dissolved water fraction, lower panel: summarized dissolved and suspended water fraction. Gaps in the time line indicate no sampling at the respective year.*

## Results for heptachlor and heptachlor epoxide

Analysis of heptachlor (HEP) and the metabolite heptachlor epoxide (HEPEP) in surface water of the Baltic Sea reveals only the detection of the more persistent metabolite heptachlor epoxide, which was additionally mainly found in the dissolved water fraction. Concentrations of total heptachlor epoxide ($HEPEP_{SUM}$[7]) ranged from 0.28 pg $l^{-1}$ in the Arkona Sea to 0.83 pg $l^{-1}$ in the Pomeranian Bight (median: 0.67 pg $l^{-1}$). Only in the areas Kiel Bight/Fehmarn Belt and Pomeranian Bight particulate heptachlor epoxide could be detected (Appendix 3).

[7] $HEPEP_{SUM}$: summarized HEPEP concentrations of dissolved and particulate water fraction

### 4.6.2 Organic hazardous substances in surface sediment

Results for DDT and metabolites

Obtained contents of DDT and metabolites in Baltic Sea surface sediment in February 2022 ranged from 29.3 ng $g^{-1}$ TOC ΣDDT (≙ 243.6 pg $g^{-1}$ DW, 0.83 % TOC) at station N1 in the Fehmarn Belt to 168.7 ng $g^{-1}$ TOC ΣDDT (≙ 50.7 pg $g^{-1}$ DW, 0.03 % TOC) at station OBBOJE in the Pomeranian Bight (Fig. 38, Appendix 4). Higher contents of the long-lived degradation products *p,p'*-DDE and *p,p'*-DDD as compared to the compound *p,p'*-DDT were found.

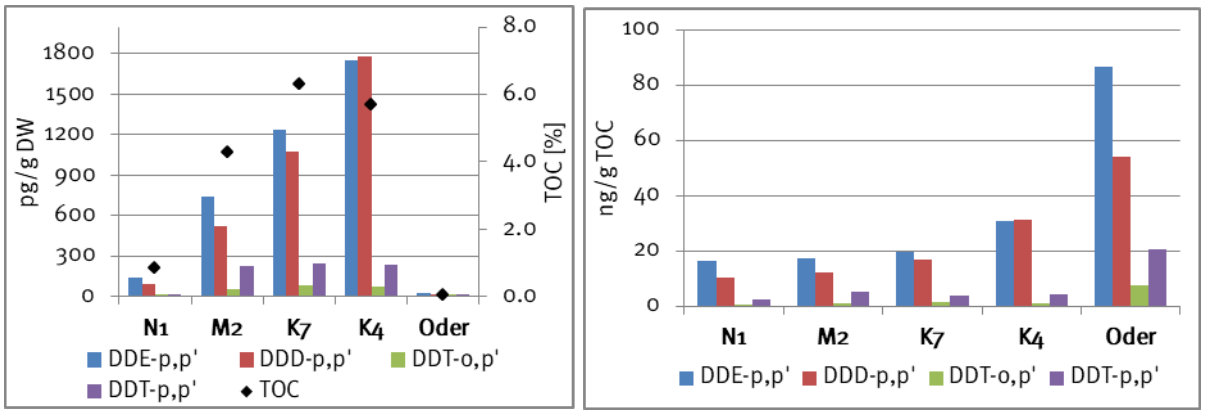


*Fig. 38: Contents of DDT and metabolites in Baltic Sea surface sediments in February 2022 in pg/g DW (DW, dry weight; left) and normalized to the organic carbon content in ng/g TOC (TOC, Total organic carbon; right).*

Time series analysis for the long-lasting DDT metabolites *p,p'*-DDE and *p,p'*-DDD showed no decreasing trends for the investigated study areas Mecklenburg Bight, Arkona Basin and Pomeranian Bight within the investigated period (Fig. 39). High variations of *p,p'*-DDD and *p,p'*-DDE contents in the Pomeranian Bight indicate infrequent high entry from the river Odra.

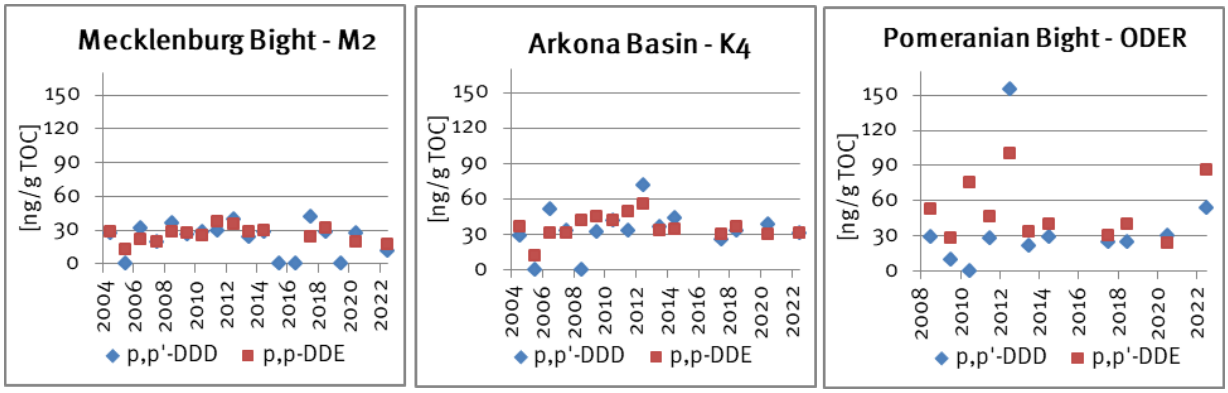


*Fig. 39: Times series of p,p'-DDD and p,p'-DDE contents in Baltic Sea surface sediments from 2004 to 2022 for the Mecklenburg Bight as well as the Arkona Basin and from 2008 to 2022 for the Pomeranian Bight. Gaps in the time line indicate no sampling in the respective year; concentrations at "0 ng/g TOC" indicate that the compound was not detected in the sample.*

Results for HCB

A similar pattern as for DDT and metabolites was observed for HCB; lowest HCB surface sediment contents of 0.34 ng $g^{-1}$ TOC (≙ 2.8 pg $g^{-1}$ DW, 0.83 % TOC) were observed at station N1 in the Kiel Bight/Fehmarn Belt area, whereas the highest HCB content of 44 ng $g^{-1}$ TOC (≙ 13.2pg $g^{-1}$ DW, 0.03 % TOC) was obtained in the Pomeranian Bight (OBBOJE, Appendix 5).

Fig. 40 depicts time series data for HCB surface sediment contents for stations in the Mecklenburg Bight, Arkona Basin and Pomeranian Bight. No decreasing trends for HCB in surface sediment can be observed within the investigated time period, but particular high variations occur in the Pomeranian Bight.

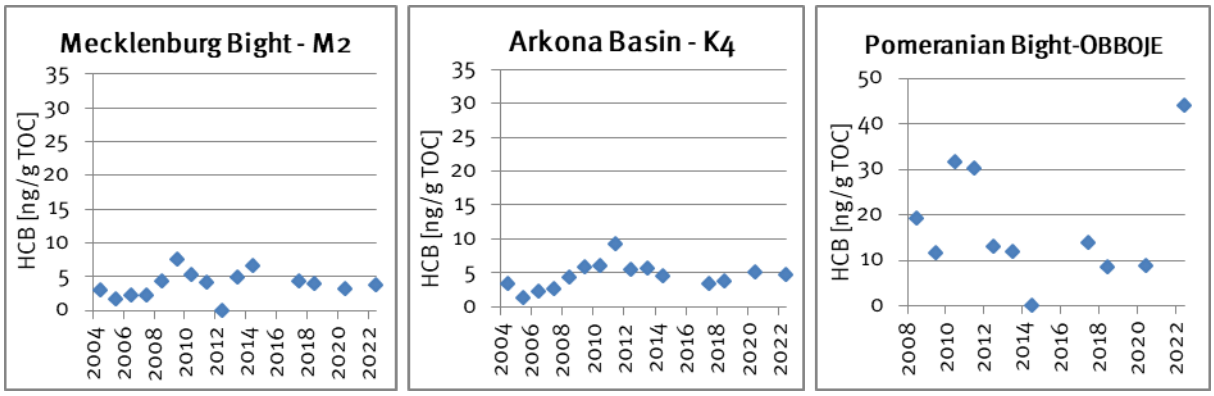


*Fig. 40: Times series of HCB contents in surface sediments from 2004 to 2022 for the Mecklenburg Bight as well as the Arkona Basin and from 2008 to 2022 for the Pomeranian Bight. Gaps in the time line indicate no sampling in the respective year; concentrations at "0 ng/g TOC" mean that the compound was not detected in the sample.*

Results for $PCB_{ICES}$

$PCB_{ICES}$ contents in the surface sediments exhibit a different distribution pattern than DDT/metabolites and HCB contents. Highest contents of $\Sigma PCB_{ICES}$ were found at the sites N1 in the Fehmarn Belt with 132.7 ng $g^{-1}$ TOC (≙ 1101.2 pg $g^{-1}$ DW, 0.83 % TOC) and at OBBOJE in the Pomeranian Bight with 166.0 ng $g^{-1}$ TOC (≙ 49.8 pg $g^{-1}$ DW, 0.03 % TOC, Fig. 41).

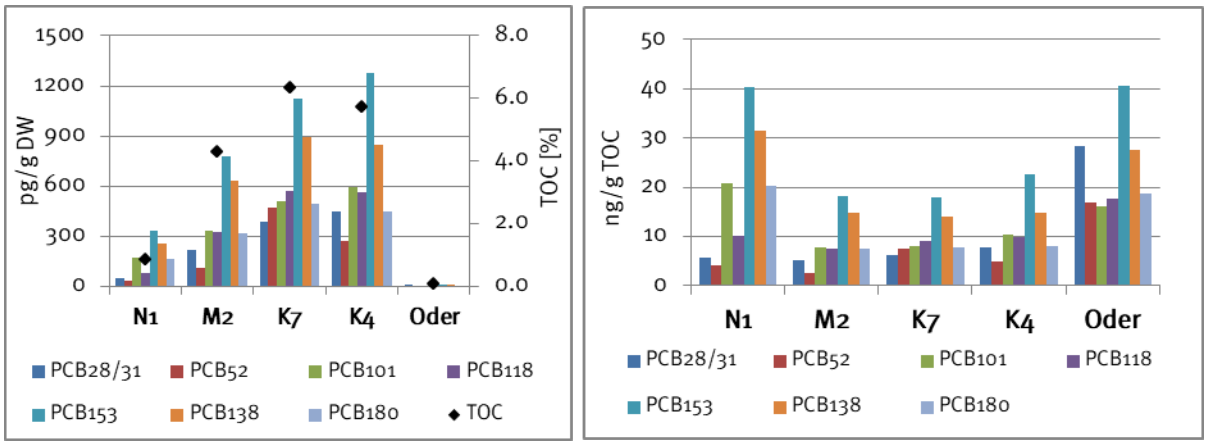


*Fig. 41: Contents of PCB$_{ICES}$ in Baltic Sea surface sediments in February 2022 in pg g$^{-1}$ DW (left) and normalized to the organic carbon content in ng g$^{-1}$ TOC (right).*

Weak declining trends can be observed for PCB$_{ICES}$ surface sediment contents in the Mecklenburg Bight and Arkona Basin. High variations are observed for the Pomeranian Bight (Fig. 42) indicating temporarily high PCB inputs through the river Odra and transportation of PCB-containing particulate material.

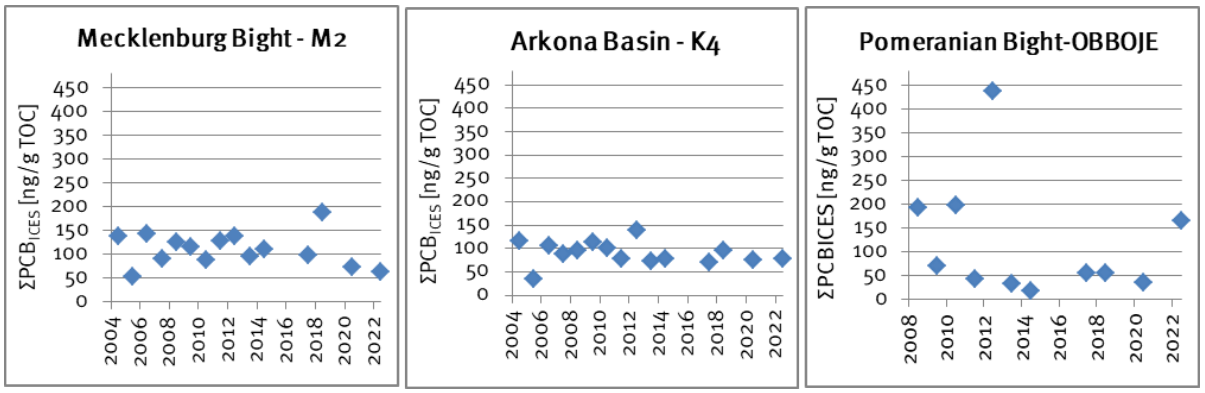


*Fig. 42: Times series of ΣPCB$_{ICES}$ contents in surface sediments from 2004 to 2022 for the Mecklenburg Bight as well as the Arkona Basin and from 2008 to 2022 for the Pomeranian Bight. Gaps in the time line indicate no sampling in the respective year.*

Results for PAH

Obtained data for ΣPAH in Baltic Sea surface sediment ranged from about 17000 ng/g TOC (≙ ca. 141 ng g$^{-1}$ DW, 0.83 % TOC) at station N1 in the Kiel Bight/Fehmarn Belt to 40000 ng/g TOC (≙ ca. 12 ng g$^{-1}$ DW, 0.03 % TOC) at the site Pomeranian Bight (OBBOJE) (Fig. 43, Appendix 7).

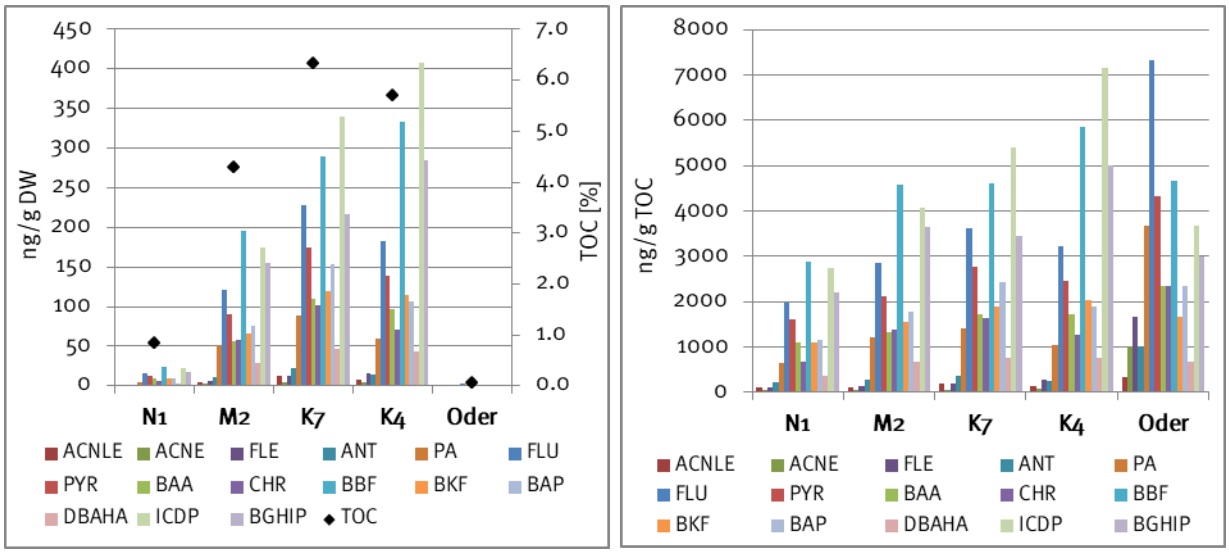


*Fig. 43: Contents of U.S. EPA PAH indicator compounds in Baltic Sea surface sediments in February 2022 in pg g$^{-1}$ DW (left) and normalized to the organic carbon content ng g$^{-1}$ TOC (right).*

Time series data for PAH surface sediment contents depict no trends within the investigated time period (Fig. 44).

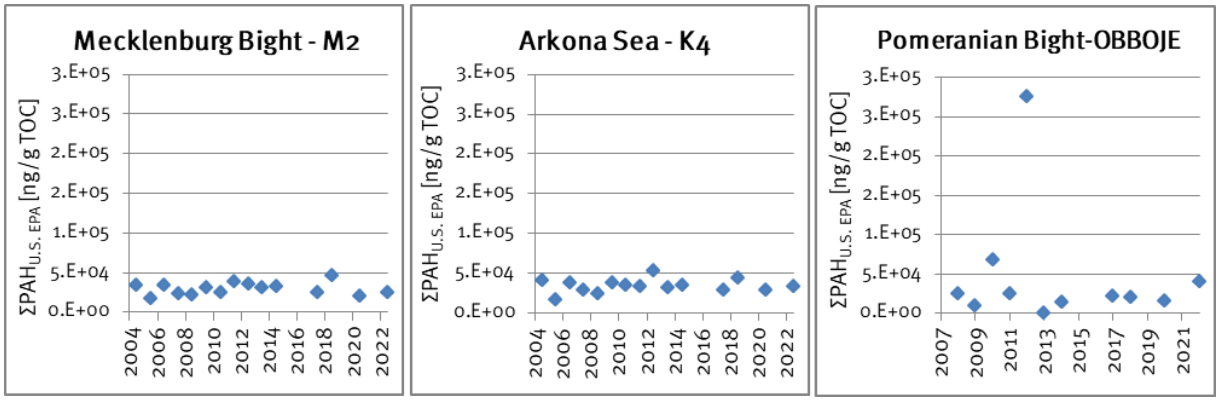


*Fig. 44: PAH surface sediment content time series data from 2004 to 2022 for the Mecklenburg Bight as well as the Arkona Basin and from 2008 to 2022 for the Pomeranian Bight. Gaps in the time line indicate no sampling at the respective year.*

A detailed analysis of pre-industrial and industrial developments of the Baltic Sea PAH pressure on the basis of surface water and sediment PAH monitoring data as well as sediment deposits can be obtained from KANWISCHER et al. (2020).

Results for Organotin

Mono- and dibutyltin (MBT, DBT) as well as TBT were found in surface sediments of the Mecklenburg Bight (M2), Arkona Basin (K7, K4) and Fehmarn Belt (N1), but not in the Pomeranian Bight (OBBOJE); triphenyltin (TPhT) was not detected at any of the studied sites (Fig. 45, Appendix 6).

MBT, DBT and TBT were detected in the Arkona Basin (K7, K4) and the Mecklenburg Bight (M2) and there, total organotin contents (ΣOT[8]) ranged from 256.7 ng $g^{-1}$ TOC (≙ 16.2 ng $g^{-1}$ DW, 6.31 % TOC) at K7 to 278.7 ng $g^{-1}$ TOC (≙ 11.9 ng $g^{-1}$ DW, 4.27 % TOC) at M2 with MBT as the predominant organotin compound. At site N1 only TBT was detected, but with highest content of 108.4 ng $g^{-1}$ TOC comparing to the other investigated sites.

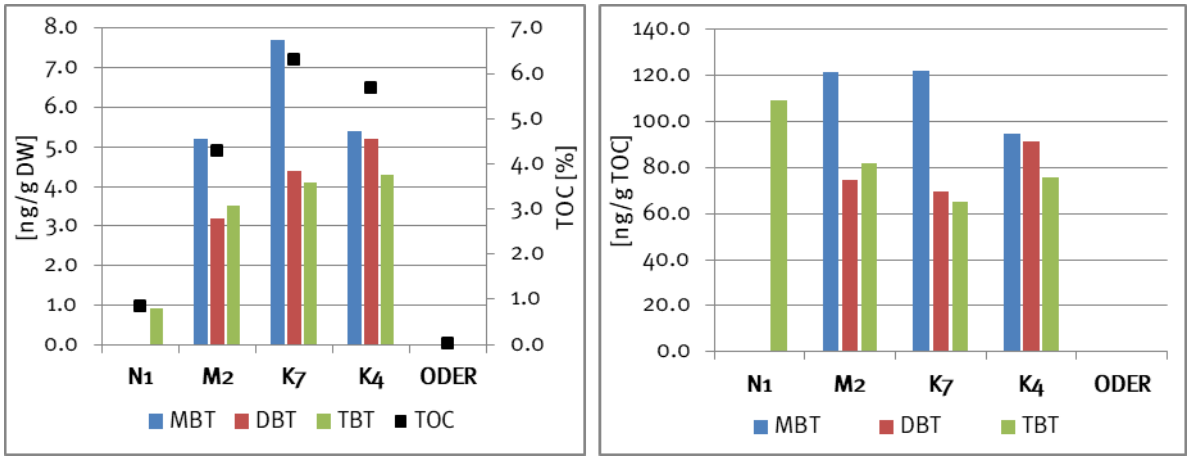


*Fig. 45: Contents of the organotin compounds MBT, DBT and TBT in Baltic Sea surface sediments in February 2022 in ng $g^{-1}$ DW (left) and normalized to the organic carbon content in ng $g^{-1}$ TOC (right).*

MBT, DBT and TBT surface sediment contents for the years 2018, 2020 and 2022 are shown in Table 13 for the sites M2 (Mecklenburg Bight), K4 (Arkona Basin) and OBBOJE (Pomeranian Bight). The short timeframe does not allow a trend analysis and therefore, the time series data will be pursued to enable the assessment of trends. However, MBT and DBT are the predominant organotin compounds most site, indicating TBT degradation at these sites. Organotin compounds largely associate to the organic carbon fraction (ABRAHAM et al. 2017). Thus, analytical limits might circumvent organotin detection at sites with low sediment TOC contents such as at the Pomeranian Bight.

*Table 13: Contents of the organotin compounds MBT, DBT and TBT in Baltic Sea surface sediments at sites M2 (Mecklenburg Bight), K4 (Arkona Basin) and OBBOJE (Pomeranian Bight) for the years 2018, 2020 and 2022.*

| | 2018 | | | 2020 | | | 2022 | | |
|---|---|---|---|---|---|---|---|---|---|
| | M2 | K4 | OBBOJE | M2 | K4 | OBBOJE | M2 | K4 | OBBOJE |
| | ng $g^{-1}$ TOC | | | | | | | | |
| MBT | 164.0 | 88.7 | n.d. | 113 | 99.8 | n.d. | 121.8 | 94.9 | n.d. |
| DBT | 111.1 | 70.9 | n.d. | 88.8 | 111 | n.d. | 74.9 | 91.4 | n.d. |
| TBT | 79.4 | 42.6 | 136.4 | 73.3 | 56.5 | 85.7 | 82 | 75.6 | n.d. |

[8] ΣOT: Sum of MBT, DBT and TBT contents in surface sediment

### 4.6.3 Assessment of the results

Quantitative threshold values for contaminants defining a good environmental status of the Baltic Sea have been defined within the framework of European water policy and the HELCOM commitment. Under European legislation, monitoring of hazardous substances in the Baltic Sea is directed through the MSFD[9] and the WFD[10]. The Environmental Quality Standards (EQS) for surface waters of the EQS-Directive[11] serve as the basis to evaluate obtained results for chlorinated hydrocarbons in Baltic Sea surface water in February 2022 (Table 14). Obtained surface sediment data were be evaluated utilizing HELCOM indicators (Table 15).

None of the obtained contaminant data in the Baltic Sea surface water exceeded defined maximum allowable concentrations (MAC-EQS, Table 14). In addition, determined concentrations for DDT and metabolites as well as HCB did not exceed annual average EQS (AA-EQS) values. However, obtained concentrations for heptachlor epoxide exceeded the annual average EQS (AA-EQS) in all investigated study areas.

Anthracene contents in surface sediment at the site Pomeranian Bight (OBBOJE) exceeded the threshold value of the HELCOM indicator *PAH*. Determined contents for TBT exceeded the threshold value for the HELCOM indicator *TBT and imposex* at the investigated sites except for the Pomeranian Bight (Table 15).

[9] Directive 2008/56/EC of the European Parliament and of the Council of 17 June 2008 establishing a framework for community action in the field of marine environmental policy

[10] Directive 2000/60/EC of the European Parliament and of the Council of 23 October 2000 establishing a framework for Community action in the field of water policy

[11] Directive 2008/105/EC of the European Parliament and of the Council of 16 December 2008 on environmental quality standards in the field of water policy; amended by directive 2013/39/EU

*Table 14: Assessment of obtained Baltic Sea surface water contaminant concentrations in February 2022 on the basis of Environmental Quality Standards (EQS) of the EQS-Directive. Red values: exceeded EQS, AA-EQS: annual average EQS, MAC-EQS: maximum allowable concentration, data for dissolved and particulate water fraction are summed.*

| Substance | Other Surface waters AA-EQS | Other Surface waters MAC-EQS | Kiel Bight/ Fehmarnbelt (T1) | Mecklenburg Bight (T2) | Arkona Sea (T3) | Pomeranian Bight (T4) | Bornholm Sea (T5) | Central Baltic Sea (T6) | Western Gotland Sea (T9) |
|---|---|---|---|---|---|---|---|---|---|
| | | | | | | µg $l^{-1}$ | | | |
| **ΣDDT$_{sum}$** | 0.025 | - | 0.000007 | 0.000008 | 0.000005 | 0.000009 | 0.000005 | 0.000005 | 0.000003 |
| ***p.p'*-DDT$_{sum}$** | 0.01 | - | 0.000001 | 0.000001 | 0.000001 | 0.000001 | 0.000001 | 0.000001 | 0.000000 |
| **HCB$_{sum}$** | - | 0.05 | 0.000008 | 0.000006 | 0.000006 | 0.000010 | 0.000005 | 0.000007 | 0.000006 |
| **Heptachlor** | $1{\cdot}10^{-8}$ | $3{\cdot}10^{-5}$ | n.d. | n.d. | n.d. | n.d. | n.d. | n.d. | n.d. |
| **Hepatchlor epoxide** | $1{\cdot}10^{-8}$ | $3{\cdot}10^{-5}$ | $71{\cdot}10^{-8}$ | $81{\cdot}10^{-8}$ | $28{\cdot}10^{-8}$ | $83{\cdot}10^{-8}$ | $30{\cdot}10^{-8}$ | $67{\cdot}10^{-8}$ | $28{\cdot}10^{-8}$ |

*Table 15: Assessment of obtained surface sediment contaminant data in February 2022 on the basis of HELCOM indicators. red values: exceeded threshold value. n.d. not detected.*

| indicator | substance | threshold value | Kiel B./Fehmarn B. (N1) | Mecklenburg B. (M2) | Arkona B. (K7) | Arkona B. (K4) | Pomeranian B. (OBBOJE) |
|---|---|---|---|---|---|---|---|
| | | | [µg $kg^{-1}$ DW. 5 % TOC] | | | | |
| PAH | **anthracene** | 24 | 11 | 13 | 18 | 13 | 50 |
| | **fluoranthene** | 3500 | 99 | 142 | 180 | 161 | 367 |
| TBT and imposex | **tributyltin** | 1.6 | 5.4 | 4.1 | 3.2 | 3.8 | n.d. |

## Acknowledgements

The authors would like to thank the staff of the Leibniz Institute for Baltic Sea Research Warnemünde who carried out measurements as part of HELCOM's Baltic Sea monitoring programme and IOW's long-term measuring programme, and the captain and crew of the research vessel Elisabeth Mann Borgese for their effort and support during monitoring and long-term programme cruises in 2022. The authors are also grateful to a number of other people and organisations for help: Weibke Aldenhoff and Jürgen Holfort of the Sea Ice Service at the Federal Maritime and Hydrographic Agency, Hamburg and Rostock, for advice in the description of the ice winter and especially for supplying the ice cover chart; the Deutscher Wetterdienst for supplying wind data from Arkona and Warnemünde from its online data portal; the Swedish Meteorological and Hydrological Institute, Norrköpping, for providing tide gauge data from its online data portal; Lotta Fyrberg from SMHI's Oceanographic Laboratory in Gothenburg for providing us with hydrographic and hydrochemical observations from Sweden's Ocean Archive (SHARK) relating to selected stations within the Swedish national monitoring programme; Tamara Zalewska and team from the Maritime Office of the Polish Institute of Meteorology and Water Management (IMGW) in Gdynia providing observational data from the Danzig Deep; Aleksandra Kowalska, IMGW in Warsaw, for providing data on solar irradiance at Gdynia.

## References


ABRAHAM, M., L. WESTPHAL, I. HAND, A. LERZ, J. JESCHEK, D. BUNKE, T. LEIPE, SCHULZ-BULL, D., 2017: TBT and its metabolites in sediments: Survey at a German coastal site and the central Baltic Sea. Marine Pollution Bulletin 121: 404–410. doi:10.1016/j.marpolbul.2017.06.020.

ALDENHOFF, W., 2022: Der Eiswinter 2021/22 an den deutschen Küsten und der gesamten Ostsee. Eisdienst, Bundesamt für Seeschifffahrt und Hydrographie Rostock, https://www.bsh.de/DE/DATEN/Vorhersagen/Eisberichte-und-Eiskarten/_Anlagen/Downloads/Beschreibung-Eiswinter/Beschreibung-Eiswinter-2021-2022.pdf?__blob=publicationFile&v=3

ALZIEU, C., 1998: Tributyltin: case study of a chronic contaminant in the coastal environment. Ocean & Coastal Management, 40(1), pp. 23-36.

ANTIZAR-LADISLAO, B., 2008: Environmental levels, toxicity and human exposure to tributyltin (TBT)-contaminated marine environment. A review. Environment International, 34(2), pp. 292-308.

BSH, 2009: Flächenbezogene Eisvolumensumme. http://www.bsh.de/de/Meeresdaten/Beobachtungen/Eis/Kuesten.jsp

V.BODUNGEN, B., GRAEVE, M., KUBE, J., LASS, H.U., MEYER-HARMS, B., MUMM, N., NAGEL, K., POLLEHNE, F., POWILLEIT, M., RECKERMANN, M., SATTLER, C., SIEGEL, H., WODARG, D., 1995: Stoff-Flüsse am Grenzfluss – Transport- und Umsatzprozesse im Übergangsgebiet zwischen Oderästuar und Pommerscher Bucht (TRUMP). Geowiss. 13, 479-485.

DIAZ, R.J., ROSENBERG, R., 2008: Spreading dead zones and consequences for marine ecosystems. Science 321 (5891), 926-929.

DUARTE, C.M., CONLEY, D.J., CARSTENSEN, J., SÁNCHEZ-CAMACHO, M., 2009: Return to Neverland: Shifting baselines affect eutrophication restoration targets. Estuaries and Coasts 32 (1), 29-36.

DWD, 2023: Monatlicher Klimastatus, Nr. 1 – 12. Deutscher Wetterdienst. https://www.dwd.de/DE/leistungen/pbfb_verlag_monat_klimastatus/monat_klimastatus.html

DWD, 2023a: Windmessungen der Station Arkona in Stundenmittelwerten des Jahres 2022. ftp://ftp-cdc.dwd.de/pub/CDC/observations_germany/climate/

DWD, 2023b: Langzeitdaten von Windmessungen der Station Arkona in Tagesmittelwerten. ftp://ftp-cdc.dwd.de/pub/CDC/observations_germany/climate/daily/kl/historical/

EFSA, E.F.S.A. 2007: Opinion of the Scientific Panel on contaminants in the food chain [CONTAM] related heptachlor as an undesirable substance in animal feed. EFSA Journal 5. John Wiley & Sons, Ltd: 478. doi:10.2903/j.efsa.2007.478.

FEISTEL, R., NAUSCH, G., HAGEN, E., 2006: Unusual Baltic inflow activity in 2002–2003 and varying deep-water properties. Oceanologia 48, pp. 21–35.

FEISTEL, R. SEIFERT, T., FEISTEL, S., NAUSCH, G., BOGDANSKA, B., BROMAN, B., HANSEN, L., HOLFORT, J., MOHRHOLZ, V., SCHMAGER, G., HAGEN, E., PERLET, I., WASMUND, N., 2008: Digital supplement. In: FEISTEL, R., NAUSCH, G. WASMUND, N. (eds.): State and evolution of the Baltic Sea 1952-2005. John Wiley & Sons, Inc., Hoboken, New Jersey, pp. 625-667.

GRASSHOFF, K., ERHARDT, M., KREMLING, K., 1983: Methods of seawater analysis. 2nd ed., Verlag Chemie, Weinheim.

GRÄWE, U., NAUMANN, M., MOHRHOLZ, V., BURCHARD, H., 2015: Anatomizing one of the largest saltwater inflows in the Baltic Sea in December 2014. J. Geophys. Res. 120, 7676-7697.

HAGEN, E., FEISTEL, R., 2008: Baltic climate change. In: FEISTEL, R., NAUSCH, G., WASMUND, N. (eds.), State and evolution of the Baltic Sea 1952 – 2005. John Wiley & Sons, Inc., Hoboken, New Jersey, pp. 93-120.

HELCOM, 2013: Approaches and methods for eutrophication target setting in the Baltic Sea region. Helsinki Commission, Helsinki, Finland.

HELCOM, 2017: Manual for marine monitoring in the COMBINE programme of HELCOM. Internet, last updated July 2017: https://helcom.fi/action-areas/monitoring-andassessment/monitoring-guidelines/combine-manual/

HELCOM, 2018a: State of the Baltic Sea - Second HELCOM holistic assessment 2011-2016. Balt. Sea Environ. Proc. 155. Helsinki, Finland. http://stateofthebalticsea.helcom.fi

HELCOM, 2018b: Sources and pathways of nutrients to the Baltic Sea - HELCOM PLC-6. Helsinki, Finland. www.helcom.fi/Lists/Publications/BSEP143.pdf

HELCOM, 2018c: Inputs of hazardous substances to the Baltic Sea. Baltic Sea Environment Proceedings 162.

HELCOM, 2023: State of the Baltic Sea - Second HELCOM holistic assessment 2016-2021. Balt. Sea Environ. Proc. 194. Helsinki, Finland. https://helcom.fi/wp-content/uploads/2023/10/State-of-the-Baltic-Sea-2023.pdf

HOCH, M., 2001: Organotin Compounds in the Environment - an Overview. Appl. Geochemistry 16 (7–8), 719–743. doi: 10.1016/S0883-2927(00)00067-6.

HOLFORT, J., 2022a: Örtliche Sturmflut am 17.01.2022 an der deutschen Ostseeküste. Bundesamt für Seeschifffahrt und Hydrographie Rostock, https://www.bsh.de/DE/THEMEN/Wasserstand_und_Gezeiten/Sturmfluten/_Anlagen/Downloads/Ostsee_Sturmflut_20220117.pdf;jsessionid=0F490C3D9B5247CC5EAA3CA7A8B04813.live11293?__blob=publicationFile&v=5

HOLFORT, J., 2022b: Sturmflut am 20./21.01.2022 an der deutschen Ostseeküste. Bundesamt für Seeschifffahrt und Hydrographie Rostock, https://www.bsh.de/DE/THEMEN/Wasserstand_und_Gezeiten/Sturmfluten/_Anlagen/Downloads/Ostsee_Sturmflut_20220120.pdf;jsessionid=0F490C3D9B5247CC5EAA3CA7A8B04813.live11293?__blob=publicationFile&v=2

IMGW, 2023: Solar radiation in J/m² at the station Gdynia 2022 – unpublished data

JACOBSEN, T.S., 1980: Sea water exchange of the Baltic. Measurements and methods. The Belt Project. The National Agency for Environmental Protection, Denmark: p107

KANWISCHER, M., BUNKE, D., LEIPE, T., MOROS, M., SCHULZ-BULL, D. E., 2020: Polycyclic aromatic hydrocarbons in the Baltic Sea — Pre-industrial and industrial developments as well as current status. Marine Pollution Bulletin 160. Elsevier: 111526. doi:10.1016/j.marpolbul.2020.111526.

KHARBUSH, J. J., CLOSE, H. G., VAN MOOY, B. A. S., ARNOSTI, C., RSMITTENBERG, . H., LE MOIGNE, F. A. C., MOLLENHAUER, G., SCHOLZ-BÖTTCHER, B., OBREHT, I., KOCH, B. P., BECKER, K. W., IVERSEN, M. H.

MOHR, W., 2020: Particulate Organic Carbon Deconstructed: Molecular and Chemical Composition of Particulate Organic Carbon in the Ocean. Frontiers in Marine Science 7(518).

KOSLOWSKI, G., 1989: Die flächenbezogene Eisvolumensumme, eine neue Maßzahl für die Bewertung des Eiswinters an der Ostseeküste Schleswig-Holsteins und ihr Zusammenhang mit dem Charakter des meteorologischen Winters. Dt. Hydrogr. Z. 42, 61-80.

KRÜGER, S., 2000: Basic shipboard instrumentation and fixed autonomic stations for monitoring in the Baltic Sea. In: EL-HAWARY, F. (ed.): The ocean engineering handbook. CRC Press, Boca Raton, USA, pp. 52-61.

KRÜGER, S., ROEDER, W., WLOST, K.-P., KOCH, M., KÄMMERER, H., KNUTZ, T., 1998: Autonomous instrumentation carrier (APIC) with acoustic transmission for shallow water profiling. Oceanology International 98: The Global Ocean Conf. Proc. 2, 149-158.

KUSS, J., ROEDER, W., WLOST, K.-P., DEGRANDPRE, M.D., 2006: Time-series of surface water $CO_2$ and oxygen measurements on a platform in the central Arkona Sea (Baltic Sea): Seasonality of uptake and release. Marine Chemistry 101, 220-232.

KUSS, J., NAUSCH, G., ENGELKE, C., LUTTERBECK, H., NAUMANN, M., WANIEK, J.J., AND SCHULZ BULL, D.E., 2020: Changes of nutrient concentrations in the western Baltic Sea in the transition between inner coastal waters to the central basins: time series from 1995 to 2016 with source analysis. Frontiers in Earth Science 8, 1-13.

LASS, H.U., MOHRHOLZ, V., SEIFERT, T., 2001: On the dynamics of the Pomeranian Bight. Cont. Shelf. Res. 21, 1237-1261.

LE MOIGNE, F. A. C., 2019: Pathways of Organic Carbon Downward Transport by the Oceanic Biological Carbon Pump. Frontiers in Marine Science 6(634).

LISITZIN, E., 1974: Sea-level changes. Elsevier Oceanography Series, Vol. 8, Amsterdam: p286

MATTHÄUS W., FRANCK, H., 1992: Characteristics of major Baltic inflows - a statistical analysis. Cont. Shelf Res., 12, 1375-1400.

MOHRHOLZ, V., 1998: Transport- und Vermischungsprozesse in der Pommerschen Bucht. Meereswiss. Ber. Warnemünde 33, 1-106.

MOHRHOLZ, V., NAUMANN, M., NAUSCH, G., KRÜGER, S. and GRÄWE, U., 2015: Fresh oxygen for the Baltic Sea – an exceptional saline inflow after a decade of stagnation. – Journal Mar. Syst. 148, 152-166.

MOHRHOLZ, V., 2018: Major Baltic inflow statistics – reviewed. Front. Mar. Sci. 5, 384. doi: 10.3389/fmars.2018.00384

MÜLLER, M. D., H.-R. BUSER, RAPPE, C., 1997: Enantioselective determination of various chlordane components and metabolites using high-resolution gas chromatography with a β-cyclodextrin derivative as chiral selector and electron-capture negative ion mass spectrometry detection. Chemosphere 34: 2407–2417. doi:10.1016/S0045-6535(97)00086-6.

NAUMANN, M., MOHRHOLZ, V., Waniek, J.J., 2017: Water exchange between the Baltic Sea and the North Sea, and conditions in the deep basins. – HELCOM Baltic Sea Environmental Fact

Sheet Online, https://helcom.fi/wp-content/uploads/2020/07/BSEFS-Water-exchange-between-the-Baltic-Sea-and-the-North-Sea-and-conditions-in-the-deep-basins-2017.pdf

NAUMANN, M., UMLAUF, L., MOHRHOLZ, V., KUSS, J., SIEGEL, H., WANIEK, J.J., SCHULZ-BULL, D.E., 2018: Hydrographic-hydrochemical assessment of the Baltic Sea 2017, Meereswiss. Ber. Warnemünde 107, 97 pp. doi:10.12754/msr-2018-0107

NAUSCH, G., NEHRING, D., 1996: Baltic Proper, Hydrochemistry. In: Third Periodic Assessment of the State of the Marine Environment of the Baltic Sea. – Balt. Sea Environ. Proc. 64B, 80-85.

NAUSCH, G., BACHOR, A., PETENATI, T., VOSS, J., V. WEBER, M., 2011: Nährstoffe in den deutschen Küstengewässern der Ostsee und angrenzenden Seegebieten. Meeresumwelt Aktuell Nord- und Ostsee 2011/1.

NAUSCH, G., FEISTEL, R., LASS, H.-U., NAGEL, K., SIEGEL, H., 2002: Hydrographisch-chemische Zustandseinschätzung der Ostsee 2001. Meereswiss. Ber. Warnemünde 49, 3-77.

NAUSCH, G., NAUMANN, M., UMLAUF, L., MOHRHOLZ, V., SIEGEL,H., 2014: Hydrographisch-hydrochemische Zustandseinschätzung der Ostsee 2013. Meereswiss. Ber. Warnemünde 93, 1-104.

NAUSCH, G., NEHRING, D., NAGEL, K., 2008: Nutrient concentrations, trends and their relation to eutrophication. In: FEISTEL, R., NAUSCH, G., WASMUND, N. (eds.): State and evolution of the Baltic Sea, 1952-2005. John Wiley & Sons, Inc. Hoboken, New Jersey, 337-366.

NEHRING, D., MATTHÄUS, W., 1991: Current trends in hydrographic and chemical parameters and eutrophication in the Baltic Sea. Int. Revue ges. Hydrobiol. 76, 297-316.

NEHRING, D., MATTHÄUS, W., LASS, H.U., 1993: Die hydrographisch-chemischen Bedingungen in der westlichen und zentralen Ostsee im Jahre 1992. Dt. Hydrogr. Z. 45, 281-331.

NEHRING, D., MATTHÄUS, W., LASS, H.U., NAUSCH, G., NAGEL, K., 1995: Hydrographisch-chemische Zustandseinschätzung der Ostsee 1994. Meereswiss. Ber. Warnemünde 9, 1-71.

REDFIELD, A. C., 1934: On the proportions of organic derivations in sea water and their relation to the composition of plankton. James Johnstone Memorial Volume. R. J. Daniel. Liverpool, University Press: 177-192.

REDFIELD, A.C., KETCHUM, B.H., RICHARDS, F.A., 1963: The influence of organisms on the composition of sea water. In: HILL, M.N. (ed.): The sea. J. Wiley & Sons, pp. 26-77.

REYNOLDS, R. W., SMITH, T.M., LIU, C., CHELTON, D.B., CASEY, K.S., SCHLAX, M.G., 2007: Daily high-resolution-blended analyses for sea surface temperature. J. Clim. 20, 5473–5496.

SCHLITZER, R., 2018: OCEAN DATA VIEW 5, ODV5 RELEASE 5.1.7 (WINDOWS 64BIT) OCT. 2018. AWI-BREMERHAVEN, 2018.

SCHMELZER, N., SEINÄ, A., LUNDQUIST, J.-E., SZTOBRYN, M.. 2008: Ice, in: Feistel, R., Nausch, G., and Wasmund, N. (Eds.), State and Evolution of the Baltic Sea 1952 – 2005. – John Wiley & Sons, Inc., Hoboken, New Jersey, p. 199-240.

SCHULZ-BULL, D., HAND, I., LERZ, A., SCHNEIDER, R., TROST, E., WODARG, D., 2011: Regionale Verteilung chlorierter Kohlenwasserstoffe (CKW) und polycyclischer aromatischer Kohlenwasserstoffe (PAK) im Pelagial und Oberflächensediment in der deutschen ausschließlichen Wirtschaftszone (AWZ) im Jahr 2010. Leibniz-Institut für

Ostseeforschung an der Universität Rostock im Auftrag des Bundesamtes für Seeschifffahrt und Hydrographie Hamburg, Rostock Warnemünde.

SEIDEL, M., MANECKI, M., HERLEMANN, D. P. R., DEUTSCH, B., SCHULZ-BULL, D., JÜRGENS K., DITTMAR, T., 2017: Composition and Transformation of Dissolved Organic Matter in the Baltic Sea. Frontiers in Earth Science 5: 31.

SIEGEL, H., GERTH, M., SCHMIDT, T., 1996: Water exchange in the Pomeranian Bight – investigated by satellite data and shipborne measurements. Cont. Shelf Res 16, 1793-1817.

SMHI, 2023a: Tide gauge data at station Landort Norra in hourly means of the year 2022; geodesic reference level RH2000. http://opendata-download-ocobs.smhi.se/explore/

SMHI, 2023b: Accumulated inflow through the Öresund 2014-2022. http://www.smhi.se/hfa_coord/BOOS/Oresund.html

SMHI, 2023c: Hydrographic and hydrochemical observations from Sweden's national monitoring programme, Ocean Archive (SHARK).

STRANDBERG, B., VAN BAVEL, B., BERGQVIST, P.-A., BROMAN, D., ISHAQ, R., NÄF, C., PETTERSEN, H., RAPPE, C., 1998: Occurrence, sedimentation, and spatial variations of organochlorine contaminants in settling particulate matter and sediments in the northern part of the Baltic Sea. Environmental Science & Technology. American Chemical Society 32 (12), pp. 1754–1759. doi: 10.1021/es970789m.

SZYMCZYCHA, B., WINOGRADOW, A., KULIŃSKI, K., KOZIOROWSKA, K. PEMPKOWIAK, J., 2017: Diurnal and seasonal DOC and POC variability in the land-locked sea. Oceanologia 59(3): 379-388.

TRUMP, 1998: Transport- und Umsatzprozesse in der Pommerschen Bucht (TRUMP) 1994-1996. Abschlussbericht, Warnemünde, 1-32 (unveröffentlicht).

WEIDIG, B. (2022): Sturmflut vom 28.01. / Niedrigwasser vom 30.01. / Sturmflut vom 30./31.01.2022. https://www.bsh.de/DE/THEMEN/Wasserstand_und_Gezeiten/Sturmfluten/_Anlagen/Downloads/Ostsee_Sturmflut_20220128-31.pdf;jsessionid=0F490C3D9B5247CC5EAA3CA7A8B04813.live11293?__blob=publicationFile&v=3

WINOGRADOW, A., MACKIEWICZ, A., PEMPKOWIAK, J., 2019: Seasonal changes in particulate organic matter (POM) concentrations and properties measured from deep areas of the Baltic Sea. Oceanologia 61(4): 505-521.

ZIMMERMAN, A.E., ALLISON, S.D., MARTINY, A.C., 2014: Phylogenetic constraints on elemental stoichiometry and resource allocation in heterotrophic marine bacteria. Environmental Microbiology 16: 1398-1410.

## Appendix: Organic hazardous substances

*Appendix 1: Concentrations of DDT and metabolites in Baltic surface water in February 2022. n.d. not detected.*

| Dissolved | Transect | *p.p'*-DDE | *p.p'*-DDD | *o.p'*-DDT | *p.p'*-DDT | ΣDDT$_{diss}$ |
|---|---|---|---|---|---|---|
| | | | | Pg l$^{-1}$ | | |
| Kiel Bight/ Fehmarn Belt | T1 | 1.9 | 1.6 | 0.13 | 0.32 | 3.9 |
| Mecklenburg Bight | T2 | 2.0 | 1.5 | 0.14 | 0.22 | 3.9 |
| Arkona Sea | T3 | 1.5 | 0.86 | 0.22 | 0.47 | 3.1 |
| Pomeranian Bight | T4 | 2.2 | 1.9 | 0.35 | 0.79 | 5.3 |
| Bornholm Sea | T5 | 1.9 | 1.4 | 0.24 | 0.50 | 4.0 |
| central Baltic Sea | T6 | 1.6 | 1.5 | 0.27 | 0.61 | 3.9 |
| western Gotland Sea | T9 | 0.86 | 0.88 | 0.17 | 0.31 | 2.2 |

| Particulate | Transect | *p.p'*-DDE | *p.p'*-DDD | *o.p'*-DDT | *p.p'*-DDT | ΣDDT$_{part}$ |
|---|---|---|---|---|---|---|
| | | | | Pg l$^{-1}$ | | |
| Kiel Bight/ Fehmarn Belt | T1 | 1.7 | 0.95 | 0.09 | 0.38 | 3.2 |
| Mecklenburg Bight | T2 | 2.2 | 1.2 | 0.11 | 0.59 | 4.1 |
| Arkona Sea | T3 | 0.74 | 0.25 | 0.09 | 0.38 | 1.5 |
| Pomeranian Bight | T4 | 2.3 | 0.91 | 0.16 | 0.55 | 3.9 |
| Bornholm Sea | T5 | 0.44 | 0.11 | 0.04 | 0.16 | 0.74 |
| central Baltic Sea | T6 | 0.48 | 0.20 | 0.04 | 0.18 | 0.90 |
| western Gotland Sea | T9 | 0.22 | 0.08 | 0.04 | 0.13 | 0.47 |

| Sum (dissolved + particulate) | Transect | *p.p'*-DDE | *p.p'*-DDD | *o.p'*-DDT | *p.p'*-DDT | ΣDDT$_{sum}$ |
|---|---|---|---|---|---|---|
| | | | | Pg l$^{-1}$ | | |
| Kiel Bight/ Fehmarn Belt | T1 | 3.6 | 2.5 | 0.20 | 0.66 | 6.9 |
| Mecklenburg Bight | T2 | 4.2 | 2.7 | 0.25 | 0.81 | 7.9 |
| Arkona Sea | T3 | 2.3 | 1.1 | 0.31 | 0.85 | 4.5 |
| Pomeranian Bight | T4 | 4.5 | 2.8 | 0.51 | 1.4 | 9.1 |
| Bornholm Sea | T5 | 2.3 | 1.5 | 0.28 | 0.66 | 4.7 |
| central Baltic Sea | T6 | 2.1 | 1.7 | 0.31 | 0.79 | 4.8 |
| western Gotland Sea | T9 | 1.1 | 0.96 | 0.21 | 0.44 | 2.7 |

*Appendix 2: Concentrations of $PCB_{ICES}$ in Baltic surface water in February 2022.*

| Dissolved | Transect | PCB 28/31 | PCB 52 | PCB 101 | PCB 118 | PCB 153 | PCB 138 | PCB 180 | $\Sigma PCB_{diss}$ |
|---|---|---|---|---|---|---|---|---|---|
| | | | | | | Pg $l^{-1}$ | | | |
| Kiel Bight/ Fehmarn Belt | T1 | 1.3 | 0.83 | 1.2 | 0.57 | 1.2 | 0.7 | 0.16 | 6.0 |
| Mecklenburg Bight | T2 | 0.80 | 0.50 | 0.72 | 0.36 | 0.76 | 0.4 | 0.08 | 3.7 |
| Arkona Sea | T3 | 0.52 | 0.24 | 0.30 | 0.19 | 0.35 | 0.2 | 0.04 | 1.9 |
| Pomeranian Bight | T4 | 0.92 | 0.38 | 0.29 | 0.23 | 0.27 | 0.2 | 0.05 | 2.4 |
| Bornholm Sea | T5 | 0.54 | 0.27 | 0.29 | 0.17 | 0.33 | 0.1 | 0.04 | 1.8 |
| central Baltic Sea | T6 | 0.66 | 0.32 | 0.22 | 0.19 | 0.20 | 0.1 | 0.03 | 1.8 |
| western Gotland Sea | T9 | 0.52 | 0.22 | 0.18 | 0.16 | 0.17 | 0.1 | 0.03 | 1.4 |

| Particulate | Transect | PCB 28/31 | PCB 52 | PCB 101 | PCB 118 | PCB 153 | PCB 138 | PCB 180 | $\Sigma PCB_{part}$ |
|---|---|---|---|---|---|---|---|---|---|
| | | | | | | Pg $l^{-1}$ | | | |
| Kiel Bight/ Fehmarn Belt | T1 | 0.32 | 0.22 | 0.71 | 0.89 | 2.3 | 1.9 | 0.79 | 7.1 |
| Mecklenburg Bight | T2 | 0.27 | 0.30 | 0.82 | 0.96 | 1.9 | 1.8 | 0.64 | 6.7 |
| Arkona Sea | T3 | 0.03 | 0.04 | 0.09 | 0.13 | 0.33 | 0.26 | 0.09 | 0.98 |
| Pomeranian Bight | T4 | 0.10 | 0.08 | 0.25 | 0.35 | 0.98 | 0.75 | 0.35 | 2.9 |
| Bornholm Sea | T5 | n.d. | 0.01 | 0.02 | 0.05 | 0.10 | 0.09 | 0.04 | 0.31 |
| central Baltic Sea | T6 | 0.01 | 0.01 | 0.04 | 0.10 | 0.13 | 0.13 | 0.06 | 0.48 |
| western Gotland Sea | T9 | n.d. | n.d. | n.d. | 0.04 | 0.06 | 0.06 | 0.02 | 0.18 |

| Sum (dissolved+ particulate) | Transect | PCB 28/31 | PCB 52 | PCB 101 | PCB 118 | PCB 153 | PCB 138 | PCB 180 | $\Sigma PCB_{sum}$ |
|---|---|---|---|---|---|---|---|---|---|
| | | | | | | Pg $l^{-1}$ | | | |
| Kiel Bight/ Fehmarn Belt | T1 | 1.6 | 1.0 | 1.9 | 1.5 | 3.5 | 2.6 | 0.92 | 13.1 |
| Mecklenburg Bight | T2 | 1.1 | 0.79 | 1.5 | 1.3 | 2.7 | 2.2 | 0.72 | 10.4 |
| Arkona Sea | T3 | 0.55 | 0.28 | 0.39 | 0.32 | 0.68 | 0.48 | 0.14 | 2.8 |
| Pomeranian Bight | T4 | 1.0 | 0.46 | 0.54 | 0.59 | 1.2 | 0.96 | 0.40 | 5.2 |
| Bornholm Sea | T5 | 0.54 | 0.27 | 0.31 | 0.22 | 0.43 | 0.28 | 0.07 | 2.1 |
| central Baltic Sea | T6 | 0.67 | 0.33 | 0.27 | 0.28 | 0.33 | 0.30 | 0.09 | 2.3 |
| western Gotland Sea | T9 | 0.52 | 0.22 | 0.19 | 0.20 | 0.23 | 0.19 | 0.04 | 1.6 |

*Appendix 3: Concentrations of HCB, HEPEP and HEP in Baltic surface water in February 2022. n.d. not detected.*

| Dissolved | Transect | HCB | HEPEP | HEP |
|---|---|---|---|---|
| | | Pg $l^{-1}$ | | |
| Kiel Bight/ Fehmarn Belt | T1 | 7.5 | 0.63 | n.d. |
| Mecklenburg Bight | T2 | 5.7 | 0.81 | n.d. |
| Arkona Sea | T3 | 5.6 | 0.28 | n.d. |
| Pomeranian Bight | T4 | 9.4 | 0.76 | n.d. |
| Bornholm Sea | T5 | 4.2 | 0.30 | n.d. |
| central Baltic Sea | T6 | 6.7 | 0.67 | n.d. |
| western Gotland Sea | T9 | 6.0 | 0.28 | n.d. |

| Particulate | Transect | HCB | HEPEP | HEP |
|---|---|---|---|---|
| | | Pg $l^{-1}$ | | |
| Kiel Bight/ Fehmarn Belt | T1 | 0.54 | 0.09 | n.d. |
| Mecklenburg Bight | T2 | 0.54 | n.d. | n.d. |
| Arkona Sea | T3 | 0.22 | n.d. | n.d. |
| Pomeranian Bight | T4 | 0.58 | 0.07 | n.d. |
| Bornholm Sea | T5 | 0.19 | n.d. | n.d. |
| central Baltic Sea | T6 | 0.18 | n.d | n.d. |
| western Gotland Sea | T9 | 0.11 | n.d. | n.d. |

| Sum (dissolved+ particulate) | Transect | HCB | HEPEP | HEP |
|---|---|---|---|---|
| | | Pg $l^{-1}$ | | |
| Kiel Bight/ Fehmarn Belt | T1 | 8.0 | 0.71 | n.d. |
| Mecklenburg Bight | T2 | 6.3 | 0.81 | n.d. |
| Arkona Sea | T3 | 5.8 | 0.28 | n.d. |
| Pomeranian Bight | T4 | 9.9 | 0.83 | n.d. |
| Bornholm Sea | T5 | 4.8 | 0.30 | n.d. |
| central Baltic Sea | T6 | 6.8 | 0.67 | n.d. |
| western Gotland Sea | T9 | 6.1 | 0.28 | n.d. |

*Appendix 4: Contents of DDT/metabolites as well as TOC in Baltic Sea surface sediments in winter 2022. Contents are in pg g$^{-1}$ DW and normalized to the organic carbon content in ng g$^{-1}$ TOC. n.d. not detected.*

| Station | DDE-*p.p'* | DDD-*p.p'* | DDT-*o.p'* | DDT-*p.p'* | Σ DDT$_{Sed}$ | TOC |
|---|---|---|---|---|---|---|
| | | | [pg g$^{-1}$ dw] | | | [%] |
| N1 (TF0010) | 134.2 | 86.5 | 4.5 | 18.4 | 243.6 | 0.83 |
| M2 (TF0012) | 742.7 | 519.3 | 49.7 | 224.7 | 1536.5 | 4.27 |
| K7 (TF0069) | 1240.7 | 1071.0 | 75.9 | 244.3 | 2631.9 | 6.31 |
| K4 (TF0110) | 1756.5 | 1779.5 | 67.9 | 232.6 | 3836.6 | 5.69 |
| ODER (OBBOJE) | 26.0 | 16.2 | 2.3 | 6.1 | 50.7 | 0.03 |
| | | | [ng g$^{-1}$ TOC] | | | |
| N1 (TF0010) | 16.2 | 10.4 | 0.5 | 2.2 | 29.3 | |
| M2 (TF0012) | 17.4 | 12.2 | 1.2 | 5.3 | 36.0 | |
| K7 (TF0069) | 19.7 | 17.0 | 1.2 | 3.9 | 41.7 | |
| K4 (TF0110) | 30.9 | 31.3 | 1.2 | 4.1 | 67.4 | |
| ODER (OBBOJE) | 86.7 | 54.0 | 7.7 | 20.3 | 168.7 | |

*Appendix 5: Contents of HCB and PCB$_{ICES}$ in Baltic Sea surface sediments in winter 2022. Contents are in pg g$^{-1}$ DW and normalized to the organic carbon content in ng g$^{-1}$ TOC. n.d. not detected.*

| Station | HCB | PCB 28/31 | PCB 52 | PCB 101 | PCB 118 | PCB 153 | PCB 138 | PCB 180 | ΣPCB$_{ICES.Sed}$ |
|---|---|---|---|---|---|---|---|---|---|
| | | | | | [pg g$^{-1}$ DW] | | | | |
| N1 (TF0010) | 2.8 | 47.3 | 34.9 | 171.5 | 84.8 | 333.9 | 261.1 | 167.8 | 1101.2 |
| M2 (TF0012) | 163.4 | 221.0 | 112.6 | 332.8 | 323.6 | 778.5 | 636.0 | 315.9 | 2720.3 |
| K7 (TF0069) | 272.5 | 386.4 | 469.4 | 513.6 | 568.7 | 1124.3 | 891.9 | 496.2 | 4450.5 |
| K4 (TF0110) | 269.2 | 447.8 | 271.9 | 591.0 | 561.9 | 1279.1 | 848.7 | 450.2 | 4450.5 |
| ODER (OBBOJE) | 13.2 | 8.5 | 5.1 | 4.8 | 5.3 | 12.2 | 8.3 | 5.6 | 49.8 |
| | | | | | [ng g$^{-1}$ TOC] | | | | |
| N1 (TF0010) | 0.34 | 5.70 | 4.20 | 20.66 | 10.22 | 40.23 | 31.46 | 20.22 | 132.7 |
| M2 (TF0012) | 3.83 | 5.18 | 2.64 | 7.79 | 7.58 | 18.23 | 14.89 | 7.40 | 63.7 |
| K7 (TF0069) | 4.32 | 6.12 | 7.44 | 8.14 | 9.01 | 17.82 | 14.13 | 7.86 | 70.5 |
| K4 (TF0110) | 4.73 | 7.87 | 4.78 | 10.39 | 9.88 | 22.48 | 14.92 | 7.91 | 78.2 |
| ODER (OBBOJE) | 44.00 | 28.33 | 17.00 | 16.00 | 17.67 | 40.67 | 27.67 | 18.67 | 166.0 |

*Appendix 6: Contents of organotin (OT) compounds in surface sediments of the Baltic Sea in winter 2022. OT contents are in ng $g^{-1}$ DW and normalized to the organic carbon content in ng $g^{-1}$ TOC. TBT tributyltin. MBT monobutyltin. DBT dibutyltin. TPhT triphenyltin. n.d. n*

| Station | TBT | MBT | DBT | TPhT | $\Sigma OT_{SED}$ |
|---|---|---|---|---|---|
| | | | [ng/g DW] | | |
| N1 (TF0010) | 0.9 | n.d. | n.d. | n.d. | 0.9 |
| M2 (TF0012) | 3.5 | 5.2 | 3.2 | n.d. | 11.9 |
| K7 (TF0069) | 4.1 | 7.7 | 4.4 | n.d. | 16.2 |
| K4 (TF0110) | 4.3 | 5.4 | 5.2 | n.d. | 14.9 |
| ODER (OBBOJE) | n.d. | n.d. | n.d. | n.d. | n.d. |
| | | | [ng/g TOC] | | |
| N1 (TF0010) | 108.4 | n.d. | n.d. | n.d. | 108.4 |
| M2 (TF0012) | 82.0 | 121.8 | 74.9 | n.d. | 278.7 |
| K7 (TF0069) | 65.0 | 122.0 | 69.7 | n.d. | 256.7 |
| K4 (TF0110) | 75.6 | 94.9 | 91.4 | n.d. | 261.9 |
| ODER (OBBOJE) | n.d. | n.d. | n.d. | n.d. | n.d. |

*Appendix 7: PAH contents in Baltic Sea surface sediments in winter 2022. Contents are presented in ng $g^{-1}$ DW and normalized to the organic carbon content in ng $g^{-1}$ TOC. n.d. not detected.*

| Station | ACNLE | ACNE | FLE | ANT | PA | FLU | PYR | BAA | CHR | BBF | BKF | BAP | DBAHA | ICDP | BGHIP | ΣPAH$_{Sed}$ |
|---|---|---|---|---|---|---|---|---|---|---|---|---|---|---|---|---|
| | | | | | | | | | [ng $g^{-1}$ DW] | | | | | | | |
| N1 (TF0010) | 0.9 | 0.5 | 0.9 | 1.9 | 5.3 | 16.5 | 13.3 | 9.1 | 5.6 | 23.9 | 9.1 | 9.6 | 3.0 | 22.8 | 18.3 | 140.6 |
| M2 (TF0012) | 4.5 | 2.6 | 5.9 | 11.5 | 52.1 | 121.6 | 89.8 | 57.0 | 58.4 | 195.2 | 66.1 | 76.4 | 28.9 | 174.0 | 155.6 | 1099.7 |
| K7 (TF0069) | 12.3 | 4.0 | 12.6 | 22.2 | 88.4 | 227.7 | 174.8 | 109.2 | 102.4 | 290.4 | 118.8 | 153.0 | 47.3 | 340.3 | 217.2 | 1920.6 |
| K4 (TF0110) | 8.5 | 4.3 | 15.7 | 14.3 | 59.2 | 183.4 | 139.1 | 97.3 | 71.7 | 333.1 | 114.9 | 107.1 | 43.2 | 407.6 | 284.6 | 1884.1 |
| ODER (OBBOJE) | 0.1 | 0.3 | 0.5 | 0.3 | 1.1 | 2.2 | 1.3 | 0.7 | 0.7 | 1.4 | 0.5 | 0.7 | 0.2 | 1.1 | 0.9 | 11.9 |
| | | | | | | | | | [ng $g^{-1}$ TOC] | | | | | | | |
| N1 (TF0010) | 108.4 | 60.2 | 108.4 | 228.9 | 638.6 | 1988.0 | 1602.4 | 1096.4 | 674.7 | 2879.5 | 1096.4 | 1156.6 | 361.4 | 2747.0 | 2204.8 | 16951.8 |
| M2 (TF0012) | 105.4 | 60.9 | 138.2 | 269.3 | 1220.1 | 2847.8 | 2103.0 | 1334.9 | 1367.7 | 4571.4 | 1548.0 | 1789.2 | 676.8 | 4074.9 | 3644.0 | 25751.8 |
| K7 (TF0069) | 194.9 | 63.4 | 199.7 | 351.8 | 1401.0 | 3608.6 | 2770.2 | 1730.6 | 1622.8 | 4602.2 | 1882.7 | 2424.7 | 749.6 | 5393.0 | 3442.2 | 30437.4 |
| K4 (TF0110) | 149.4 | 75.6 | 275.9 | 251.3 | 1040.4 | 3223.2 | 2444.6 | 1710.0 | 1260.1 | 5854.1 | 2019.3 | 1882.2 | 759.2 | 7163.4 | 5001.8 | 33110.7 |
| ODER (OBBOJE) | 333.3 | 1000.0 | 1666.7 | 1000.0 | 3666.7 | 7333.3 | 4333.3 | 2333.3 | 2333.3 | 4666.7 | 1666.7 | 2333.3 | 666.7 | 3666.7 | 3000.0 | 40000.0 |

Naumann, M., Gräwe, U., Umlauf, L., Burchard, H., Mohrholz, V., Kuss, J., Kanwischer, M., Osterholz, H., Feistel, S., Hand, I., Waniek, J.J., Schulz-Bull, D.E.: Hydrographic-hydrochemical assessment of the Baltic Sea 2022

# CONTENT



Leibniz-Institut für Ostseeforschung Warnemünde
IOW